EFFECT OF HYDROQUININE AGAINST PATHOGENIC MICROORGANISMS AND ITS MECHANISM

NONTAPORN RATTANACHAK

A Thesis Submitted to the Graduate School of Naresuan University
in Partial Fulfillment of the Requirements
for the Doctor of Philosophy in Biomedical Sciences
2023

EFFECT OF HYDROQUININE AGAINST PATHOGENIC MICROORGANISMS AND ITS MECHANISM

NONTAPORN RATTANACHAK

A Thesis Submitted to the Graduate School of Naresuan University
in Partial Fulfillment of the Requirements
for the Doctor of Philosophy in Biomedical Sciences
2023

Thesis entitled "Effect of hydroquinine against pathogenic microorganisms and its mechanism"

By Nontaporn Rattanachak

has been approved by the Graduate School as partial fulfillment of the requirements for the Doctor of Philosophy in Biomedical Sciences of Naresuan University

Oral Defense Committee

..... Chair
(Assistant Professor Robert Baldock, Ph.D.)

..... Advisor
(Assistant Professor Jirapas Jongjitwimol, Ph.D.)

..... Internal Examiner
(Assistant Professor Yordhathai Thongsri, Ph.D.)

..... Internal Examiner
(Napaporn Apiratmateekul, Ph.D.)

..... External Examiner
(Assistant Professor Thanwa Wongsuk, Ph.D.)

Approved

.....
(Associate Professor Krongkarn Chootip, Ph.D.)
Dean of the Graduate School

Title	EFFECT OF HYDROQUININE AGAINST PATHOGENIC MICROORGANISMS AND ITS MECHANISM
Author	Nontaporn Rattanachak
Advisor	Assistant Professor Jirapas Jongjitwimol, Ph.D.
Academic Paper	Ph.D. Dissertation in Biomedical Sciences, Naresuan University, 2023
Keywords	Hydroquinine, Pseudomonas aeruginosa, Antimicrobial activity, RND-type efflux pump, Anti-infection, Virulence factors, Transcriptomic analysis

ABSTRACT

Hydroquinine is an organic compound closely related to quinine-derivative drugs known to possess anti-malarial activity. Hydroquinine has also been found in abundance in some natural extracts and has been suggested to have antibacterial properties. However, there is limited evidence demonstrating the antibacterial properties of hydroquinine. Further, the exact mechanism of hydroquinine action against *Pseudomonas aeruginosa* has not yet been studied. Therefore, this study aimed to investigate the antibacterial properties of hydroquinine using broth microdilution method. In addition, this research has uncovered the mechanism of action of hydroquinine against *P. aeruginosa* by examining transcriptional changes using high-throughput transcriptomic analysis. We further validate these findings using both genotypic analysis using PCR-based methods and phenotypic analysis. This study found that hydroquinine inhibited all eight bacterial reference strains tested. The minimum inhibitory concentration (MIC) and the minimum bactericidal concentration (MBC) values of hydroquinine against all eight bacterial strains investigated ranged from 650–2,500 and 1,250–5,000 µg/mL, respectively. Transcriptomic analysis demonstrated that at ½ MIC of hydroquinine (1.250 mg/mL), 254 genes were differentially expressed (97 downregulated and 157 upregulated). Hydroquinine induced the upregulation of the RND-type efflux pump genes, a drug-resistant mechanism (4.90 to 9.47 Log_2 fold change) and downregulation of virulence

factor genes associated with flagella assembly, pathogenicity factors (-2.93 to -2.18 Log_2-fold change) in *P. aeruginosa* ATCC 27853. Furthermore, the expression of RND-type efflux pump genes were validated by multiplex quantitative reverse transcription PCR (mRT-qPCR) and an *effluxR* detection assay with multiplex reverse transcription digital PCR (mRT-dPCR) methods. It showed that ½ MIC of hydroquinine significantly induced the expression of the *mex*D and *mexY* genes in the *P. aeruginosa* strains. In addition, using the RT-qPCR method, the virulence factor gene expression associated with flagella assembly and quorum sensing showed significantly downregulated in *P. aeruginosa* ATCC strains under ½ MIC of hydroquinine treatment. Additionally, by analyzing cellular phenotypes of *P. aeruginosa* associated with virulence factors, treatment with ½ MIC of hydroquinine exhibited inhibition of motility, pyocyanin production and impaired biofilm formation. These results offer a detailed view of the global transcriptomic changes in *P. aeruginosa* in response to hydroquinine exposure, which is helpful in the understanding of the cellular strategies utilized during hydroquinine conditions and indicates a possible mechanism for *P. aeruginosa* inhibition after hydroquinine exposure.

ACKNOWLEDGEMENTS

First of all, I would like to express my deepest appreciation and sincere gratitude to my advisor, Assistant Professor Dr. Jirapas Jongjitwimol for his kindness in providing an opportunity to be his advisee and for allowing me to pursue mine. I am also grateful for his valuable supervision, valuable suggestions, all kinds of support, encouragement, guidance, and criticism throughout the course of my study.

I wish to sincerely thank Associate Professor Dr. Touchkanin Jongjitvimol for their help and for giving me an opportunity for this PhD study.

My greatest appreciation and sincere gratitude are also addressed to my graduate committees, Dr. Robert Baldock, Assistant Professor Dr. Yordhathai Thongsri, Dr. Napaporn Apiratmateekul, and Assistant Professor Dr. Thanwa Wongsuk for their helpful suggestions and criticisms.

I also appreciated the scholarship (Grant number 3/2563) from the Ministry of Higher Education, Science, Research, and Innovation of Thailand, for this Ph.D. study.

I sincerely thank Dr. Robert Baldock for his help, correction, and suggestions in my thesis. Special thanks are also for taking me as a member of his lab to conduct experiments and support and provide valuable suggestions while working at the University of Portsmouth, UK. Also, I wish to thank Kelly Doughty for her help and providing valuable suggestions during the time in UK.

My special additional thanks are also to Associate Professor. Dr. Chalermchai Pilapong, and Dr. Krai Daowtak for helping me in the analysis of the result of transcriptomic analysis as well as Mr. Theerasak Jaifoo for his assistances with the drug sensitivity test part.

Appreciation is also expressed to all academic staff and members of the Biomedical Sciences Program for their valuable suggestions, practical helps, providing the wonderful environment and friendship during the time of this study.

Finally, I would like to express my sincere gratitude and appreciation to my dear parents, my husband and my family for their love, push-up, cheerfulness, devotion and encouragement throughout my life.

Nontaporn Rattanachak

TABLE OF CONTENTS

Page

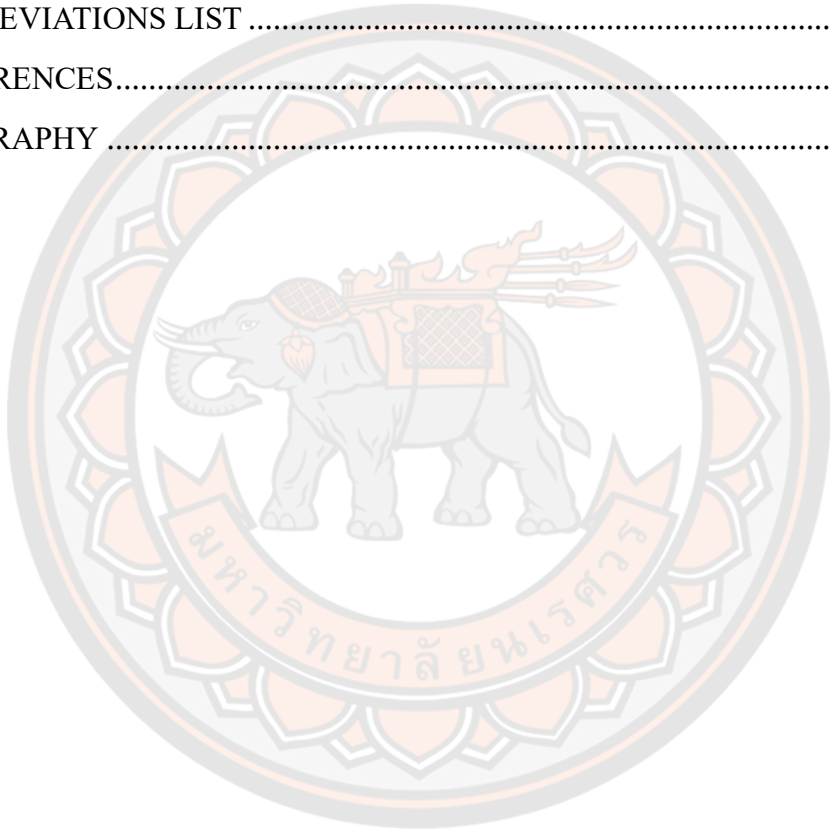

List of tables

Page

List of figures

Page

CHAPTER I

INTRODUCTION

Background and significance of the study

The emergence of drug-resistant pathogens is one of the most severe public health problems in many countries, leading to the difficulty in treating microbial infections and a significant cause of human mortality (1). *Enterobacteriaceae*, *Pseudomonas aeruginosa*, and *Acinetobacter* have been classified by the World Health Organization (WHO) as the most concerning pathogens ("critical priority") (1). In addition, there are currently many drug-resistant bacteria that were assessed by the Centers for Disease Control and Prevention (CDC) as presenting urgent, serious, and concerning threats. This includes *Streptococcus pneumoniae*, *Staphylococcus aureus*, *Mycobacterium tuberculosis*, *Enterococcus* spp., *Escherichia coli*, *Salmonella* spp., *Klebsiella pneumoniae*, *P. aeruginosa*, *Acinetobacter baumannii*, and *Neisseria gonorrhoeae* (2-4). Some of these bacteria are the primary causes of opportunistic infection in hospitalized patients and with drug resistance, have limited therapeutic options for treatment. One of the reasons is the ability of microorganisms to resist and evade the activity of antibiotics (5). These microorganisms are able to adapt and/or avoid destruction from antibiotics through several mechanisms such as production of beta-lactamase, decreased outer membrane permeability, efflux pump expression, production of aminoglycoside-modifying enzymes, and target modification (6). These mechanisms can enable resistance to many types of antimicrobial classes including aminoglycosides, fluoroquinolones, beta-lactamase, chloramphenicol etc. This is considered as multidrug resistance (MDR) (7-11).

P. aeruginosa is an opportunistic pathogen with a high propensity for multidrug resistance in hospitalized patients. The National Nosocomial Infections Surveillance (NNIS) System reported that *P. aeruginosa* has been the second common microorganism isolated in nosocomial pneumonia (17% of cases) (12). It was the third common pathogen isolated in both urinary tract infections (UTI) and surgical site infection patients (11% of cases) (12). Overall, *P. aeruginosa* is the fifth microorganism isolated from all specimens in nosocomial infection patients (about 9% of cases). Significantly, nosocomial infection by MDR *P. aeruginosa* causes mortality rates of 18–61% (13). *P. aeruginosa* infection in neutropenic patients leads to high mortality of 50–70% (6). For these reasons, treatment of either *P. aeruginosa* or MDR *P. aeruginosa* infections requires effective antibiotics or potentially combination treatments to overcome resistance. Discovery and development of novel agents obtained from natural products may be another choice inhibiting the growth of MDR *P. aeruginosa*. Several researchers propose the utilization of some natural products based on their antimicrobial properties. Previous research has discussed chemicals found in natural products from plants, such as flavonoids, alkaloids, and terpenoids (14). Many natural products have been documented as a potential antimicrobial agent to inhibit the growth of pathogenic microorganisms and also highlighting their potential as a synergistic agent or a potentiator of the currently used antibiotics (15).

Recently, Jongjitvimol *et al.* (2020) (16) reported that the ethanolic nest entrances extracts from *Tetrigona apicalis* possess antibacterial, antifungal, and anti-proliferative activities. Significantly, hydroquinine was found as the major content of chemical compounds in the extracts. Hydroquinine is an organic compound and a cinchona alkaloid, which was closely related to quinine alkaloid compounds (17). As a therapeutic drug, hydroquinine has been approved for use in medical treatment for nocturnal cramps in the Netherlands at 300 mg daily for 2 weeks (18). Moreover, it may reduce light-brown patches on the skin and skin discolorations associated with pregnancy. In addition, hydroquinine has been documented that it has anti-malarial and demelanizing activities (19). Furthermore, other alkaloid compounds have been reported to possess antimicrobial properties and anti-virulence factors in both gram-positive and gram-negative bacteria, such as inhibition of quorum sensing (QS) signaling and pigment production in *P. aeruginosa* (20), inhibiting biofilm formation in *E. coli* and *P. aeruginosa* (21), and inhibiting virulence gene expression in *S. aureus* (22).

According to these reports, hydroquinine might have potential as both an antimicrobial and anti-infective agent. However, either antibacterial or anti-infective activities of hydroquinine has not yet been studied, furthermore the mechanism of hydroquinine against pathogenic bacteria remains unknown. The objectives of this research, were to investigate the antibacterial properties of hydroquinine against pathogenic bacteria. And to investigate the mechanisms of action of hydroquinine against *P. aeruginosa*.

Objective of the study

This study consists of two main objectives. The first objective was to investigate the antibacterial activity of hydroquinine against pathogenic bacteria. The second was to investigate the mechanisms of action of hydroquinine against *P. aeruginosa*.

Scope of the study

The scope of this study was to find a novel active compound with antibacterial properties. In this research, hydroquinine was studied in three main parts: (1) characterizing the properties of hydroquinine against pathogenic bacteria, (2) characterizing global transcriptional profiles of a *P. aeruginosa* reference strain with hydroquinine treatment, and (3) investigating mechanisms of action of hydroquinine against *P. aeruginosa* strain.

The first part was evaluation of hydroquinine characterization. This was divided into four issues. Firstly, the antimicrobial susceptibility of all bacteria tested in this study (reference strains) was checked using a method from the Clinical and Laboratory Standards Institute (CLSI) guideline. Secondly, antibacterial activity of hydroquinine against both gram-negative and gram-positive bacteria was investigated using broth microdilution method. Next, time to kill DS *P. aeruginosa* ATCC 27853 and MDR *P. aeruginosa* ATCC BAA 2108 was tested using a time-kill assay. Lastly, the synergistic effect of hydroquinine with certain antibiotics was observed against MDR *P. aeruginosa* ATCC BAA 2108 by checkerboard assay.

The second part the global transcriptional profile of *P. aeruginosa* ATCC 27853 was evaluated by transcriptomic analysis after treated with ½ MIC of hydroquinine 1 h. This part provided the globally transcriptomic information of *P. aeruginosa* in response to hydroquinine.

In the last part, after transcriptomic analysis was used to identify differentially expressed genes. Further investigation of up-regulated or down-regulated genes was performed to investigate the mechanisms by which hydroquinine is able to target DS and MDR *P. aeruginosa* strains. Target validation was performed using with either genotypic analysis using polymerase chain reaction (PCR) based methods, phenotypic analysis or both.

The experiments in this research were performed in the Biosafety Level 2 (BSL-2) Laboratory and Central laboratory at Faculty of Allied Health Science, Naresuan University, Phitsanulok, Thailand. Some experiments were performed in Microbiology Laboratory, Department of Medical Technology, Faculty of Allied Health Science, Naresuan University, Phitsanulok, Thailand.

CHAPTER II

LITERATURE REVIEW

1. Hydroquinine

Hydroquinine or dihydroquinine is an organic compound. It is found in natural alkaloids (Cinchona Alkaloids) and is closely related to quinine. Moreover, it can be found in commercial pharmaceutical formulations of quinine. Its chemical formula is $C_{20}H_{26}N_2O_2$, and its molecular weight is 326.4334 g/mole (Figure 1) (19).

In the Netherlands, hydroquinine (Inhibin®) has been used in medical treatment for nocturnal cramps (18, 19). It has been an over-the-counter medicine in the Netherlands since March 1990 (19). The dose of hydroquinine for nocturnal cramp treatment is 200 mg with dinner and 100 mg at bedtime for 14 days. Hydroquinine also has anti-malarial with a dose of 129 nM [IC50] (23) as well as demelanizing activity (19). It may reduce light-brown patches on the skin, skin discolorations associated with pregnancy, abrasions on the skin or the use of birth control pills (19). Moreover, hydroquinine also decreases melanin by slowing the synthesis of the tyrosinase enzyme, which changes the protein compound that forms melanin into another compound (19). Therefore, hydroquinine has the property to use as an effective bleaching agent. It also is used for composition in skin-lightening creams and lotions. In addition, it may be used as a derivative of many drugs used in pharmacology, such as cabotegravir, capmatinib, tazemetostat etc (19). Furthermore, it was used in derivatives of drug resistance in malaria, such as chloroquine, tafenoquine, mefloquine, quinidine, cyproquinate etc. (19). Moreover, Nontprasert, A. *et al.* (1996) (23) evaluated the anti-malarial effects in vitro of quinine, dihydroquinine and 3-hydroxyquinine, alone and in combination. Quinine and dihydroquinine have comparable anti-malarial activities, approximately ten times higher than the metabolite 3-hydroxyquinine. Furthermore, dihydroquinine has been reported to affect deoxyribonucleic acid (DNA), ribonucleic acid (RNA) and protein during the in vitro erythrocytic growth cycle of *Plasmodium knowlesi* (24). A recent study reviewed the ethanolic Nest Entrances Extracts (eNEEs) extract from nest entrances of *Tetrigona apicalis*, which have hydroquinine as the significant content of chemical compounds in the eNEEs. The result showed antibacterial, antifungal, and anti-proliferative activities (16).

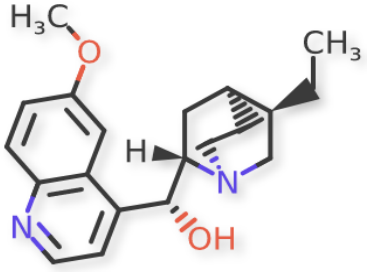

Figure 1 Structure of hydroquinine (19)

1.1 Cinchona alkaloids

Cinchona alkaloids are rigid molecules containing four chiral carbons. The cinchona alkaloids comprise quinine, quinidine, cinchonidine, and cinchonine. It has been found in the genus Cinchona, which has approximately 40 species and belongs to the Rubiaceae family (25, 26). The amount of alkaloid compounds found in each Cinchona species is different. For example, 5–7% alkaloid content was found in the "red" bark of Cinchona succirubra. The bark of Cinchona calisaya has an alkaloid content of 4–7%. In contrast, the Cinchona officinalis "ledgeriana" bark has 5–14% alkaloid content. In addition, given favorable growing conditions, certain the bark of cinchona hybrids could produce alkaloids up to 17%, which is more than the wild-type cinchona. The bark analysis of different cinchona species shows quinine is the most abundant alkaloid, usually comprising 50–90% of the alkaloids' sum. The structures of four major cinchona alkaloids are similar (Figure 2), and in the bark of Cinchona found about 30–90% (26).

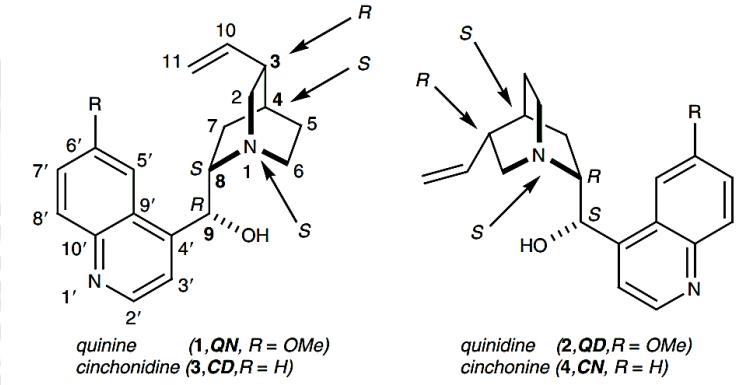

Figure 2 Structure of four major cinchona alkaloids (26)

1.2 Quinine

Quinine ($C_{20}H_{24}N_2O_2$) is an alkaloid compound extracted from the bark of the cinchona tree. The discovery of quinine is widely regarded as the most fortunate medical discovery of the 17th century (27). The first chemical molecule successfully used to treat an infectious disease was using quinine to treat malaria (27). In Peru, the Spanish Countess of Chinchon caught a fever and was cured by the bark of a tree. She introduced quinine to Europe in 1638 after returning to Spain with the bark, and in 1742, botanist Carl Linnaeus named the tree Cinchona in her honour (27). Before 1820, consumers used the cinchona tree bark by mixing the fine powder of the cinchona tree bark with wine. Pierre Joseph Pelletier and Joseph Caventou named quinine in 1820 after it was isolated and extracted from the bark. Therefore, purified quinine replaced the use of bark and was used in the standard malaria treatment (28). Besides quinine, used for anti-malaria, other cinchona alkaloids, such as quinidine, cinchonine, and cinchonidine, are also used for malaria treatment. From 1866 to 1868, cinchona alkaloid efficacy was evaluated by treating 3,600 patients using sulfate alkaloids. All four alkaloids were comparable in terms of "cessation of febrile paroxysms," with higher than 98% cure rates. However, after 1890, quinine alkaloids became commonly used for malaria treatment as they had access sources of cinchona bark that had increased quinine content (Javan cinchona bark). Until the 1920s,

quinine continued to be used for malaria treatment, even with increased efficient synthetic anti-malarials were available. Chloroquine was the most important of these medications, and it was extensively utilized, especially beginning in the 1940s. However, by the late 1950s, chloroquine in areas of Southeast Asia and South America was resisted by *Plasmodium falciparum*. Throughout the 1980s, malaria that was resistant to chloroquine spread to almost every location. Therefore, with the rise in chloroquine resistance, quinine has become more critical, especially in treating severe malaria and plays a vital role in treating malaria today (27).

1.2.1 Biological activity of quinine

Quinine has been used as an anti-malarial therapy in medicine for centuries because it has specific toxicity against Plasmodium. Besides its anti-malarial activity, quinine has been shown to have other pharmaceutical properties, such as anti-inflammation and anti-cancer (29). Krishnavenil and Suresh (2015) (30) found that quinine has anti-cancer activity, effectively inhibiting cell proliferation and inducing cell death in cancer cells through protease activity. Along with this, Ning *et al.* (2016) (29) reported that quinine has potency as an anti-obesity by activating adipogenesis through ERK/S6 signaling. Quinine possesses antimicrobial properties, as revealed by several studies. Quinine inhibits *E. coli*, *K. pneumonia*, and *S. aureus*. Moreover, Antika *et al.* (2020) (31) revealed that quinine derivatives demonstrated middle antimicrobial activity when compared with quinine on common pathogenic bacteria strains, e.g. *E. coli, S. aureus, P. aeruginosa*, and *Bacillus substiles*. Moreover, among other quinine derivatives, ester quinine propionate was found to exhibit the highest antibacterial activity (9 to 23.5 mm) when compared to streptomycin (8 to 12 mm) on common pathogenic bacteria strains (31).

2. Antibacterial mechanism of natural alkaloids and derivatives

The relation of unique chemical structures of alkaloids causes antibacterial mechanisms (32, 33). Alkaloid mechanisms for inhibiting bacterial growth consist of inhibiting the bacterial proteins and nucleic acid synthesis and modifying the permeability of the bacterial cell membrane. Alkaloids also inhibit bacteria from growing by destroying cell membranes and cell wall, bacterial metabolism, and efflux pump inhibition (Figure 3) (34).

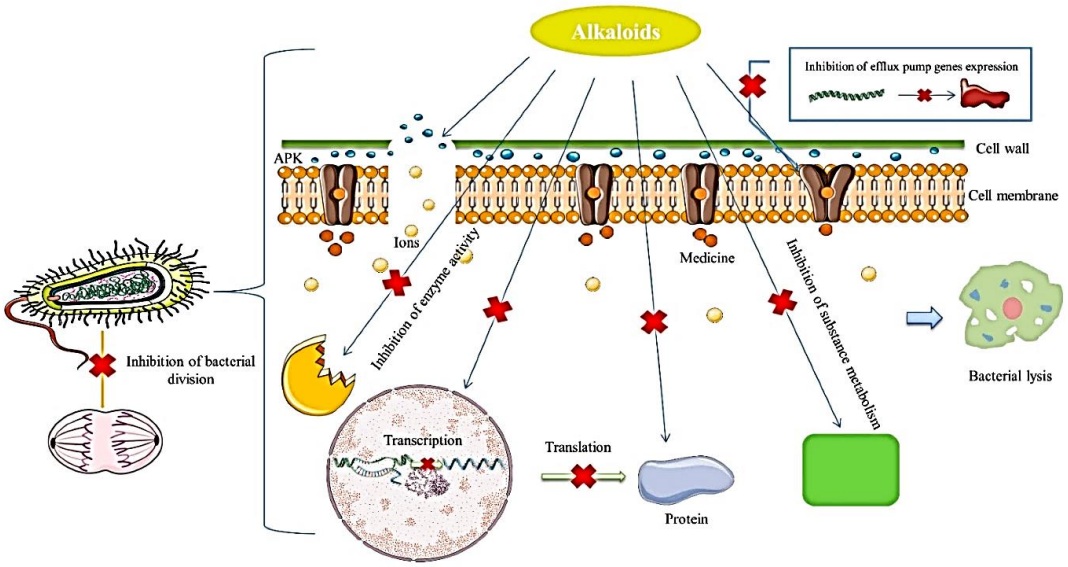

Figure 3 Antibacterial mechanism of natural alkaloids (32)

2.1 Inhibition of bacterial nucleic acid and protein synthesis

Deoxyribonucleic acid (DNA) and ribonucleic acid (RNA) are compositions of bacterial nucleic acids involved in storing and expressing genetic information. DNA function stores all of the genetic information to develop, maintain, and reproduce for cell growth and living (35). There are three types of RNA molecules that function as messenger molecules from DNA to cellular protein synthesis (36). The functionality of different types of RNA: Messenger RNA (mRNA) is a single-stranded molecule that is transcribed genetic code from DNA that acts as a protein blueprint or template translated into protein (36). Transfer RNA (tRNA) acts as a specific adaptor during the genetic code translation into protein, bringing the appropriate amino acid to mRNA, which recognizes a codon on mRNA (36). Ribosomal ribonucleic acid (rRNA) is the RNA component of ribosomes, associated with a set of proteins to form ribosomes (36). Therefore, inhibition of DNA replication or DNA/RNA molecules were damaged, preventing the expression of genes or DNA replication, affecting the characteristics of microorganisms and their growth and reproduction (37). For example, DNA gyrase enzymes act to releive supercoiling and allow uncoiling bacterial DNA during DNA replication. DNA gyrase is essential for synthesis, replication, repair, and transcription, as a result it is a good target for antibiotics (38). Heeb, S. *et al.* (2011) reported that type II topoisomerase enzyme was the target of natural or synthetic quinolone alkaloids, consequently inhibiting DNA replication (39). Similarly, berberine, an isoquinoline alkaloid, has exhibited activity against bacteria, fungi, protozoa, and viruses. This compound inhibited the bacteria through various mechanisms, such as inhibiting cell division and inhibiting protein and DNA synthesis, leading to bacterial death (40-42). Matrine inhibited the synthesis of proteins involved in cell development and division in *E. coli* and *S. aureus*, preventing bacteria from dividing and growing. Matrine is bound with proteins in cells, producing aggregates, which cause the disintegration of the cytoplasm and, finally, the death of the bacteria (32). Moreover, sanguinarine and berberine are naturally

occurring alkaloids capable of altering the functionality of filamentous temperature-sensitive protein Z (FtsZ). FtsZ is essential for the cell cycle, especially in controlling the bacterial cell division process, diaphragm formation, and forming a ring structure at the division site (43).

2.2 Effect on the bacterial cell membrane and cell wall

The bacterial cell membrane consists of phospholipid bilayers and proteins that are elastic and semi-permeable (44, 45). The cell membrane functions relate to the protective barrier, recognition, identification, and electron transport (44). It provides an environment inside the cell, a somewhat stable and constant environment for bacteria's life activities. When the bacterial cell membrane is broken, it will cause a high number of molecules to be released out of the cell. Moreover, if the cell wall protection function is lost, the cell membrane transport and information transfer functions are blocked. All of these contribute to inhibiting bacterial growth or livelihood, leading to biological death (44, 45). Moreover, it has various indicators representing the bacteria cell membrane was damaged. Significantly, the conductivity of the culture medium increases as intracellular electrolytes leak into the medium. Therefore, changing the conductivity of the culture supernatant is able to indicate that the permeability of the bacterial cell membrane has changed (46). In addition, increasing the permeability of the bacterial cell wall leads to leaks of alkaline phosphatase (AKP) out of the cells, which is found primarily between the cell wall and cell membrane of bacteria. Consequently, the integrity of the bacterial cell wall can be measured from AKP activity (47, 48). Moreover, various targets may be involved in damaging the cell membrane of alkaloid mechanisms, such as proton motive force (PMF), electron flow, nutrient uptake, or other unrelated enzyme activities (49). Alkaloids from *Dicranostigma leptopodum* can change the cell permeability and significantly affect antibacterial activity (*K. pneumonia*), which displayed that the conductivity of the culture medium with and without the alkaloid was significantly different (50).

2.3 Efflux pumps inhibition

Efflux pumps are transmembrane protein complexes found in gram-positive and gram-negative bacteria, and eukaryotic organisms (51). The function of efflux pumps is to pump toxic substrates, including antibiotics and compounds, from within the cells to the external environment. The pumps may be specific for one or many substrates, including various antibiotics or agents with structurally different molecules. Therefore, the pumps are able to transport a variety of antibiotics out of the cell as a result, efflux pump activity is linked to multiple drug resistance (MDR) (52). If the efflux pump removes membrane-permeable antibacterial agents, the bacterial cell may avoid toxicity resulting from the antibacterial agents. This reduces the effectiveness of the agent and promotes resistance (53). Major facilitator (MF), multidrug and toxic efflux (MATE), resistance-nodulation-division (RND), small multidrug resistance (SMR), and ATP binding cassette (ABC) are five major families of an efflux transporters found in bacteria (54). All these families use proton motive force for energy, except the ABC family, which applies ATP hydrolysis to actively transport the substrates out of the cell (55). Steroidal alkaloid conessine is one of the alkaloids found in *Holarrhena antidysenterica* barks. This compound has shown potential antibacterial activity against both gram-positive and gram-negative bacteria.

Moreover, conessine showed significant synergistic effects when combined with conventional antibiotics. The available studies indicate that conessine has displayed efflux pump inhibiter activity against the AdeIJK efflux pump, which plays a vital role in pumping the multiple antibiotics in *Acinetobacter baumannii* (56). Moreover, Siriyong *et al.* (2017) (15) reported that conessine reduced the minimum inhibitory concentrations (MICs) value of all antibiotics by at least 8-fold in *P. aeruginosa* MexAB-OprM overexpressed K1455 strain compared with *P. aeruginosa* PAO1 strain. Therefore, conessine could be an inhibitor of the MexAB-OprM efflux pump. The researchers discussed that the mechanism of conessine for efflux pump inhibition might be caused by competition inhibition and/or block the substrate-binding site of MexB. Therefore, conessine may compete for substrate-binding site of MexB. It is also suggested that conessine compounds may interact with the "G-loop" or "switch loop" of the efflux pump structure, in which the distal and proximal binding sites were separated, compared to the mechanism of MexB-specific PAßN. Therefore, in vitro studies have shown that the inhibition of the efflux pump is able to reduce the levels of MDR efflux pump activities. Consequently, antibacterial effects are improved, and bacterial resistance is prevented (57). For this reason, efflux pump inhibitors may be a valuable asset promote and synergize with existing antibiotics (58).

2.4 Bacterial metabolism inhibition

Interfering with the energy metabolism of bacteria may occur from the antibacterial activities of alkaloids, causing inhibition of bacterial activity to maintain or grow. One of the potential targets is adenosine triphosphate (ATP), which is usually synthesized through respiration. It is the most direct source of energy in organisms and the energy supply for a variety of living processes in cells. ATP is a critical component of respiration, primary metabolism, and energy source for various enzyme reactions. Therefore, inhibition of ATP synthesis affects many fundamental metabolic systems in microorganisms, which may lead to the death of bacteria (32, 59). Berberine can affect *Streptococcus pyogenes* (Group A streptococcus, GAS) carbohydrate metabolism by enhancing the conversion and uptake of carbohydrates and decreasing carbohydrate consumption (60). Berberine stimulated the exchanging pathway of other compounds to monosaccharides and their derivatives, which increased the conversion and absorption of carbohydrates. In addition, berberine up-regulated ATP-binding cassette transported phosphotransferase systems, which were also involved in carbohydrate uptake. Moreover, the disturbance of the carbohydrate metabolism by berberine in GAS cause stimulates excessive reactive oxygen species (ROS), ultimately inhibiting the bacteria. In addition, berberine inhibits the growth of intestinal bacteria by reducing ATP and Nicotinamide adenine dinucleotide hydrogen (NADH) production (50). Furthermore, alkaloids from *Dicranostigma leptopodum* (Maxim) Fedde have shown *K. pneumoniae* inhibition via intracellular enzyme activities and disrupt normal cell metabolic functions, all contributing to the bacteria inactivation (61).

3. Anti-virulence factor of natural alkaloids and derivative

The virulence factor of pathogenic bacteria encompasses the molecules that assist the bacteria in colonizing the host as well as damaging host tissue at the cellular level (62). The infection process of pathogenic bacteria occurs from the coordinated action of virulence factors via the following steps: (i) host invasion, (ii) tissue colonization, (iii) tissue damage, and (iv) host defence evasion (63). The virulence factors of pathogenic bacteria include quorum sensing (QS), bacterial biofilms, bacterial motility, bacterial toxins, bacterial pigments, bacterial enzymes and bacterial surfactants (64). The natural alkaloids and derivatives for inhibiting virulence factors of pathogenic bacteria consist of (i) quorum sensing inhibition, (ii) biofilms forming inhibition, (iii) motility inhibition, (iv) bacterial toxins inhibition, (v) bacterial pigments inhibition (Figure 4) (64).

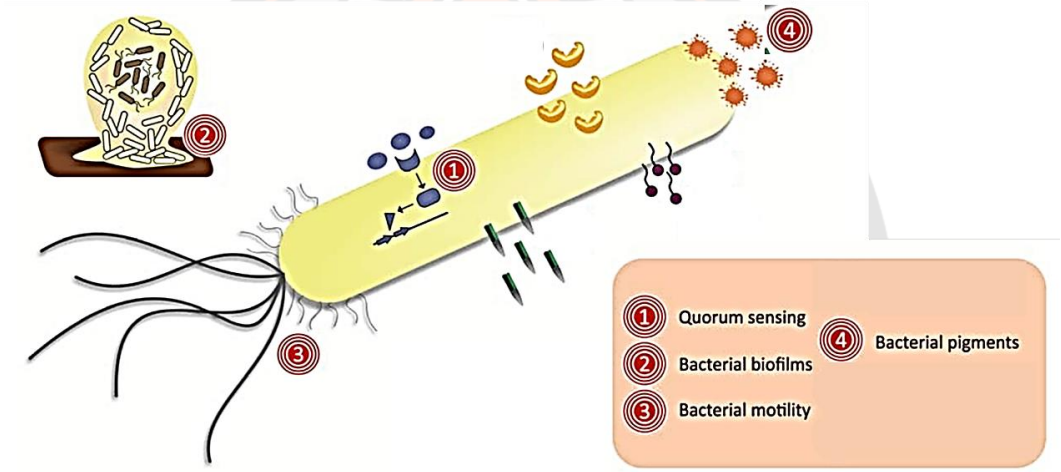

Figure 4 Virulence factors of pathogenic bacteria (64)

3.1 Alkaloids and derivatives against quorum sensing (QS)

Quorum sensing (QS) is a chemical communication system of bacteria used for cell-to-cell communication, and gene expresses regulation in response to the inconstancy of cell density (65). The QS of bacteria produces, detects, responds and recognizes small signal molecules called autoinducers that it self-secreted to define various physiological activities, including virulence, motility, spore production, symbiosis, unification, antibiotic production, and biofilm formation (65). Generally, the typical autoinducer class of gram-negative bacteria is Nacylated L-homoserine lactones (AHLs), which the bacteria recognize. The AHLs are able to pass across membranes and attach to cytoplasmic receptors to make a regulatory effect. The other autoinducers of gram-negative bacteria include autoinducers AI-2 and (S)- 3-hyroxytridecan-4-one (CAI-1), which are produced depending on molecule S-adenosylmethionine (SAM) (66, 67). In contrast, gram-positive bacteria use either a membrane-bound histidine kinase or cytoplasmic receptors to recognize peptides with various post-translational modifications as autoinducers or autoinducer peptides (AIP) (68). Interestingly, the inhibition of QS is an alternative strategy for reducing the

virulence of infectious diseases (64). Caffeine, an alkaloid isolated from the *Leguminosae Trigonella*, has been reported to be able to have anti-QS properties against *P. aeruginosa* PA01 via inhibiting the AHL signaling molecules production (69). Moreover, the steroidal alkaloid tomatidine was shown as a biological activity that is able to reduce hemolysis production of *S. aureus* via inhibiting the expression of QS accessory gene regulation (*agr*) system, including *hla*, *hld*, *geh*, *nuc*, *plc*, and *splC* (22).

3.2 Alkaloids and derivatives against biofilms forming capacity

Biofilms are microbial cell communities covered by the matrix of extracellular polymeric substances (EPS) that are self-produced. The biofilms are necessary for cellular adhesion to both biotic and abiotic surfaces. It usually occurs in natural environments and is the most prevalent type of microbial organization (70, 71). The process of biofilm formation includes (i) bacterial adhesion on surfaces, (ii) bacterial colonization, (iii) bacterial preform mature biofilms and biofilm exopolysaccharide (EPS) matrix, and (iv) bacterial release from biofilms as shown in Figure 5 (64). Biofilms pose a significant challenge in several areas, especially in medical and food industry settings, which play an essential role in the exhibition of morphological, physiological, and genetic differences from free-living (planktonic) bacteria (72). In recent years, biofilms have received significant attention due to their enormous impact on medicine and public health. Bacteria in the biofilm form are primarily responsible for the chronicity of persistent infections because they can attach to many devices such as medical devices namely, central venous catheters, endotracheal tubes, intrauterine devices, mechanical heart valves, pacemakers, peritoneal dialysis catheters, replacement joints, and urinary catheters (73, 74). The bacterial biofilm form causes resistance in most medical settings, resulting from the bacteria that elude the host immune defences and withstand antibacterial therapies (75, 76). Opportunistic bacterial pathogen *P. aeruginosa* is one of the bacterial biofilm formation capacity strains that can colonize the lungs of cystic fibrosis patients, causing persistent disease from biofilm-based that is self-produced (77). Interestingly, alkaloids and derivatives received from plants have been reported to have an essential role in inhibiting the biofilm formation of *P. aeruginosa*. Four strategies of alkaloids and derivatives to inhibit biofilm formation have been reported, including (A) preventing bacterial adhesion, (B) preventing biofilm maturity, (C) disabling the EPS matrix of mature biofilms, and (D) killing microorganisms in mature biofilms (78). The biofilm produced by *P. aeruginosa* was inhibited from plant-derived indole isolated from cruciferous vegetables. The 3-indolyl acetonitrile can reduce polymeric matrix production via virulence-related genes (*pqsE* and *pvcC*) and motility-related genes (z2200, *pilI*, *flhF*, and *motD*) (21). Many plants derived indoles were also shown to significantly decrease the ability of *P. aeruginosa* biofilm formation, such as 3-Indolylacetonitrile, indole-3-carboxyaldehyde, indole-3-acetamide, and isatin (79). Moreover, the formation of biofilm and mature biofilm disruption of gram-positive bacteria namely *S. aureus* and *S. epidermidis* were inhibited by sanguinarine and chelerythrine, which were extracted from Macleya cordata (80). Both compounds inhibited the biofilm formation of S. aureus by affecting some cytoskeleton elements (80).

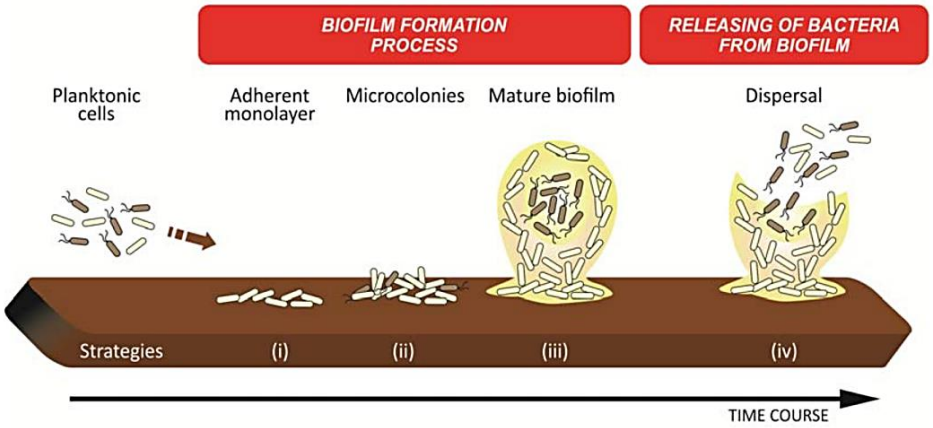

Figure 5 The process of biofilm development
(i) bacterial adhesion on surfaces, (ii) bacterial colonization, (iii) bacterial preform mature biofilms and biofilm exopolysaccharide (EPS) matrix, and the (iv) bacterial releasing from biofilm (64).

3.3 Alkaloids and derivatives against motility activity of bacteria

Bacterial motility is an essential activity of both pathogens and commensals. The activity is an initiation step for bacterial adhesion, colonization and persistence, allowing them to survive under challenging environmental conditions. The movement and attachment of bacteria occur from assembling structural cell-surface elements, including flagellum, fimbriae or pili, capsule and adhesins. Typically, the movement and colonization of bacteria from motile to attachment and reverse occurs from chemotaxis, the capacity to orient along specific chemical gradients. Moreover, the bacteria are able to detect and track the nutrients to find new areas for colonization, which occur from complex interactions between cell-cell signaling, motility, and chemotaxis (81, 82). Two bacterial motility types depend on flagella, including swimming and swarming motility, which are able to encourage the virulence factors production of pathogens via host colonizing and other formations such as biofilm. Bacterial swimming motility uses rotating flagella to move, unlike swarming motility, which occurs as individual cells move in liquid environment conditions. The flagella-independent motility of bacteria is twitching motility, which uses the extension and contract of type IV pili. The different type of bacterial motility without a motor is sliding, which uses surfactants to reduce surface tension for the spreading of bacteria to develop colonies (81-83). The motility of bacteria is essential to facilitate infection, which also involves other virulence factors, even from mutant bacteria strains unable to motile. Bacterial motility is related to host attachment and colonizing, contributing to bacteria invasion, promoting biofilm formation, virulence factor secretions and activation of immune defences (81). Previously, alkaloids and derivatives received from plants have been reported to inhibit the motility of gram-positive and gram-negative bacteria (64). Indole alkaloid reserpine and the piperidine alkaloid piperine at subinhibitory concentrations affected flagellar function via decreased expression of the flagellar gene (*fliC*) and motility genes (*motA* and *motB*), causing a reduction in swimming and swarming motilities of *E. coli* (84). However, genes involved in adhesin genes (*fimA*, *papA*, *uvrY*) of *E. coli* showed up-regulated when treated with both alkaloids, resulting in increased biofilm formation and exhibit antibiotic

resistance (84). The alkaloid derivative, caffeine isolated from the *Trigonella foenum-graecum* L. was reported to decrease the swarming motility of *P. aeruginosa*, determined by short and undefined tendrils of bacterial colony. It decreased the motility by interfering with the QS-regulated virulence factors (69). Moreover, the indole-3- carbinol was reported to the effecting on sliding motility of *S. aureus* (85).

3.4 Alkaloids and derivatives against bacterial toxins

The bacterial toxins are considered a significant factor in microbial virulence and play a critical role in establishing infection, triggering many cellular functions within the host (86-88). They are divided into two categories following the classification of chemicals, including lipopolysaccharides and proteins. The lipopolysaccharides or endotoxins are large chemical molecules of gram-negative bacteria's cell membrane structure, consisting of a lipid and a polysaccharide. The proteins or exotoxins are secreted from gram-negative and gram-positive bacteria and diffuse out of the cell. There are three exotoxin categories, including cytolytic toxins, AB toxins, and superantigens (64). Both gram-negative and gram-positive bacteria produce cytolytic toxins, allowing interaction with host membrane components with penetration into the lipid bilayer, which transforms into a small molecule by changing the molecule structure from toxin oligomerizes into prepore (89). Several studies have been reported about therapeutic strategies to inhibit toxins produced by bacteria using alkaloids and derivatives (64). Indole, the derivatives of 3-indolylacetonitrile have ability to inhibit hemolysis caused by *P. aeruginosa* (79). Moreover, a steroidal alkaloid found in tomatoes, which is tomatidine, can inhibit the hemolytic activity of several *S. aureus* strains through decreased expression of *hld* gene related to lyse red blood cells (22).

3.5 Alkaloids and derivatives inhibit bacterial pigment production.

The bacterial pigments are secondary metabolic products. It can enhance pathogen survival in the host environment and promote bacterial virulence by interfering with the host’s immune clearance mechanism or expressing pro-inflammatory or cytotoxic properties (90). Most pigments produced by gram-positive, namely *S. aureus*, are staphyloxanthin, which is unnecessary for growth but has a role in bacterial virulence. The ability of staphyloxanthin involves the metabolism of isoprenoids, which is similar to the generation of cholesterol (91). Moreover, this pigment was reported to reduce the function of oxygen radicals (O_2 −) and hydrogen peroxide (H_2O_2) generated from the host's immune system (91). The important pigments gram-negative pseudomonas species produce are pyoverdines and pyocyanins, which are necessary for bacterial growth via regulating iron in the environment. Pyoverdine is in a large family of bright green-yellowish pigments synthesized when the bacteria lake iron conditions to obtain iron from other sources like the extracellular medium. Pyoverdine is organized in a large family of bright green-yellowish pigments synthesized when the bacteria are subjected to iron shortage conditions to receive iron from other sources like the extracellular medium. The pyoverdines serve as primary siderophores, which are effective iron (III) transporters and robust iron (III) scavengers (92). Most of the pyocyanin pigment produced from *P. aeruginosa* is blue-green and is referred to as "blue pus.". It is a recognized virulence factor that has endured via evolution (93). Pyocyanin, a secondary metabolite highly generated in low-iron environments and is redox-active, is crucial

for iron metabolism by reducing and liberating it from transferrin. Moreover, the pyocyanin functions contribute to the iron uptake of *P. aeruginosa* and serve as a signaling molecule to control a limited set of genes involved in efflux and redox processes. In addition, pyocyanin produced from *P. aeruginosa* is regulated by the QS system, namely *Las*/*Rhl* and PQS and is affected by *AmpR* (94, 95). Interestingly, pyocyanin has been demonstrated as a broad spectrum for destroying the cell, including suppression of cell respiration and ciliary function, inhibition of epidermal cell development, and release of prostacyclin, as well as disruption of calcium homeostasis (96). Many studies reported that alkaloids and derivatives play a role in decreasing pyocyanin and pyoverdine pigment production. The indole derivative from plants, 3-Indolylacetonitrile, can modulate the QS system of *P. aeruginosa*, consequently reducing the production of pyocyanin and pyoverdine pigment (21). Furthermore, caffeine interfered with the QS-regulated virulence factors of *P. aeruginosa*, resulting in a drop in pyocyanin production in a dose-dependent manner (97).

4. *Pseudomonas aeruginosa*

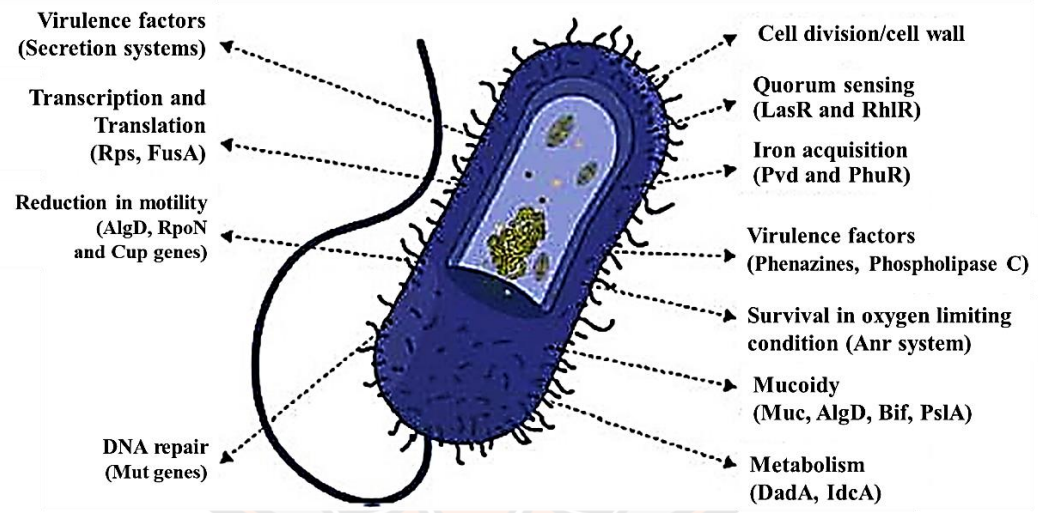

Figure 6 Morphology of *Pseudomonas aeruginosa* (98)

4.1 Taxonomic hierarchy

Kingdom	Bacteria
Subkingdom	Negibacteria
Phylum	Proteobacteria
Class	Gammaproteobacteria
Order	Pseudomonadales
Family	Pseudomonadaceae
Genus	*Pseudomonas*
Species	*Pseudomonas aeruginosa* (99)

4.2 Classification

P. aeruginosa is a gram-negative bacterium, rod-shaped (Figure 6), non-spore-forming, oxidase-positive, and lactose non-fermenters. *P. aeruginosa* is a facultative anaerobe because it can grow in aerobic and anaerobic conditions. It receives energy from anaerobic respiration or fermentation when it lacks oxygen and produces energy from aerobic respiration for cell growth or survival. Motility is provided by a single polar flagella and pili (45). *P. aeruginosa* also grows in moist environments such as soil and water. Moreover, it can be found in various fresh fruits and vegetables (100). *P. aeruginosa* can colonize a wide range of habitats because of its high metabolic versatility and broad adaptation capacity to changing environments (101). Furthermore, it can produce water-soluble pigments, pyocyanin and pyoverdine, which cause blue-green color colonies on the solid medium. Moreover, *P. aeruginosa* produces indophenol oxidase, which separates it from other gram-negative bacteria (making them positive in the "oxidase" test) (6). In addition, some *P. aeruginosa* can produce biofilm, which promotes tolerance and living in adverse conditions. Significantly, it can live in slime-encased biofilms that allow it to survive and replicate within human tissues and medical devices. *P. aeruginosa*, in the form of biofilm, will protect host-produced antibodies and phagocytes, which contribute to the organism's drug resistance. The optimum temperature for *P. aeruginosa* growth is 37°C, but it can also live at temperatures ranging from 4°C to 42°C (102). *Pseudomonads* are the group that requires minimal nutrition for growth. There are only acetate and ammonia as carbon and nitrogen sources that *P. aeruginosa* needs for growth. Moreover, *P. aeruginosa* can use nitrate or nitrite as a terminal electron acceptor and does not operate fermentation, causing it to grow in anaerobic conditions. Without oxygen, *P. aeruginosa* can metabolize arginine and pyruvate by substrate-level phosphorylation pathways for growth (103). Therefore, from the reason above, the adaptable dietary requirements of *P. aeruginosa* result in difficulty eliminating from various areas that become contaminated. They are permitted growth in various environments, even in inappropriate conditions, such as operating rooms, hospital rooms, clinics, and medical equipment (6).

4.3 Pathogenesis

P. aeruginosa has several virulence factors and produces many factors that may aid the virulence and pathogenesis of the host cell (Table 1) (98, 104). All strains can produce endotoxin, a significant virulence factor in bacteremia and septic shock. Toxin A, a diphtheria-like exotoxin, is produced by most isolated strains. Basined *P. aeruginosa* is one of the opportunistic pathogen infections in hospitalized patients and can produce many virulence factors. Moreover, *P. aeruginosa,* which presents biofilms, can survive and grow within human tissues and medical equipment when biofilms are present. Because biofilms protect the cell from the invasion of antibodies and phagocytes, resulting in antibiotic resistance of this organism. Therefore, *P. aeruginosa* can infect various site organisms in patients or even humans with weakened immune systems (Figure 7). Consequently, infections in patients from medical equipment are not uncommon, such as corneal infections following eye surgery or injury, urinary tract infections on catheters or in irrigating solutions, respiratory tract infections, or necrotizing pneumonia following the use of contaminated respirators, patients suffering from a severe wound, and children with

middle ear infections. After treatment, *P. aeruginosa* infection in hospitalized patients may cause many diseases. For example, cardiac surgery and lumbar puncture may result in endocarditis and meningitis, respectively, and are also associated with some diarrheal disease episodes. Furthermore, *P. aeruginosa* most infects and colonizes patients with cystic fibrosis patients, causing them to die ultimately. *P. aeruginosa* infection is associated with a 50% overall mortality rate of patients.

Table 1 Virulence factors of *P. aeruginosa* strains

virulence factors	Action to cell host	Reference
Flagella	Invasion, mobility, and adhesion	(105)
Pili	Adhesion and transfer of secretions	(106, 107)
Exopolysaccharides	Pathogen persistence and adhesion	(108, 109)
Lipopolysaccharide	Endotoxin; inflammatory agent, adherence and biofilm formation	(108, 109)
Elastase	- Elastin degradation, membranes disruption - Monocyte chemotaxis and complement proteins degradation	(110)
Lipase A	Participation in degradation	(111)
Phospholipase C	- Disruption of lung surfactant - Hydrolysis of lecithin	(112, 113)
Proteolytic	Degrades complement factors, host tissue, and destroy immunity of host (plasmin, IgG, fibrinogen)	(110, 114, 115)
Pigments	Inhibit lymphocyte proliferation via neutrophils apoptosis	(116-118)
Exotoxin A	Interrupt protein synthesis of eukaryotes cell	(119)
Exoenzyme S	Antiphagocytic factor	(119, 120)
Biofilm	- Protection cells from antibiotics and immune system effectors - Reduce the permeability of antibodies (Ab), antibiotics, and biocides into the cell	(121, 122)

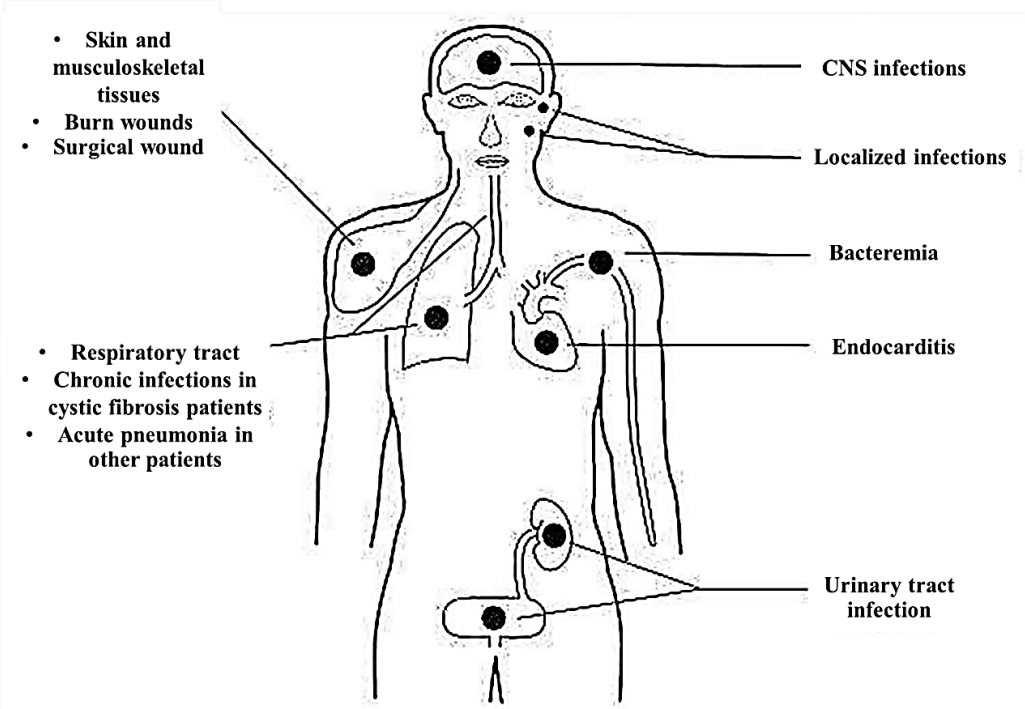

Figure 7 Various sites infection of *P. aeruginosa* (104)

4.4 Antibiotic resistance mechanisms of *P. aeruginosa*

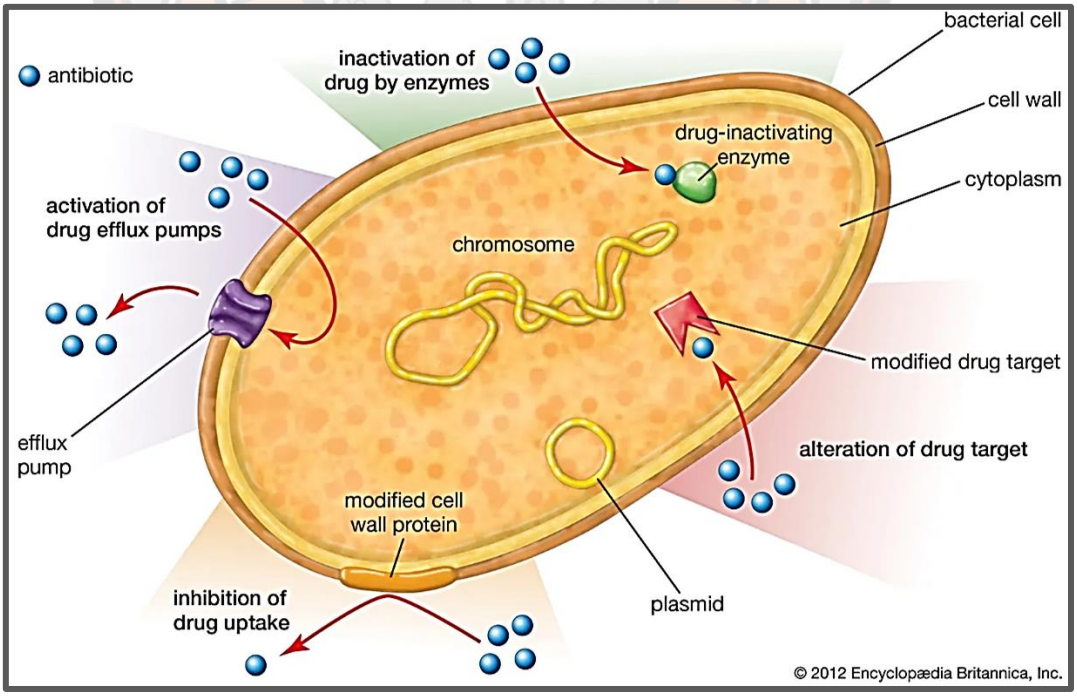

Figure 8 Examples of antibiotic resistance mechanisms of microorganisms (123)

4.4.1 Intrinsic antibiotic resistance

Reducing the specific antibiotic efficacy of *P. aeruginosa* strains through inherent structural or functional characteristics is intrinsic antibiotic resistance (124). Restriction of outer membrane permeability, pumping antibiotics out of the cell by efflux systems, and production of antibiotic-inactivating enzymes are the common intrinsic antibiotic resistance mechanisms of *P. aeruginosa* strains (125).

4.1.1.1 Restriction of outer membrane permeability

The outer membrane structure of *P. aeruginosa* consists of peptidoglycan and cell membrane. The outer membrane plays a vital role in protecting the bacteria from phagocytosis of the host cell and cell survival. Furthermore, The outer membrane structure of *P. aeruginosa* acts as a selective barrier function to prevent antibiotic penetration, which has characteristics of an asymmetric bilayer of phospholipid and lipopolysaccharides (LPS), packed with porins that form ß -barrel protein channels (126). The porin family can be divided into four classes: specific porins, which have specialized binding sites for a particular set of molecules; non-specific porins, which allow the small hydrophilic molecules that diffuse slowly; gated porins, which are ion-regulated outer membrane proteins involved in ion complex absorption; and efflux porins, which are important components of efflux pumps that pump the toxic or antibiotics out of the cell (127). In *P. aeruginosa*, the OprF protein is the major non-specific porin; specific porins include OprB, OprD, OprE, OprO and OprP; the class of gated porins consists of OprC and OprH, and OprM, OprN, and OprJ belong to the class of efflux porins (128). Bouffartigues *et al*. (2015) (129) reported that OprF protein is related to the upregulation of bis-(3′-5′)-cyclic dimeric guanosine monophosphate (c-di-GMP), which is an essential substance for controlling biofilm formation. Therefore, overexpression of OprF in *P. aeruginosa* may result in antibiotic resistance. Moreover, Li *et al.* (2012) (130) reported that carbapenems have binding sites with OprD protein, which involves increased antibiotic uptake. Therefore, the absence of OprD in *P. aeruginosa* reduces antibiotic uptake and increases the resistance to carbapenems (imipenem and meropenem) (131).

4.1.1.2 Efflux pump systems

Efflux pumps are transmembrane proteins that penetrate the bacterial cell membrane. It significantly pumps toxic compounds or antibiotics out of the cell (132). The RND family is one of the efflux pump families of *P. aeruginosa* that plays a crucial role in antibiotic resistance. The structure of the RND family consists of three components: cytoplasmic membrane transporters, periplasmic linker proteins, and outer membrane porin channel proteins. The three components of the RND protein work together to pump toxic compounds or antibiotics from the periplasmic space and cytosol out of the cell. The four pumps of the RND family include MexAB-OprM, MexCD-OprJ, MexEF-OprN, and MexXY-OprM, which have a role in contributing to antibiotic resistance (133). The wild-type *P. aeruginosa* has been reported to find expression of MexAB-OprM pump. This pump resisted several antibiotics such as tetracycline, chloramphenicol, quinolones, novobiocin, macrolides, trimethoprim, ß-lactams and ß-lactamase inhibitors (134-137).

4.1.1.3 Inactivating antibiotics by enzymes

One of the effective mechanisms of intrinsic resistance in bacteria is the production of enzymes to inactivate antibiotics' activity by destroying or modifying them. ß-lactamases and aminoglycoside-modifying enzymes are enzymes commonly produced by *P. aeruginosa* hydrolysis antibiotics at the amides bond of the ß-lactam ring and esters bonds, which are chemical bonds of antibiotics (138-140). Moreover, the inducible *ampC* gene in *P. aeruginosa* encodes the hydrolytic enzyme-lactamase. This enzyme can destroy the amide bond of the ß-lactam ring, leading to the inactivation of ß-lactam antibiotic function (138). In addition, ß-lactamases can be divided into four classes based on their amino acid sequences: A, B, C, and D (141). *P. aeruginosa* produces class C of ß-lactamase, an anti-pseudomonal cephalosporin (142). Furthermore, extended-spectrum-ß-lactamases (ESBLs) enzymes produced from some *P. aeruginosa* are able to be broader and more resistant to the majority of ß-lactam antibiotics (143). *P. aeruginosa* shows resistance to aminoglycoside, an antibiotic commonly used to treat *P. aeruginosa* infections. Moreover, aminoglycoside resistance of *P. aeruginosa* may occur from various contributing mechanisms, such as decreased cell membrane permeability, enhanced efflux, ribosomal changes, and enzyme modification. However, the most crucial mechanism in resistance to aminoglycoside is the modification of the molecular structure of aminoglycoside (amino and glycoside groups) by enzymes (144).

4.4.2 Acquired antibiotic resistance

The bacteria that develop antibiotic resistance via mutation or horizontal gene transfer is referred to as acquired antibiotic resistance (145).

4.4.2.1 Resistance to antibiotics by mutations

Overexpression of efflux pumps, production of enzymes to inactivate antibiotics, lowering expression of membrane proteins controlling permeability, and modification of target sites in bacteria are all mechanisms that can cause reduced antibiotic effectiveness. These factors contribute to bacteria's ability to survive in the presence of antibiotic compounds. Increasing mutation frequencies in *P. aeruginosa* occur when the DNA oxidative repair mechanism is inactivated. It results in overexpression of the MexCD-OprJ efflux pump and increased lactamase production (146). Natural mutations can alter the exhibition and function of porin, reducing bacterial membrane permeability and enhancing antibiotic resistance. For example, in *P. aeruginosa*, a lack of OprD grants a significant level of carbapenem resistance, particularly to imipenem. Moreover, the overexpression of efflux pumps has decreased susceptibility to antibiotics. For instance, overexpression of efflux pump, which occurred from transcriptional regulators gene mutations: *mexR*, *nalB nalC* or *nalD* of MexAB-OprM, *mexZ* of MexXY-OPrM, and *nfxB* of MexCD-OprJ increased the bacterium resistance to chloramphenicol, macrolides, novobiocin, quinolones, tetracycline, and cephems, but exhibit high susceptibility to many ß-lactams (147-150). Moreover, chloramphenicol, quinolones, trimethoprim, and carbapenems increase resistance by strains with mutations in *nfxC* (151-153). Antibiotic resistance can occur from mutational modifications of the target sites in *P. aeruginosa*. For example, mutations in genes encoding DNA gyrase (*gyrA* and *gyrB*) and/or topoisomerase IV (*parC* and *parE*) at the drug target sites can

prevent binding by quinolones. Therefore, these gene mutations reduce susceptibility of *P. aeruginosa* to quinolones (154). The overexpression of antibiotic-inactivating enzymes in *P. aeruginosa* is also characteristic of the acquired resistance mutation mechanism (145). For example, the *ampC* gene encodes ß-lactamases, and the *ampD* gene acts as a regulator of *ampC* expression and encodes a cytosolic N-acetyl-anhydromuramil-l-alanine amidase, so inactivating mutations in *ampD* gene cause overproduction of ß-lactamases (155).

4.4.2.2 Resistance to antibiotics by resistance gene acquisition

The same or different bacterial species can transfer antibiotic-resistance genes via horizontal gene transfer, which is carried on plasmids, transposons, integrons, and prophages. Transformation, transduction and conjugation are the significant mechanisms of horizontal gene transfer (156). Direct physical contact to transfer DNA from a donor cell to a recipient cell is the conjugation process. Bacteriophages transfer DNA from one bacterium to another, called transduction. Transformation is a process of genetic alteration in bacteria by direct uptake of free DNA fragments released into the environment and combined into their genome through the cell membrane (5). Diffusion of antibiotic resistance among *P. aeruginosa* strains may be caused by the acquisition of antibiotic resistance genes. The imipenemase (IMP), Verona integron-encoded metallo-ß-lactamase (VIM), sao-paulo metallo-ß-lactamase (SPM), Germany imipenemase (GIM), new delhi metallo-ß-lactamase (NDM) and Florence imipenemase (FIM) are antibiotic resistance proteins that are encoded from genes in *P. aeruginosa*. These genes are carried on integron and class 1 integron, which are transferred via horizontal gene transfer mechanisms (5). Fluoroquinolone is one of the antibiotic classes resisted by bacteria transfer of plasmids that carry resistance genes. Mutations or alter the drug target sites of fluoroquinolones (DNA gyrase and topoisomerase IV) or even reduce the membrane's permeability or transfer of plasmids into the cell of bacteria, causing the bacteria to develop resistance to fluoroquinolones (7, 157-159).

4.4.3 Adaptive antibiotic resistance

Adaptive antibiotic resistance in bacteria is induced by transitory changes in the gene and/or protein expression, which respond to environmental stimuli. Then, it can be reversible when the stimulus is removed, resulting in antibiotic resistance the following time. The best-characterized mechanisms of adaptive resistance of *P. aeruginosa* are biofilm formation and the building of persister cells. Consequently, patients with cystic fibrosis may experience persistent infection (160).

4.4.3.1 Resistance resulting from biofilm formation

A biofilm is matrices of extracellular polymeric substances (EPSs) that bacteria produce, including exopolysaccharides, proteins, metabolites, and extracellular DNA (eDNA) (161). Bacteria biofilm formation helps bacteria colonize living and non-living surfaces as well as enabling expansion and growth in adverse conditions. Microbes that can produce biofilms are less sensitive to antimicrobial agents and have fewer responses to host immune than microbial unable to produce. One of the essential characteristics of microbial biofilms is that bacteria may tolerate even high dosages of antibiotics. Therefore, a high antibiotic dose may be needed to destroy the bacteria biofilm. The general biofilm mechanisms for protecting bacteria

from antibiotic attack or immunity of host cells are avoidance permeability of antibiotics that slow growth of biofilm cells, adaptation to the stress response, and persister cell differentiation (162). The biofilm-forming properties of *P. aeruginosa* make it impervious for the antibiotic to penetrate through the biofilm layer or little through and evade the immune response, which causes the treatment to be unsuccessful and may cause the bacteria to become antibiotic-resistant (162). The matrix components for the biofilm formation of many *P. aeruginosa* strains are exopolysaccharides. They synthesize three exopolysaccharides: Pel, Psl, and alginate (163-165). Furthermore, eDNA functions as a vital matrix component of the biofilm formation of *P. aeruginosa* strains (166, 167). In addition, rhamnolipids have been shown to have a role in the production of microcolonies in *P. aeruginosa* biofilms (168). Overexpression of biofilm matrix in *P. aeruginosa* isolated from the clinical show significantly protects cells against antimicrobial treatment (169). Alginate-overproducing *mucA* mutant of *P. aeruginosa* demonstrated significantly higher increased antibiotic tolerance than wild-type. Similarly, overproducing Pel and Psl exopolysaccharide of *wspF* and *yfiR P. aeruginosa* mutants leads to significantly higher antibiotic tolerance than wild type. Overproduction of biofilm matrix components improved *P. aeruginosa* aggregates' resistance to tobramycin and ciprofloxacin (170).

4.4.3.2 Antibiotic resistance of persister cells

Persister cells are bacteria-produced cells that build a biofilm. The persister cells are organisms that are not mutants but are tolerant to high concentrations of antibiotics and avoid destruction from the immune system. As a result, the persister cells can grow and spread, causing recurring infections in patients and reducing the effectiveness of treatment (171). The *P. aeruginosa* isolated from cystic fibrosis patients typically shows higher levels of persister cells than wild-type strains, resulting in *P. aeruginosa* high levels of resistance to antibiotics and a greater propensity to become multidrug-resistant (172).

5. Omic- Technology

'Omic' technologies are the new "global" techniques for measuring cellular molecules, such as RNA, proteins, and intermediary metabolites, based on their capability to characterize all or most members of the molecules family in a single examination (Figure 9) (173). The terms "ome" and "omics" are derived from the "ome" suffix, which has been added to a variety of existing biological terms such as "genome," "proteome," "transcriptome," and "metabolome" to create names for fields of study. The "omics" technologies are high-throughput technologies that can investigate and simultaneously increase the number of proteins/genes. Also, the technologies have the potential to detect expression profiles of genes or proteins to reveal the function of some complicated mixture that results in complex effects. Moreover, identifying unknown targets via all gene products present in biological samples is also the primary goal of "omic" technology. The technology helps understand biological processes, discover biomarkers and identify signaling molecules involved with cell growth, cell death, and cellular metabolism. Therefore, using these new technologies, the activity of functional biochemical pathways and differences in the genetic sequence of each species and among individuals that had

previously been unrealizable can be investigated. Furthermore, "omic" technology might have a potential role in diagnosing and treating diseases more accurately in the future.

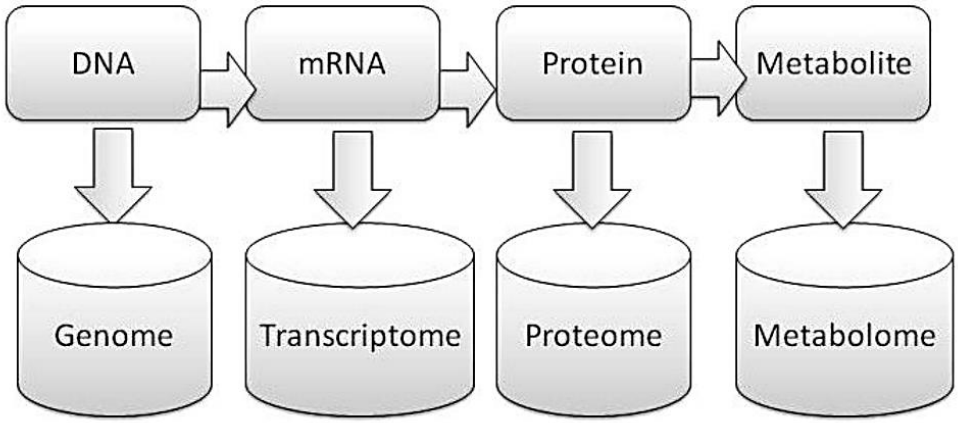

Figure 9 The "ome" study types include genome, proteome, transcriptome and metabolome
(173)

5.1 Transcriptomics technologies

Transcriptomics technologies are the methods used to analyze the transcriptome of an organism, expression of an organism's genes. All informational content of an organism are encoded in its genome and expressed via transcription. In this situation, mRNA operates as a temporary intermediary molecule in the information network, while noncoding RNAs carry out additional, different roles. A transcriptome records a moment in time when all the transcripts in a cell were present. The transcriptomic analysis can reveal information about an organism's biology and the function of a regulated gene by measuring the organism's gene expression in the time points or different conditions. Additionally, it can infer the roles of previously unannotated genes. Moreover, transcriptome analysis can explain how gene expression changes in different organisms and helps us understand how instruments contribute to human disease. Gene expression analysis identifies broad coordinated trends that more targeted assays cannot discern. Extensively, measuring RNA transcripts can be accomplished through either individual transcript sequencing (ESTs or RNA-Seq) or transcript hybridization to nucleotide probes ordered array (microarrays) (174).

5.1.1 RNA-Sequencing (RNA-Seq)

RNA-Seq refers to the combination technique of high-throughput sequencing and computational analysis to identify and count the number of transcripts present in an RNA extract (175). More than 10^9 short DNA sequences can be produced by RNA-Seq method, which must be aligned with reference genomes made up of millions to billions of base pairs. Sequence generation depends on the sequencing technique employed; the length of the produced nucleotide sequences can range from 30 bp to over 10,000 bp, but they are frequently around 100 bp. RNA-Seq takes advantage of transcriptome deep sampling with many short fragments received from the RNA transcript. These enable quantification of the original transcriptome by aligning reads to a reference genome (de novo assembly) (176). Moreover, the

theoretical maximum quantification in RNA-Seq is infinite, and the background signal for 100 bp reads in nonrepetitive areas is relatively low (175). In addition, at a particular time, RNA-Seq can specify the genes within a genome or which genes are active. The read quantification can also simulate the accurate level of gene expression. Therefore, the advancement of high-throughput sequencing technologies has significantly impacted the approach (175).

5.1.2 Microarray

Microarrays consist of probes, which are short nucleotide oligomers that are arranged in an ordered pattern on a solid substrate like glass (177). The hybridisation of these probes with transcripts labelled fluorescent is used to investigate the abundance of transcripts. The transcript abundance is detected from the intensity of fluorescence at each probe location on the array (178). Before array transcript abundance, some information of interest organism must first know to generate the probes, including annotated genome sequence or ESTs library. The data of transcript analysis by microarray is reported as images of high resolution, which feature detection and spectral analysis necessary. The size of raw image files is about 750 MB, whereas files around 60 MB are the processed intensities. The intron and exon structure can be revealed by a number of short probes matching a single transcript, necessitating statistical models to validate the signal.

5.1.3. Applications

5.1.3.1 Diagnostics and profiling of disease

In several fields of biological research, including illness detection and profiling, transcriptomic techniques have seen widespread application (175). Using RNA-Seq techniques allowed transcriptional initiation sites to be identified on a large scale, and unique splicing changes and alternate promoter usage were discovered. These regulatory components have a significant role in human disease; recognizing such variations is essential for adequately interpreting disease-association research (179). To further understanding of disease causative variations, RNA-Seq can also detect allele-specific expression, gene fusions, and single nucleotide polymorphisms (SNP) associated with disease (180). Retrotransposons are transposable elements that multiply within eukaryotic organisms' genomes by reverse transcription. The transcription of endogenous retrotransposons may affect the transcription of nearby genes through various epigenetic pathways and result in disease, which RNA-Seq can reveal (181). Similarly, the possibility for using RNA-Seq to study immune-related disease is fast growing due to the capability to separate populations of immune cells and sequence patient-derived T cell and B cell receptor repertoires (182).

5.1.3.2 Responses to environment

Transcriptomics can uncover genes and pathways identification that the organism responds to and retaliate the stresses of biotic and abiotic environments. Transcriptomics' nontargeted approach enables the discovery of new transcriptional networks in complicated networks. For example, during the biofilm formation of *Candida albicans*, the gene expression was investigated to understand a coregulated group of genes essential for producing and maintaining biofilms (183). Moreover, the

drug resistance mechanisms of pathogenic bacteria are able to be provided from transcriptomic profiling (184).

5.1.3.3 Noncoding RNA

Transcriptomics is most frequently used to study a cell's mRNA content. However, the same methods also apply to non-coding RNAs that perform direct tasks rather than being translated into proteins, such as those involved in protein translation, DNA replication, RNA splicing, and transcriptional regulation (185, 186). Numerous of these non-coding RNAs impact disease states, such as cancer, cardiovascular, and neurological disorders (187).

5.1.3.4 Transcriptome databases

Studies on transcriptomics produce much data that could be used for purposes far beyond the experiments themselves. As a result, raw or processed data may be published into public databases, such as National Center for Biotechnology Information (NCBI) or noncode.org, to ensure their usefulness for the larger scientific community.

5.1.3.5 Gene ontology (GO)

Gene Ontology (GO) is the most extensive database that describes the knowledge of gene functions and products, including proteins and noncoding RNAs. Large-scale molecular biology and genetics investigations in biomedical research can be computationally analyzed based on this knowledge, which is both machine- and human-readable. Usually, ontologies comprise several classes, terms, or concepts involved in their relations. The "molecular biology domain" is the fundamental framework for GO, and it uses three categories of functional features to define gene function, including Molecular function (MF), Cellular component (CC), and Biological process (BP). The MF describes the molecular functions carried out by a gene product. The CC exhibit the locations where MFs operate with cellular structures. The BP describes a "biological program" comprising molecular activities acting in concert to achieve a particular outcome; this program can be at the cellular or organism levels of multicellular organisms (188).

CHAPTER III

METHODOLOGY

In this study the experiments were divided into three main parts as shown in Figure 10. The first part aimed to characterize the properties of hydroquinine and is further divided into four subsections. Firstly, the antimicrobial susceptibility test of all bacteria in this study (reference strains) was checked using methods that following the Clinical and Laboratory Standards Institute (CLSI) guideline M07-A9 (189). Secondly, the antibacterial activity of hydroquinine against both gram-negative and gram-positive bacteria was determined from minimal inhibitory concentration (MIC) and minimal bactericidal concentration (MBC) by broth microdilution method. Next, the bactericidal effect of hydroquinine was examined against *P. aeruginosa* strains using a time-kill assay. Lastly, synergistic effects of hydroquinine with specific antibiotics were observed against MDR *P. aeruginosa* ATCC BAA 2108 by checkerboard assay. The synergistic effects of hydroquinine were determined from the calculation fractional inhibitory concentration index (FICI) value (190). In the second part, global transcriptional profiles of *P. aeruginosa* ATCC 27853 were determined by transcriptomic analysis with and without treatment with ½ MIC of hydroquinine for 1 h. In the last part, we validated the observed up-regulation of RND-type efflux pump genes and down-regulated virulence factor genes to uncover the mechanisms of action of hydroquinine against *P. aeruginosa*. Both genotypic and phenotypic analysis was performed to characterize the mechanism of hydroquinine action.

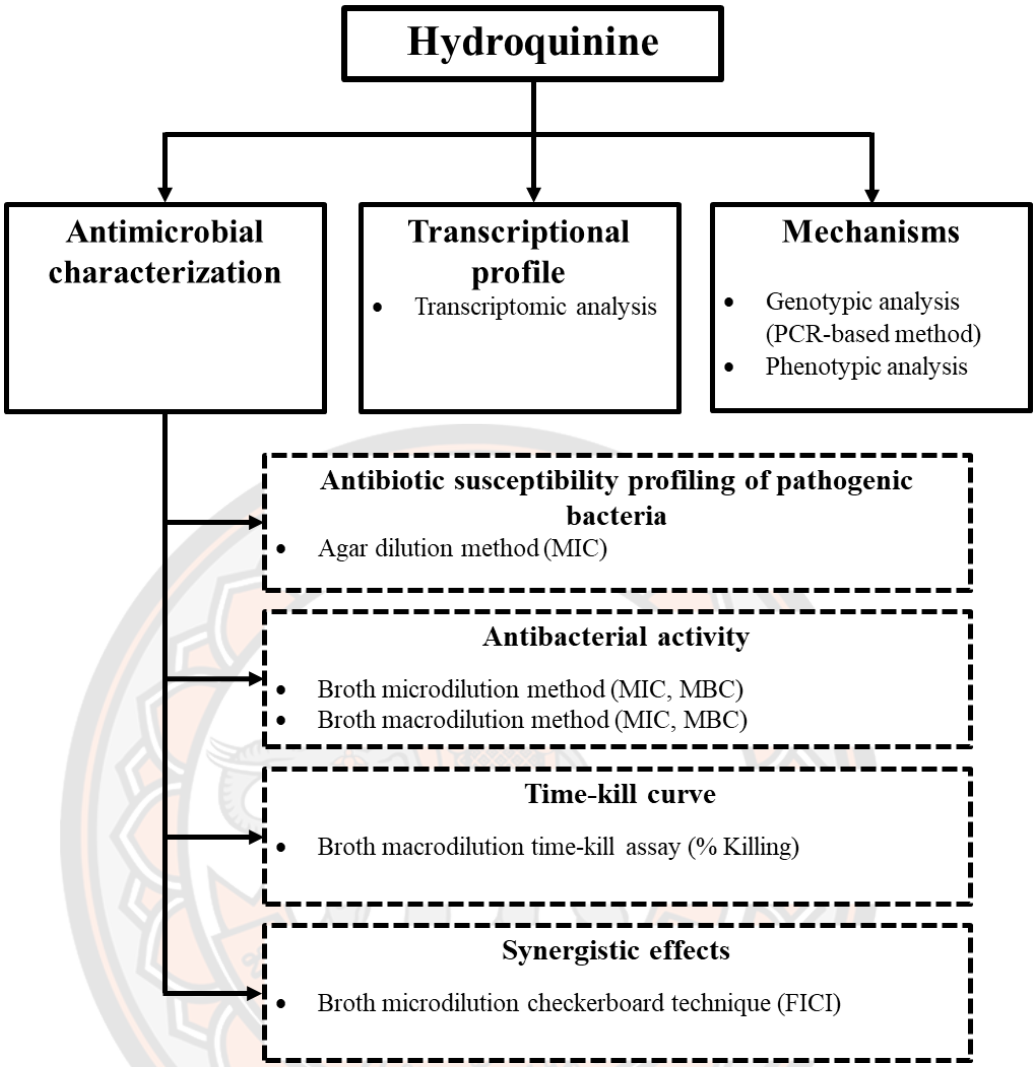

Figure 10 Conceptual framework of the study

1. Microorganism cultivation

The bacteria used in this study purchased from American Type Culture Collection (ATCC) strains consist of *Pseudomonas aeruginosa* ATCC 27853, *P. aeruginosa* ATCC BAA-2108, *Staphylococcus aureus* ATCC 29213, *S. aureus* ATCC 25923, *Escherichia coli* ATCC 25922, *E. coli* ATCC 2452, *Klebsiella pneumoniae* ATCC 1705 and *Enterobacter cloacae* ATCC 2341. Clinical isolates (PA.CI) of *P. aeruginosa* strains were received from hospitalized patients at Kamphaeng Phet Hospital, Kamphaeng Phet, Thailand in 2022. At least three to five similar colonies of all bacteria tested in this study were inoculated on tryptone soya agar (TSA) by streak plate technique and culture at 35±2°C for 18-24 h. In the case of subculture, bacterial colonies were re-streaked on the appropriate media and then incubated at 35±2°C for 18–24 h. Before using inoculum in each experiment, the turbidity of inoculum was adjusted in exponential growth phases to achieve turbidity equivalent to a 0.5 McFarland standard ($1–2\times10^8$ CFU/mL).

2. Preparation antibiotics and hydroquinine

The antibiotics used in this study were dissolved in sterile deionized water or proper solvents recommended by CLSI standard (191). Hydroquinine was prepared by dissolving with 50% DMSO and Tween 80. After that, the concentration of hydroquinine was diluted in Mueller-Hinton broth (MHB) to achieve the required initial concentration.

3. Characterizing the antimicrobial properties of hydroquinine

3.1 Antibiotic susceptibility teat

The antibiotic susceptibility testing of all bacteria tested in this study was re-evaluated by agar dilution method with Vitek®2 compact mechanical device. The principle of the Vitek®2 compact automatic instrument for susceptibility testing is to measure the turbidity value of the change that occurs from bacteria growth in the test well compared with the initial value. Briefly, 40 µL of inoculum (0.5 McFarland) was added to the specific bacteria group Vitek®2 Identification test card, which has an antibiotic coat. The card test was measured every 15 min for 18 h at 35.5±1°C by the wavelength of 660 nm in each well at 16 different positions and repeated triplicate. The MIC values were reported as results of this experiment. The antibiotics tested in this study were selected from some antibiotics (group A–C) according to the CLSI M100 recommendation (192) shown in Table 2 (191).

Table 2 Types of antibiotics to evaluate antibiotic susceptibility test (AST)

Strains	Antibiotic groups			Mode of action to inhibit bacteria
	A	**B**	**C**	
P. aeruginosa	Ceftazidime (193)	Cefoperazone (194), Cefepime (195), Doripenem, Imipenem, Meropenem (196)	-	cell wall synthesis
		Amikacin (197), and Tigecycline (198)		protein synthesis
		Ciprofloxacin (199), and Levofloxacin (200)		DNA replication
K. pneumoniae *E. cloacae* *E. coli*	Ceftazidime (193)	Amoxicillin (201), Piperacillin (202), Ceftriaxone (203), Cefoperazone (194), Doripenem, Ertapenem, Imipenem, and Meropenem (196)		cell wall synthesis
		Amikacin (197), Tigecycline (198)		protein synthesis
		Ciprofloxacin (199), and Levofloxacin (200)		DNA replication
S. aureus	Oxacillin (204)	Vancomycin (205)		cell wall synthesis
	Erythromycin (206)	Linezolid and Tetracycline (207)	Gentamicin (208)	protein synthesis
	Trimethoprim (209)	Rifampicin (210), and Ciprofloxacin (199)	Moxifloxacin (211)	DNA replication

3.2 Antibacterial activity assays

The antibacterial activity of hydroquinine against bacteria tested in this study was determined from MIC and MBC. It was tested by broth macrodilution and microdilution assay in accordance with the CLSI guideline M07-A9 (189). All tests were performed in triplicate experiments. Hydroquinine was prepared by dissolving with 50% DMSO and Tween 80. After that, the concentration of hydroquinine was diluted in Mueller-Hinton broth (MHB) to achieve the initial concentration of 20 mg/mL. Bacterial inoculum preparation was performed by inoculating at least the similar three to five colonies of the bacteria into 2 mL of tryptose soya broth (TSB) and incubated at 35±2°C for 2–6 h. The turbidity of the bacterial culture was adjusted with sterilized normal saline solution (NSS) to achieve turbidity of about 0.5 McFarland standard (1–2×10^8 CFU/mL).

3.2.1 Determination of minimal inhibitory concentration (MIC) by broth microdilution assay

To investigate the antibacterial activity of hydroquinine, all microdilution methods were conducted using microplates in the 96-well platform. Briefly, 100 µL of MHB was added to each well. A serial two-fold dilution of hydroquinine concentration was performed by adding hydroquinine at a concentration of 20 mg/mL (100 µL) into the first well and mixing. Then, 100 µL of the mixture in the first well was transferred to the second well and continued to make the two-fold dilution series until the last well. The final concentrations of hydroquinine were between 0.02 and 10 mg/mL. Meanwhile, ciprofloxacin (CIP) stock solution was used as the quality control (QC). It was performed a series of two-fold dilutions (CIP concentration range from 0.0002 to 2 µg/mL), like the above-mentioned processes. *P. aeruginosa* ATCC 27853 and *S. aureus* ATCC 29213 were tested as QC strains. Then, 10 µL of inoculum was added in each well to achieve the final inoculum concentration of approximately 5×10^4 CFU/well. Moreover, the well-contained MHB with the serial dilution of hydroquinine concentration without inoculum represented the blank control. At the same time, the well-contained MHB with inoculum was the growth control. The MHB was mixed with 50% v/v DMSO and Tween 80 as vehicle control and only MHB as sterility control. The 96-well plate was incubated at 35±2°C for 16–20 h. The lowest concentration of hydroquinine inhibited the growth of the bacterial strains performed by unaided eyes. The results of this experiment were recorded as MIC of hydroquinine. The MIC of QC ranges for the bacteria reference strain was shown in the CLSI document M100-S (192).

3.2.2 Determination of minimal inhibitory concentration (MIC) by broth macrodilution assay

In order to investigate the antibacterial activity of hydroquinine, all macrodilution method was performed using a test tube. Briefly, 1 mL of MHB was added to each tube. A serial two-fold dilution of hydroquinine concentration was performed by adding hydroquinine at a concentration of 20 mg/mL (1 mL) into the first tube and mixing. Then, 1 mL of the mixture in the first tube was transferred to the second tube and continued to make the two-fold dilution series until the last tube. The final concentrations of hydroquinine were between 0.02 and 10 mg/mL. Then, 1 mL of inoculum (1×10^6 CFU/mL) was added into each tube to achieve the final

inoculum concentration of approximately 5×10^5 CFU/mL. Moreover, the tube containing MHB with hydroquinine without inoculum represented the blank control. At the same time, the tube containing MHB with inoculum was referred as the growth control. The MHB was mixed with DMSO and Tween 80 as vehicle control and only MHB as sterility control. The tube was incubated at 35±2°C for 16–20 h. The lowest concentration of hydroquinine inhibited the growth of the bacteria strains performed by unaided eyes. The results of this experiment were recorded as MIC of hydroquinine. The MIC of QC ranges for the bacteria reference strain was shown in the CLSI document M100-S (192).

3.2.3 Determination of minimal bactericidal concentration (MBC)

The MBC of hydroquinine were determined by pipetting 10 µL of each sample that received from MIC tested on MHA plate. The plate was then incubated at 35±2°C for 24 h to observe the number of colonies. The MBC normally means the 99.99% killing of the original inoculum. The results of this experiment were recorded as MBCs of hydroquinine.

3.3 Time-kill of hydroquinine against *P. aeruginosa* ATCC 27853 strains

Time-kill assay is the common method for investigating the bactericidal effect. It can show both a concentration-dependent manner and a time-dependent manner of bactericidal effect between the antimicrobial agents and the microbial strains (212). After knowing MIC and MBC values of hydroquinine against *P. aeruginosa* strains from antibacterial assays mentioned above, the concentrations of hydroquinine were prepared by making a serial two-fold dilution. The concentration of hydroquinine required 4×MIC, 2×MIC, MIC, MIC/2, and MIC/4 values.

For preparation of the bacterial inoculum, one colony of *P. aeruginosa* was inoculated into 2 mL of TSB and incubated at 35±2°C for 2–6 h. The turbidity of inoculum was adjusted with sterilized normal saline solution (NSS) to achieve turbidity of about 0.5 McFarland standard ($1–2\times10^8$ CFU/mL). The inoculum added to each flask has a final inoculum concentration of approximately 5×10^5 CFU/mL.

To evaluate the bactericidal effect of hydroquinine, the time-dependent or concentration-dependent bactericidal effect was shown by broth macrodilution time-kill assay. Briefly, the final concentrations of hydroquinine at 4×MIC, 2×MIC, MIC, MIC/2, and MIC/4 were prepared with 30 mL of MHB in each flask. The sterility control contained only MHB without hydroquinine and microorganisms. At the same time, the growth control contained MHB with the microorganisms tested. The inoculum at 3 mL was then added to each flask except the sterility control. The sample was incubated at 35±2°C, and 1 mL of each culture was taken every 2 h until 8 h to do the serially diluted in phosphate-buffered saline (PBS). The dilutions were spread on MHA and incubated at 35±2°C for 16–20 h.

The bactericidal effect of hydroquinine was shown as the percentage of killing (%killing). The number of living cells of each flask was counted as colony-forming unit (CFU) in order to calculate the percentage of killing compared to the growth control. The percentage of killing cells was calculated from the formula (2) (213, 214) The definition of “bactericidal” effect normally means the 90% killing for 6 h, equivalent to 99.9% killing of lethality for 24 h of the original inoculum (215). All tests performed in the triplicate experiments.

$$\text{killing cells\%} = [1 - (\text{CFU sample}/\text{CFU control})] \times 100\% \qquad (2)$$

3.4 *In vitro* evaluation of synergy using the checkerboard method

This experiment focused only on the MDR *P. aeruginosa* strain because it has been reported as one of the representative bacteria that is the opportunistic and MDR pathogen in hospitalized patients. Moreover, its serious limitation in effective therapeutic options because of its remarkable capacity to resist antibiotics (5).

By modulating antibiotic resistance in MDR *P. aeruginosa* with hydroquinine, *P. aeruginosa* ATCC BAA-2108 strain was selected to study. The broth microdilution checkerboard technique was used to assess the synergistic effect of hydroquinine plus antibiotics, which followed and modified the method from Fratini *et al*. (2017) and Cheypratub *et al*. (2018) (216, 217). The synergy was determined by the Fractional Inhibitory Concentration (FIC) index value according to the FICI equation (1) (216, 217).

$$FICI = (MIC_{HQ + antibiotic} / MIC_{HQ}) + (MIC_{antibiotic + HQ} / MIC_{antibiotic}) \quad (1)$$

The antibiotics used in this study were selected based on some antimicrobial resistance reported by MDR *P*. *aeruginosa*, according to the ATCC (218). They consisted of gentamicin (GT), imipenem (IM), and ampicillin (AP). The final concentrations of antibiotics in combination ranged as 2 × MIC, MIC, MIC/2, MIC/4, MIC/8, MIC/16, MIC/32, and MIC/64 for each hydroquinine concentration. All antibiotics were dissolved in sterile deionized water. Hydroquinine was dissolved with 50% DMSO and Tween 80. The concentration of hydroquinine was then diluted in MHB to achieve the required initial concentration.

The MIC of hydroquinine and antibiotics were determined before starting this experiment. The MIC values of hydroquinine were received from antibacterial activity assays and antibiotics followed by CLSI M100 guidelines (192). Briefly, 100 µL of MHB was added into the first well; in contrast, 75 µL of MHB was added into the second to 10 well in 96-well microtiter plates, then, added 50 µL of (4×) antibiotics into the first well and mixed. After that, 75 µL of the mixture in the first well was transferred to the second well and continued to make the series of two-fold dilution until the 8 well. 25 µL of 4x hydroquinine concentration was then added to each row. The final concentrations of hydroquinine were 2×MIC, MIC, MIC/2, MIC/4, MIC/8, MIC/16, MIC/32, and MIC/64 in rows A to H, respectively. Similarly, the final concentrations of antibiotics in columns 1-8 after adding 25 µL of (4×) hydroquinine ranged from 2×MIC, MIC, MIC/2, MIC/4, MIC/8, MIC/16, MIC/32, and MIC/64 (µg/mL) respectively. The final inoculum approximately 5×10^4 CFU/well was then added into each well. Moreover, only MHB was the sterility control in well 9, whereas MHB with inoculum was the growth control in well 10. The MHB mixed with DMSO and Tween 80 was vehicle control (Figure 10). The 96-well plate was incubated at 35±2°C for 16–20 h. The naked eye and a microplate reader (EnSpire, PerkinElmer) at the wavelength of 620 nm were used to observe the turbidity to determine growth.

A 4-fold or more significant reduction in MIC values of antibiotics after adding hydroquinine was considered significant compared to MIC values of only antibiotics and calculated FICI. The synergy, additivity, and antagonism were defined as FICI <1; =1; >1, respectively (190, 219)

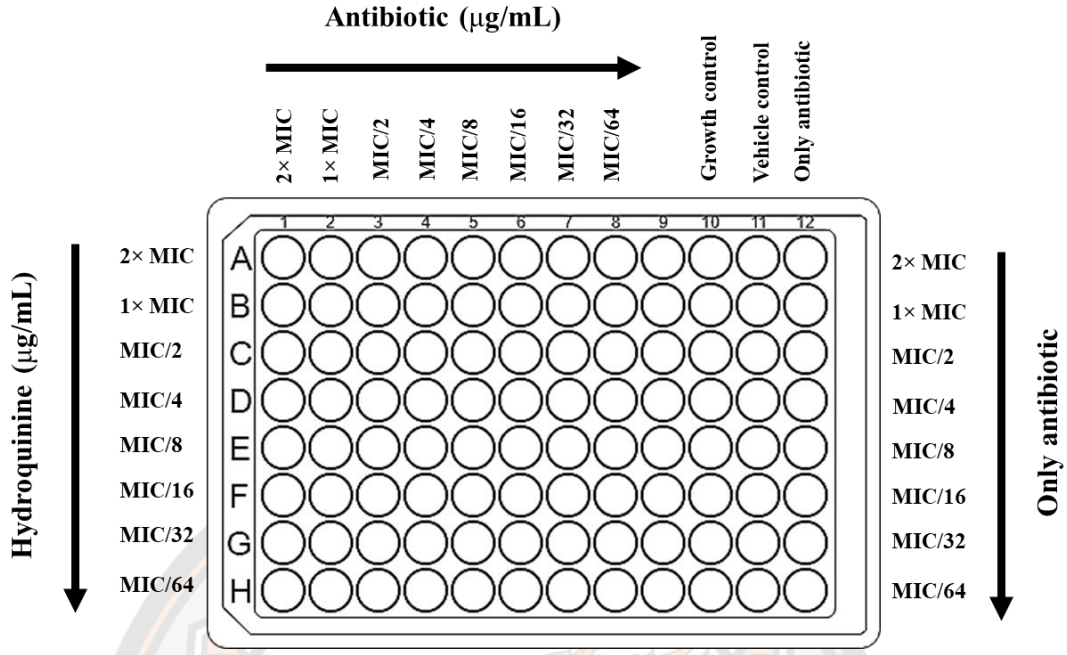

Figure 11 The 96-well plate for checkerboard method (220)

4. *In vitro* evaluation of transcriptional profile of *P. aeruginosa* ATCC 27853 under hydroquinine treatment condition.

This experiment evaluated the transcriptional profile of *P. aeruginosa* ATCC 27853 growing in ½ MIC of hydroquinine, conducted by transcriptomic analysis. The results of this experiment showed the *P. aeruginosa* transcriptional responded to hydroquinine. The probable mechanisms of hydroquinine against the *P. aeruginosa* strain were also shown in this experiment.

4.1 Hydroquinine treatment and total RNA extraction

One colony of *P. aeruginosa* ATCC 27853 was cultured in 100 mL of MHB and shaking incubated at 200 rpm, 35±2°C, until reaching the mid-exponential phase (2–6 h). The turbidity of the bacterial culture was then adjusted with sterilized normal saline solution (NSS) at 600 nm (OD600) to achieve turbidity of about 0.5 McFarland standard (1–2×10^8 CFU/mL). After that, 30 mL of the cultures were aliquoted into two falcon conical tubes. In the first tube, hydroquinine was added, a final concentration of roughly ½ MIC (1.25 mg/mL) representing the treatment group. The second tube had the culture with hydroquinine solvent dissolved (DMSO and Tween 80), which represents to control group. Each culture was shaken incubated at 200 rpm, 35±2°C for 1 h. Total RNA were then isolated by RNeasy Mini Kit (QIAGEN) and DNase was used to remove the residue DNA, following the manufacturer instructions. Total RNA was than analyzed quantification and purity using Colibri Microvolume Spectrophotometer (Titertek Berthold, Pforzheim, Germany). The purity of total RNA was investigated from the A260:A280 nm ratio, around 1.8–2.1 and A260:A230

around 2.0. The integrity of RNA was verified by 1% agarose gel electrophoresis at 100 V for 40 min.

The RNA extraction was performed by RNeasy Mini Kit of QIAGEN following the manufacturer's instructions. Briefly, the bacteria cells were harvested by centrifuging at 5,000×g 4°C for 5–10 min. RNA protection was then mixed at concentration 2X with 1X of MHB and incubated at room temperature for 5 min. After that, the pellet cell was harvested by centrifuging at 5,000×g for 5 min. The bacterial cell was lysis with RLT buffer containing ß-mercaptoethanol about 350–700 µL. Also, cells were disrupted by the Probe Sonicator at 30% power and 20% pulse for 3 min. The supernatant was then harvested by centrifugation at maximum speed for 3 min. 70% ethanol was then added to an equal volume of the supernatant and mixed well by pipetting. The lysate was transferred to the RNeasy spin column and placed in a 2 mL collection tube. After that, the lysate was centrifuged for 15 sec at ≥ 8,000×g, and the flow-through was discarded. The buffer RW1 (350 µL) was then added into the RNeasy spin column and centrifuged to remove the buffer RW1 at ≥ 8,000×g for 15 sec. The DNases enzyme (80 µL) was added into the column and incubated at room temperature for 15 min. The sample was washed with buffer RW1 at 350 µL and removed the buffer at ≥ 8,000×g for 15 sec. The buffer RPE (500 µL) was then added into the column and the buffer was removed by centrifugation at ≥ 8,000×g for 15 sec. Then, about 30–50 µL of RNase-free water was added directly to the spin column membrane and eluted the RNA by centrifugation at ≥ 8,000×g for 1 min. The RNA sample was collected at about -80°C for the next experiment.

4.2 Transcriptomic analysis

The transcriptome of the samples was performed by Macrogen Inc. (Seoul, South Korea), and the experiment overview was shown in Figure 12**.** Before transcriptomic analysis, the quality and quantity of the total RNA sample were checked. Briefly, the total RNA integrity of *P. aeruginosa* treated with hydroquinine was checked using Agilent 2100 Bioanalyzer (Agilent, USA) with an RNA integrity number (RIN) greater than or equal to 7. The TruSeq stranded total RNA kit (Illumina, San Diego, CA, USA) was then used for library construction. The cDNA library was prepared by cDNA random fragmentation, followed by 5' and 3' adapter ligation. Adapter-ligated fragments were then PCR amplified and gel purified. The library size and library quantity were checked. Briefly, the template size distribution was checked to verify the size of PCR-enriched fragments using Agilent Technologies 2100 Bioanalyzer. The standard curve of fluorescence readings and the library sample concentration calculation were performed with a Qubit standard Quantification solution and calculator. After the library quality passes, the cDNA library was sequenced on a flow cell using high-throughput 2×150 nt, pair-end mode on an Illumina HisSeq 2100 platform (Illumina, San Diego, CA, USA). Total read bases (bp), total reads, GC content (%), AT content (%), phred quality score 20 (Q20) (%), and Q30 (%) were then calculated. Quality checks for raw sequencing data, read mapping and expression quantification of RNA sequencing were analyzed. The passed filter reads were mapped onto *Pseudomonas aeruginosa* PAO1 genome reference using Bowtie2.

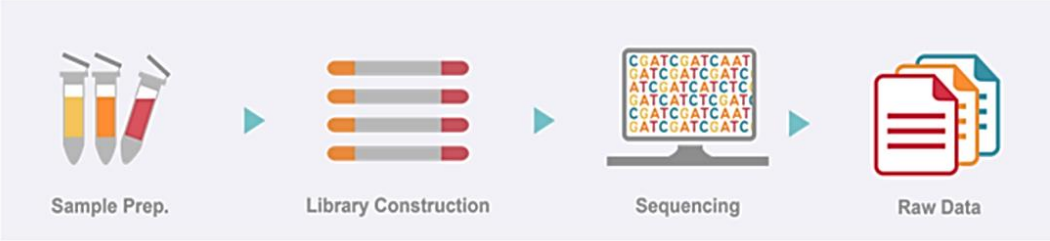

Figure 12 Transcriptomic experiment overview

4.3 The differentially expressed genes (DEGs) analysis.

Transcript quantification analysis, fragments per kilobase of transcript per million (FPKM) form was used to analyze DEGs. Briefly, transcript quantification conducted using Feature count. The differential expression analysis of the hydroquinine-treated sample was then conducted with edgeR, which was compared with the hydroquinine untreated sample. The results of DEGs were summarized using the significant criteria of $-2 \geq \log_2$ fold change ≥ 2 and a false discovery rate (FDR) $P \leq 0.05$.

4.4 Gene ontology (GO) terms and Kyoto encyclopedia of genes and genomes (KEGG) pathway analysis

The significant DEGs were used to analyze functional annotation in Gene ontology (GO) terms and Kyoto encyclopedia of genes and genomes (KEGG) pathway using the Database for Annotation, Visualization, and Integrated Discovery (DAVID) (https://david.ncifcrf.gov/ 2021 updated database, accessed on 20 September 2022). Briefly, the "Start Analysis" function on the DAVID program home page was chosen. The name genes received from DEG results were submitted in the "Enter gene list" box. After that, the "REFSEQ _PROTEIN" was selected in the select identifier step. The type of "Gene list" was then chosen. In the last step, click "Submit list" to let the program choose the items you wish to examine, as shown in Figure 13.

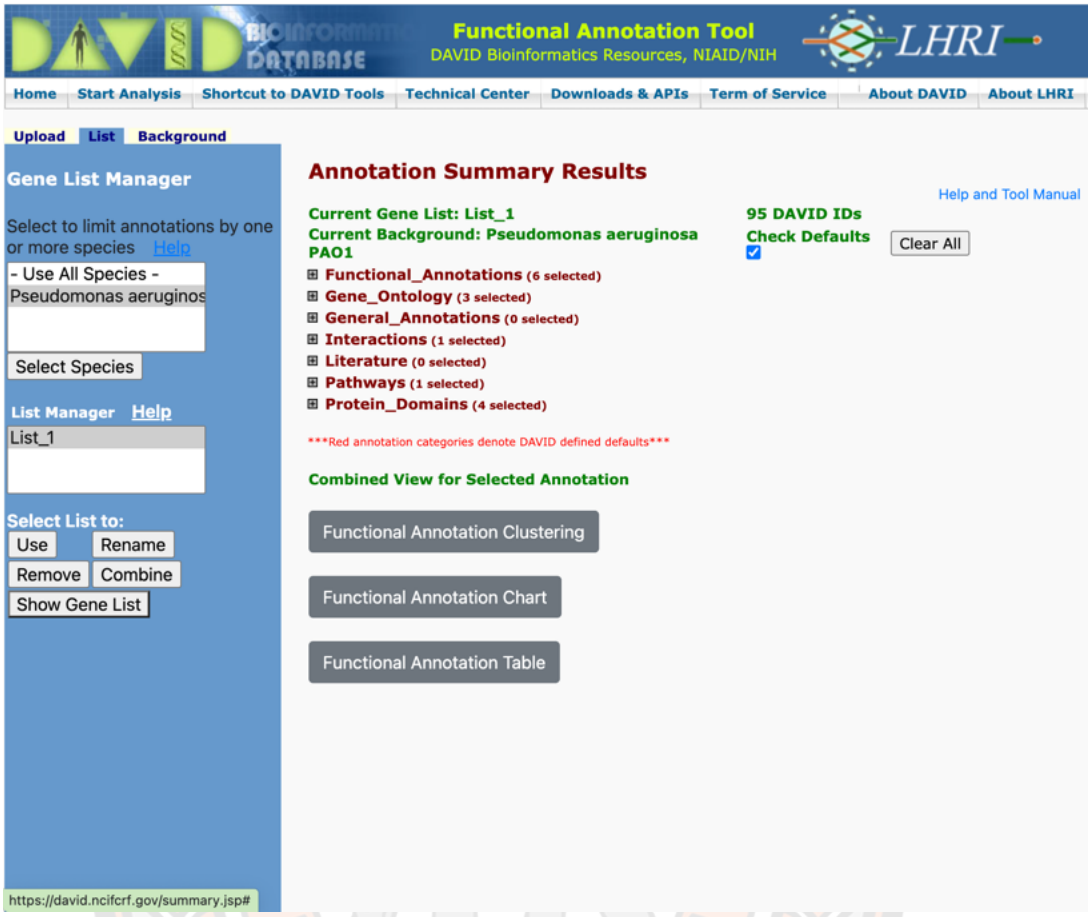

Figure 13 Functional annotation analysis example

5. *In vitro* evaluation the exact mechanisms of hydroquinine against *P. aeruginosa* strains

According to the transcriptomic analysis results, some of the RND-type efflux pump upregulated genes and virulence factor downregulated genes were selected. These genes were selected to verify the exact mechanism of hydroquinine against *P. aeruginosa* strains. Both of DS *P. aeruginosa* ATCC 27853 and MDR *P. aeruginosa* ATCC BAA 2108 represented pathogenic bacteria for this study.

To verify the exact mechanism of hydroquinine affect RND-type efflux pump in *P. aeruginosa* strains, the genotypic analysis was conducted using a reverse transcription polymerase chain reaction (RT-PCR) system. Whereas the effect of hydroquinine on virulence factors in *P. aeruginosa* strains was verified with genotypic and phenotypic analysis.

5.1 Verification of RND-type efflux pump upregulated gene expression of *P. aeruginosa* strains

5.1.1 Genotypic analysis

This experiment, the expression of RND-type efflux pump gene in *P. aeruginosa* were verified to find exact mechanism of hydroquinine. Three representative RND-type included *mexB*, *mexD*, and *mexY* of *P. aeruginosa* were

selected. This experiment, multiplex PCR base systems, including multiplex quantitative reverse transcription PCR (mRT-qPCR) and multiplex reverse transcription digital PCR (mRT-dPCR) methods were used to identify the expression of three *mex* genes in *P. aeruginosa* strains under hydroquinine treatment condition. Therefore, in order to detect the expression of *mex* genes, the optimal conditions for amplifying the *max* genes in *P. aeruginosa* including annealing/extension temperature and gDNA concentration, were first investigated with multiplex quantitative PCR (mqPCR) method and confirm with DNA agarose gel electrophoresis methods. Moreover, to use mRT-dPCR for detecting the expression of *mex* genes in *P. aeruginosa* strain, the *effluxR* detection assay with multiplex digital PCR (mdPCR) was developed in this experiment using the optimal conditions from the mqPCR. The *effluxR* detection assay with mdPCR was also evaluated optimal gDNA concentration, limit of detection, sensitivity, and specificity to amplify representative RND-type efflux pump genes in *P. aeruginosa* strains. The conceptual framework of this experiment is shown in Figure 14.

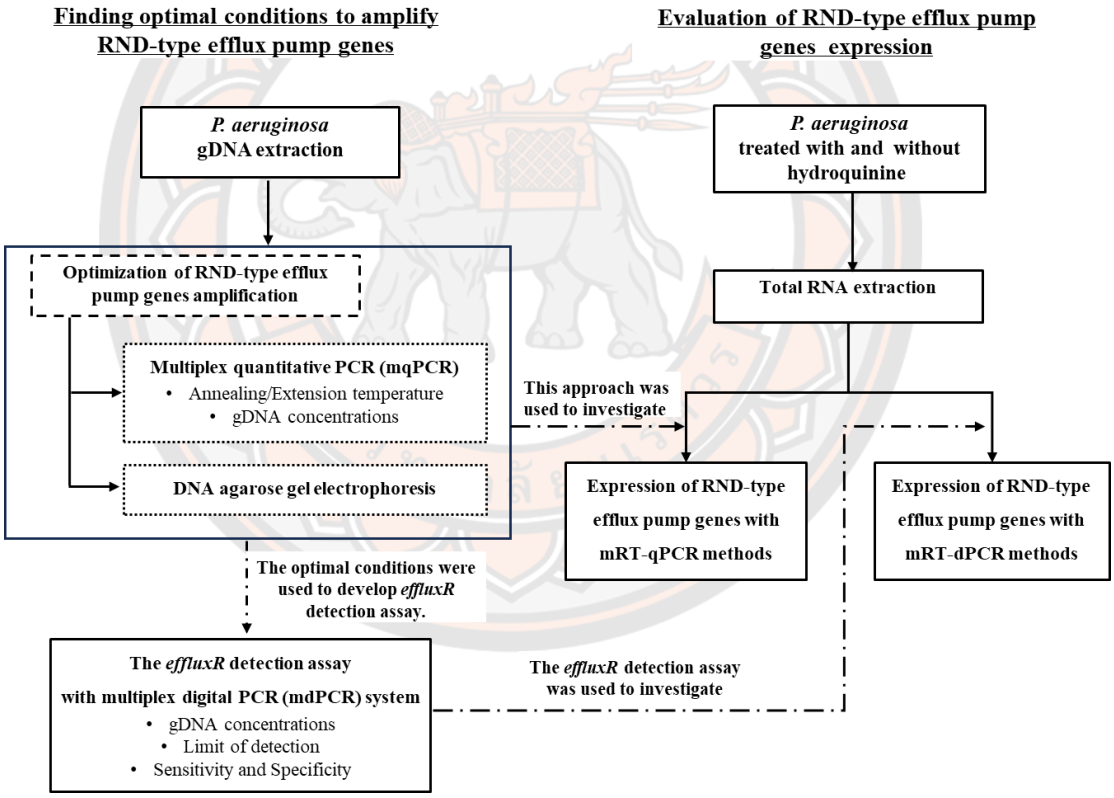

Figure 14 The framework of genotypic analysis for RND-type efflux pump gene verification of *P. aeruginosa*

5.1.1.1 Genomic DNA extraction

All bacteria cells grown in TSB were harvested at 24 h by centrifugation at 5,000×g 4°C for 5–10 min. Genomic DNA of all bacterial strains was isolated with Genomic DNA Isolation Kit (Bio-Helix, Taiwan) as following the manufacture's instruction (221). Briefly, the pelleted cells were lysis by lysis buffer. The samples were then mixed with vortex and incubated at 60°C for 10 min. RNA in

samples were degraded by adding 5 µL of 10 mg/mL RNase and incubated at room temperature for 5 min. To remove protein, protein buffer was added to the sample tubes. After that the samples were centrifuged at 12,000 rpm for one minute. Each supernatant was then collected and transferred in 2-mL collection tube. After centrifugation, washing buffer was added in the tube at two time to wash the sample. The gDNA sample in column was collected by eluted with 50 µL DNase-free water and then centrifugation at 14,000 rpm for 2 min. gDNA concentration and purity were verified using a Colibri Microvolume Spectrophotometer (Titertek-Berthold, Pforzheim, Germany).

5.1.1.2 Total RNA extraction and cDNA synthesis

Total RNA extraction of *P. aeruginosa* treated with and without hydroquinine was performed synonymous with the RNA extraction protocol mentioned in Section 4.1 (221). In a step of complementary DNA (cDNA) synthesis, the QuantiNova Reverse Transcription Kit (QIAGEN, Hilden, Germany) was used to synthesize as the manufacturer suggested. Briefly, 2 µL of gDNA Removal Mix was added in 1 µg of RNA in a PCR tube to remove gDNA. The RNase-free water was added to the PCR tube to adjust a final volume of 15 µL. The sample was then incubated at 45 ◦C for 2 min. After that, 4 µL of Reverse Transcription Mix and 1 µL of reverse transcription enzyme were added to the reaction tube to synthesize cDNA. The reaction was incubated at the annealing step at 25 ◦C for 3 min, and the reverse-transcription step was performed at 45 ◦C for 10 min, followed by inactivation of the reaction at 55 ◦C for 5 min. The concentration of cDNA synthesized was measured prior to downstream analysis.

5.1.1.3 Primer and probe design

The genes of interest from transcriptomic analysis results were selected. Whole genome sequencing of interest was searched from the NCBI database. Subsequently, copied and pasted the whole genome sequencing on the SnapGene viewer program (version 5.2.5.1) to design a primer or probe. Then, to ensure the primer or probe melting temperature was suitable, the Oligo Calc: Oligonucleotide Properties Calculator software (http://biotools.nubic.northwestern.edu/) was used to check. Subsequently, the Basic Local Alignment Search Tool (Nucleotide BLAST) and the Pseudomonas database (https://www.pseudomonas.com) were used to confirm a specific primer to the gene of interest. Guidelines for designing suitable PCR primers or probes are described below for specific amplification by polymerase chain reaction with highly effective results (222). 1) The length of PCR primers and probe should be 18-22 and 22–24 bp. 2) Primer Melting Temperature (Tm): The optimal range is 52–58 °C 3) Primer Annealing Temperature (Ta): The optimal Ta is about 5°C below the Tm of primers (223) 4) GC Content: The total bases G and C of primer should have many G and C in the primer of about 40-60% 5) GC Clamp: should have many G or C bases at the 3' end of the primer about not exceeding 3 bases 6) Avoid primer secondary structures and repetition of continues of four or more bases and dinucleotide repetitions (for example, AGGGG or CGCGCGCG) 7) Avoid homology of self-primer and forward and reverse primers (more than three bases). These conditions cause self-dimers or primer-dimers.

5.1.1.4 Investigation of optimal conditions of RND-type efflux pump genes amplification using multiplex qPCR (mqPCR) system

This experiment was performed to provide the optimal conditions for developing another downstream method: the *efluxR* detection assay using a multiplex digital PCR (mdPCR) system (224). These conditions were also used to detect the expression of the representative RND-type efflux pump genes in *P. aeruginosa* strains with RT-qPCR method.

1) Investigation of optimal annealing/extension temperature of mqPCR system to amplify RND-type efflux pump genes

The optimal annealing/extension temperature of the multiplex qPCR system was investigated to amplify the RND-type efflux pump and reference genes of *P. aeruginosa* strain. Three representative RND-types of *P. aeruginosa* strain, including *mexB*, *mexD*, and *mexY*, and reference gene *16s rRNA* were amplified in this experiment. Five temperatures, 58°C, 59°C, 60°C, 61°C, and 62°C were analyzed. The multiplex qPCR reactions were prepared following QIAcuity Probe PCR Kit guidelines (QIAGEN, Hilden, Germany). Briefly, each reaction consists of 5 ng of gDNA template, 800 nM of each forward and reverse primer (Table 3), 400 nM of each probe (Table 3) (221), 5 µL of 4×Probe PCR Master Mix were added and adjusted to a 20 µL final volume with RNase-free water. After reaction preparation, the LineGene 9600 Plus Real-Time PCR Detection System (Bioer Technology, Hangzhou, China) was uses to analyze the *mex* genes of *P. aeruginosa* strains. The thermal cycler conditions of the mqPCR program to amplify *mex* genes, followed by 40 cycles of denaturation at 95°C for 15 sec and combined annealing/extension at tested temperatures for 30 sec. The cycle threshold (Ct) value was reported as a result. In each run, all tests were performed in triplicate with a non-template control (NTC).

Table 3 The sequences of primers and probes were used in this study.

Name	Oligonucleotide sequences (5' to 3')	PCR product size (bp)	References
mexB			
F_primer	GATAGGCCCATTTTCGCGTGG	199	(221)
R_primer	CGATCCCGTTCATCTGCTGC		
Probe	(FAM)CGCCTTGGTGATCATGCTCGCG(BHQ1)		
mexD			
F_primer	TCATCAAGCGGCCGAACTTC	131	(221)
R_primer	GGTGGCGGTGATGGTGATCTG		
Probe	(HEX)CTGGCCGGCCTGCTGGTCATTTC(BHQ1)		
mexY			
F_primer	CGCAACTGACCCGCTACAAC	168	(221)
R_primer	CGGACAGGCGTTCTTCGAAG		
Probe	(Texas Red)CGAAGCCATGCAGGCGATGGAGG(BHQ2)		
16s rRNA			
F_primer	CATGGCTCAGATTGAACGCTG	225	(221)
R_primer	GCTAATCCGACCTAGGCTCATC		
Probe	(Cy5)CGAGCGGATGAAGGGAGCTTGCTC(BHQ2)		

2) Investigation of optimal gDNA concentration of *P. aeruginosa* strains using mqPCR system

In order to amplify representative RND-type efflux pump as well as housekeeping genes, four gDNA concentrations of *P. aeruginosa* strains were detected (224). The reaction was prepared by added each gDNA concentration of 5.0 ng, 2.5 ng, 1.0 ng, and 0.5 ng into a PCR tube containing 800 nM of each forward and reverse primer (Table 3), 400 nM of each probe (Table 3), and 5 µL of 4×Probe PCR Master Mix. The total volume was then adjusted to 20 µl with RNase-free water. The thermal cycler conditions of the mqPCR program to amplify representative *mex* genes, followed by 40 cycles of denaturation at 95°C for 15 sec and combined annealing/extension at the optimal temperature for 30 sec. The Ct value was reported as a result. In each run, all tests were performed in triplicate with a non-template control (NTC).

5.1.1.5 Detection of RND-type efflux pump genes by DNA agarose gel electrophoresis

Representative RND-type efflux pump genes including *mexB*, *mexD*, and *mexY* of *P. aeruginosa* ATCC stains (27853 and BAA-2108) and *P. aeruginosa* clinical strains 1–3 (PA.CI1, PA.CI2, and PA.CI3) were validated using gel electrophoresis (224). To prepare 2% Tris-borate-EDTA (TBE) agarose gel, 2 g of agarose (GeneDireX, Inc., Taoyuan, Taiwan) was added to 100 mL of TBE, and then the gel solution was melted until homogeneously. Once the gel solution has cooled down, UltraPure™ Ethidium Bromide (EtBr) (Thermo Fisher Scientific, Waltham, Massachusetts, USA) was added. The gel solution with EtBr was then poured into a casting tray to create a gel slab. After that 10 µl of each gDNA sample with 1x of loading dry buffer (GeneDireX, Inc., Taoyuan, Taiwan) was loaded into the solid gel, it was in chamber filled with TBE buffer. A DNA marker was also loaded as reference for sizes (GeneDireX, Inc., Taoyuan, Taiwan). The representative *mex* and *16s rRNA* were analyzed at 120 V for 30–40 min. The DNA size of each target and reference gene was shown in Table 3. The band intensity of genes was visualized and photographed under UV light with a gel documentation system (Aplegen, Ramsey, USA).

5.1.1.6 Development of the *effluxR* detection assay to detect the representative RND-type efflux pump gene using multiplex digital PCR (mdPCR)

In this experiment, to achieve the effective *effluxR* detection assay with mdPCR system for detecting RND-type efflux pump gene in *P. aeruginosa* strains, the optimal gDNA concentrations, the limit of detection, sensitivity and specificity were studied (224). The multiplex QIAcuity Digital PCR system (QIAGEN, Hilden, Germany) was used in this experiment. The mdPCR reactions were performed by QIAcuity Probe PCR Kit (QIAGEN, Hilden, Germany), following the manufacturer's instructions. Briefly, all mdPCR reactions were performed at a final volume of 40 µL. Each reaction contained different quantities of gDNA (as indicated), 0.8 µM of each forward and reverse primer, 0.4 µM of each probe (Table 3), and 10 µL of PCR Master Mix and RNase-free water. The mdPCR reactions were then pipetted to a 24-well QIAcuity Nanoplate (QIAGEN, Hilden, Germany). The nanoplate was sealed with a rubber sheet and loaded in the QIAcuity Digital PCR instrument (QIAGEN, Hilden, Germany) (Figure 15). The thermal cycler conditions

of the mdPCR system were as follows: 40 cycles of denaturation at 95 °C for 15 sec and combined annealing/extension at 59 °C for 30 sec. Fluorescence measurements were then made for each reaction. A non-template control (NTC) was used as a negative control. All analyzable partitions, including the valid, positive, and negative partitions, were used to calculate the total number of copies of the target molecule (λ) in all valid partitions (copies per partition) according to Equation (1). The absolute quantification (λ_{volume} as the unit of copies/µL) was then calculated as shown in Equation (2), where the estimated partition volume (V) is 0.91 nL for the 26k-nanoplate system.

$$\lambda = -\ln\left(\frac{\text{Number of valid partitions - Number of positive partitions}}{\text{Number of valid partitions}}\right) \text{ ---------- equation (1)}$$

$$\lambda_{volume} = \frac{\lambda}{V\ [\mu L]} \text{ ---------- equation (2)}$$

The different gDNA concentrations of *P. aeruginosa* strain 5.00, 2.50, 1.00, 0.50, 0.05 ng were used to determine the optimal gDNA concentration. The presented results were interpreted as a positive partition percentage. For analyzing the limit of detection of the assay to detect *mex* genes in *P. aeruginosa*, the various gDNA concentrations, including 2.50, 1.25, 0.50, 0.05, 0.005, 0.003, 0.001 and 0.000 ng were used. The *mex* genes were detected as partition and then interpreted as the absolute quantification in the unit of copies/µL. The 95% confidence interval (CI) in copies/µL is also reported following the manufactures calculation (QIAGEN, Hilden, Germany). Also, 69 positive-*mex* efflux pump gene samples and 15 negative samples were used to analyze the sensitivity and specificity of the assay with a blind test technique. The *mexB*, *mexD*, and *mexY* genes were detected from the relative fluorescence intensity and then interpreted as present or absent gene.

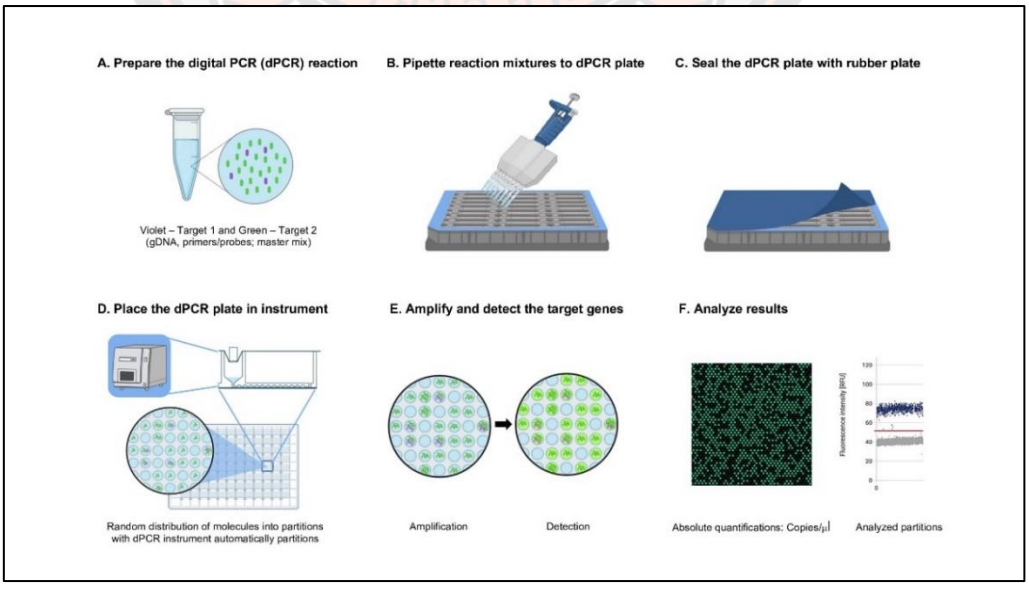

Figure 15 The schematic amplification of target genes using digital PCR (224)

5.1.1.7 Detection of RND-type efflux pump gene expression using Multiplex Quantitative Reverse Transcription PCR (mRT-qPCR)

The representative RND efflux pump genes expression of *P. aeruginosa* ATCC 27853 and MDR ATCC-BAA 2108 were verified (221). This study evaluated the *mexB, mexD,* and *mexY* gene expression of both *P. aeruginosa* strains at different treatment times with ½ MIC of hydroquinine. Briefly, the bacterial strains were treated and untreated with ½ MIC hydroquinine for 1, 2, and 4 h. The total RNA was then collected and synthesized cDNA. The mRT-qPCR reactions and thermal cycler conditions were synonymous with the mqPCR protocol mentioned in Section 5.1.1.4, which changed the template from gDNA to cDNA. The concentration of cDNA template used in this study was 100 ng. The thermal cycler conditions for amplification were the same with mqPCR, which annealing/extension temperature was 59 °C. After analyzing, the CT values of the reference gene (*16s rRNA*) and the *mex* target genes in each sample set were used to calculate the fold change of gene expression levels with ΔΔCt method ($2^{-\Delta\Delta ct}$). The fold change of gene expression levels was given relative to the untreated sample. Each test was performed in triplicate together with a non-template control (NTC) in each run.

5.1.1.8 Detection of RND-type efflux pump gene expression using the *effluxR* detection assay with mRT-dPCR

This experiment verified the representative RND-type efflux pump gene expression of DS *P. aeruginosa* ATCC 27853 using the *effluxR* detection assay with mRT-dPCR (221). All materials used for gene expression were synonymous with the *effluxR* detection assay with mdPCR system mentioned in Section 5.1.1.6, which changed the template from gDNA to cDNA. Briefly, the total RNA of *P. aeruginosa* was extracted after treatment with and without ½ MIC of hydroquinine for one hour. The cDNA was then synthesized following the cDNA synthesis method mentioned in Section 5.1.1.2. The thermal cycler conditions for amplification were the same with the *effluxR* detection assay. After the reaction was finished, the fluorescent signals were statistically calculated as positive and negative partitions. Non-template controls (NTC) were used as negative controls to calculate the appropriate threshold (cut-off) between positive and negative partitions. Data were expressed as absolute quantification in the unit of copies/µL using Poisson statistics. Fold changes in mRNA were calculated as the average ratio of normalized mRNA copies per microliter in the hydroquinine-treated condition compared to the non-treated control.

5.2 Verification of virulence factor downregulated gene expressions of *P. aeruginosa* strains

In this experiment, the virulence factor downregulated gene expressions were verified to find the exact mechanism of hydroquinine against the infection activity of both DS and MDR *P. aeruginosa* strains. The representative virulence factor genes involved in the flagella assembly (*flgK*, *flgH*, *flgC* and *fliF*) were selected to validate by genotypic analysis with the RT-qPCR method. In addition to genes present in this experiment's transcriptomic results, quorum sensing (QS) ‑ related genes (*rhlI* and *rhlR*) were also studied to investigate in this experiment. Moreover, phenotypic analysis of flagella assembly that play an essential role in movement and attachment of *P. aeruginosa* was also investigated with swimming and swarming motility assay.

Furthermore, phenotypic analysis of pigment production and biofilm formation of both DS and MDR *P. aeruginosa* strains were investigated in this study (225).

5.2.1 Genotypic analysis

5.2.1.1 Detection of *P. aeruginosa* virulence factor downregulated gene expressions using RT-qPCR method

Six representative virulence factor genes included *flgH*, *flgK*, *fliF*, *flgC, rhlI* and *rhlR* of *P. aeruginosa* were selected. These genes were detected using RT-qPCR methods. Briefly, both of DS and MDR *P. aeruginosa* were treated with ½ MIC of hydroquinine for 1 h. The total RAN extraction and cDNA synthesis was performed synonymous with the total RAN extraction method in Section 4.1 and 5.1.1.2, respectively (225).

The LineGene 9600 Plus Real-Time PCR Detection System (Bioer Technology, Hangzhou, China) was used to analyze the gene expression in this study. The RT-qPCR reaction was performed following the manufacturer's instructions of HOT FIREPol® EvaGreen® qPCR Mix Plus (Cat. No. 08-25-00001, Solis Bio-dyne, Tartu, Estonia). The cDNA synthesized was then used as a PCR template. The specific primers for each gene are shown in Table 4 (225). The *16s rRNA* of *P. aeruginosa* was used as a reference gene. The RT-qPCR cycling conditions were as follows: 40 cycles of denaturation at 95 °C for 15 sec, proper annealing step ranging at 56.0–58.5 °C for 20 sec, and extension at 72 °C for 20 sec. The *16s rRNA* gene was used as a housekeeping reference to calculate the relative expression levels of the genes. After amplifying, the Ct values of reference gene and target genes in each sample set were used to calculate the relative expression levels of gene using a $2^{-\Delta\Delta Ct}$ method. All the experiments were performed in triplicate.

Table 4 Summary of primer sequences and annealing temperatures used

Primer name	Oligonucleotide sequences (5' to 3')	Annealing temperature (°C)	References
flgH F	CGAGCAGAACCTCTACGACG	57.5	(225)
flgH R	TCGGGTTGTTGGTGGTCATG	57.5	(225)
flgK F	CCAGCAAGCTGAATTCCAGC	56.0	(225)
flgK R	GGTCGTCTCGATATCGCTGG	56.0	(225)
fliF F	AGATGTACAACCCGGACCAG	57.5	(225)
fliF R	TCGGATCGATGATGGTCTGG	57.5	(225)
flgC F	TTCTCCACCATGTTCCAGCAG	57.5	(225)
flgC R	TCCTCGACCACGTTCACATTG	57.5	(225)
rhlI F	CAGGAATTCGACCAGTTCGACC	58.5	(225)
rhlI R	CGAAGACGTCCTTGAGCAGG	58.5	(225)
rhlR F	GTAGCGAGATGCAGCCGATC	57.0	(225)
rhlR R	CCTTGGGATAGGTGCCATGG	57.0	(225)
16s rRNA F	CATGGCTCAGATTGAACGCTG	58.0	(221)
16s rRNA R	GCTAATCCGACCTAGGCTCATC	58.0	(221)

5.2.2 Phenotypic analysis

5.2.2.1 Determination of *P. aeruginosa* flagella assembly

The flagella assembly was investigated via ability of *P. aeruginosa* motility using swimming and swarming motility assay (225) following modifications from She *et al.* 2018 (226). Briefly, Luria-Bertani (LB) solidified with 0.3% of agarose was prepared for swimming motility investigation. For investigating swarming motility used LB with 0.5% agarose and D-glucose. Both assays were performed in 6-well plates (35 mm diameter) containing 3 mL of corresponding media with hydroquinine at concentrations of MIC, ½ MIC and ¼ MIC values including 2.500, 1.250 and 0.625 mg/mL for the DS strain as well as of 1.250, 0.625 and 0.312 mg/mL for the MDR strain. DMSO was use as vehicle control and only the media as sterility control. The swimming motility assay was performed by strapping the inoculum in the center of the agar thickness. Whereas 2 µL of the inoculum was pipetted on the central agar for swarming motility investigation. After that 6-well plates were incubated at 35 ± 2 °C for 24 h. The diameter zones of the swimming and swarming motility were then measured and reported. Also, percentage of swimming and swarming motility inhibition were reported in this experiment.

5.2.2.2 Detection of *P. aeruginosa* pyocyanin production

The effect of hydroquinine to pyocyanin production of *P. aeruginosa* was determined (225) using colorimetric spectrometry (226). Briefly, both of DS and MDR *P. aeruginosa* strains were treated with and without hydroquinine in MHB at a concentration of MIC, ½ MIC and ¼ MIC. The corresponding inoculum with DMSO and only MHB were used as vehicle control and untreated control, respectively. The samples were incubated at 35 ± 2 °C for 24 h. The pyocyanin pigment was then separated by centrifugation at 4,000 rpm for 15 min. The supernatant was then collected and filtered with syringe (a 0.2 µm in pore size filter). The pyocyanin pigment of each sample was extracted with chloroform at a ratio of 2:3 and re-extracted with 1.0 mL of 0.2 M HCl. MHB with the corresponding inoculum was the untreated control. The pyocyanin pigment was measured at 540 nm using a microplate reader (PerkinElmer, Waltham, MA, USA). Also, the percentage of pyocyanin production inhibition was calculated and reported in this experiment.

5.2.2.3 Detection of *P. aeruginosa* biofilm formation

In this experiment, the biofilm mass formation of both DS and MDR *P. aeruginosa* strains were detected after treatment with and without hydroquinine (225). The hydroquinine concentrations used in this experiment were MIC, ½ MIC and ¼ MIC including 2.500, 1.250 and 0.625 mg/mL for the DS strain as well as of 1.250, 0.625 and 0.312 mg/mL for the MDR strain. The biofilm mass formation of *P. aeruginosa* strains was investigated using crystal violet retention assay with the following modifications (227, 228). Briefly, the experiment was performed in 96-well plates, which containing MHB (200 µL), each hydroquinine concentration tested and 10% DS or MDR inoculum. For control groups including untreated control and vehicle control. DMSO and Tween 80 was used as a vehicle control. The plates were then incubated at 35 ± 2 °C for 24 h. The planktonic cells were then carefully removed and washed with sterile distilled water three times. After that the biofilm mass in each well was dried at 60 °C for 45 min. Crystal violet at concentration 0.1%

(w/v) was used to stain the adherent biofilm cells on the plate for 20 min at room temperature. The crystal violet was then washed with sterile distilled water three times. After that the samples were re-dissolved with 95% ethanol (v/v). The biofilm mass formation was measured via the optical density, which used microplate reader (PerkinElmer, Waltham, USA) at 595 nm. Also, the percentage of biofilm formation inhibition that caused from hydroquinine was calculated and reported.

Statistical analysis

All the experiments were performed independently in triplicate. Where appropriate results are shown as means ± standard deviation (SD). An independent student t-test using IBM SPSS statistics version 23 (Armonk, NY, USA) was used to test statistically significant mean differences between both comparing treated and untreated groups and comparing treated and vehicle control groups. GraphPad Prism version 8.2.0 (San Diego, CA, USA) was created and analyzed all graphs. For all analyses, significant differences were reported for p-values < 0.05.

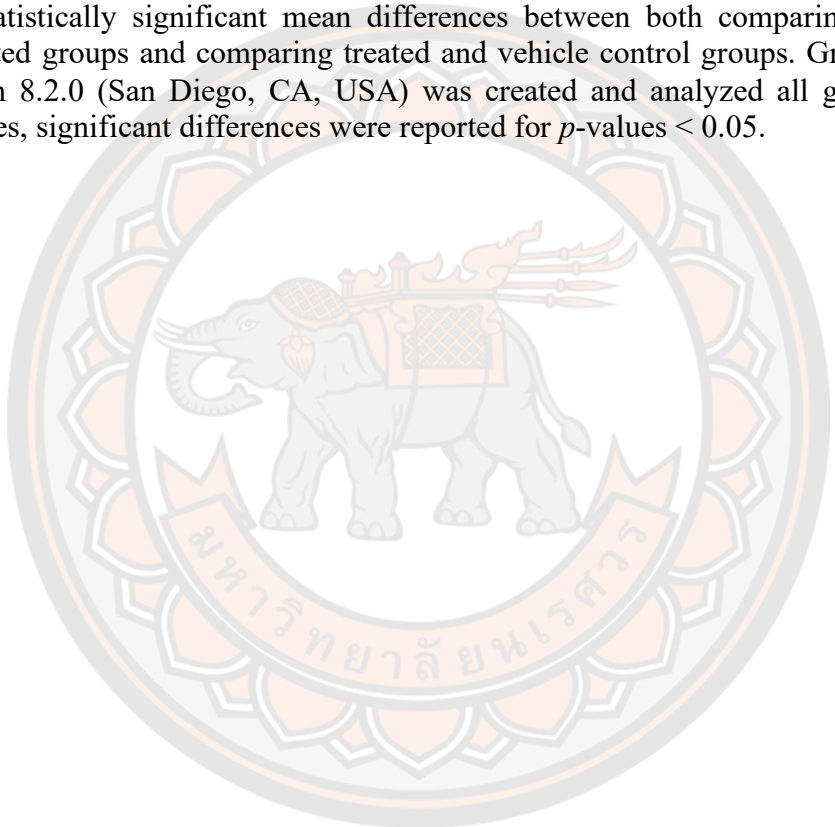

CHAPTER IV

RESULTS

1. Characterizing the antimicrobial properties of hydroquinine

1.1 Antibiotic susceptibility profiling of pathogenic bacteria using phenotypic method

To characterize the antimicrobial properties of hydroquinine, we sought to determine the susceptibility profiles of the pathogenic bacteria included in this study. Eight pathogenic bacteria tested were re-evaluated for antibiotic susceptibility to antibiotic groups A-C according to the CLSI M100 recommendation (192) using the Vitek®2 compact mechanical device. Results of the antibiotic susceptibility test showed that all the bacteria included in this study still possessed the expected antibiotic susceptibility profiles following the guideline of CLSI M100. *P. aeruginosa* ATCC 27853, a drug-sensitive (DS) strain accordant with ATCC reported, showed susceptibility to most antibiotics except for tigecycline, which affects protein synthesis, as shown in Table 5. *P. aeruginosa* ATCC BAA-2108, a multidrug resistance (MDR) strain reported by ATCC, was only susceptible to four of the antibiotics tested: ceftazidime, cefoperazone, cefepime and ciprofloxacin (Table 5). In contrast, the ATCC BAA-2108 strain showed resistance and intermediate results to antibiotics of more than three classes that function in inhibiting cell wall synthesis (doripenem, imipenem and meropenem), protein synthesis (amikacin and tigecycline) and DNA replication (levofloxacin) (Table 5). These antibiotics must be used in combination with another antibiotic to clear infections with this strain of *P. aeruginosa*.

Table 5 Antibiotic susceptibility report of *P. aeruginosa* strains

Antibiotic	**Mode of action**	***P. aeruginosa* ATCC 27853**		***P. aeruginosa* ATCC BAA-2108**	
		MICs	**Interpretation**	**MICs**	**Interpretation**
Ceftazidime	cell wall synthesis	≤1	S	4	S
Cefoperazone	cell wall synthesis	≤8	S	≤8	S
Cefepime	cell wall synthesis	2	S	8	S
Doripenem	cell wall synthesis	0.5	S	≥8	R
Imipenem	cell wall synthesis	2	S	≥16	R
Meropenem	cell wall synthesis	0.5	S	4	I
Amikacin	protein synthesis	≤2	S	≥64	R
Tigecycline	protein synthesis	≥8	R	≥8	R
Ciprofloxacin	DNA replication	≤0.25	S	0.5	S
Levofloxacin	DNA replication	1	S	2	I

Note: S; Susceptible, I; intermediate, R; Resistant

For *K. pneumoniae* (ATCC 1705), the antibiotic susceptibility results confirmed resistance to all antibiotics tested except for tigecycline, which affects protein synthesis, as shown in Table 6. Moreover, the antibiotic susceptibility result of *E. cloacae* ATCC 2341 showed resistance to all antibiotics tested except for amikacin, which affects protein synthesis, as shown in Table 6. All antibiotics that inhibit cell wall synthesis and protein synthesis (amikacin) were resisted by *E. coli* strain ATCC 2452, as shown in Table 7. At the same time, *E. coli* strain ATCC 2452 was susceptible to antibiotics, affecting DNA replication (tigecycline and ciprofloxacin) and protein synthesis (tigecycline). Antibiotic susceptibility results of *E. coli* strain ATCC 25922 showed susceptibility to all antibiotics tested in this study (Table 7). Moreover, both gram-positive bacteria strains tested in this study, namely *S. aureus* ATCC 29213 and ATCC 25923, showed susceptibility to all antibiotics tested, as shown in Table 8.

Table 6 Antibiotic susceptibility profiles of *K. pneumoniae* and *E. cloacae* strains

Antibiotic	**Mode of action**	***K. pneumoniae* ATCC 1705**		***E. cloacae* ATCC 2341**	
		MICs	**Interpretation**	**MICs**	**Interpretation**
Ceftazidime	cell wall synthesis	≥64	R	≥64	R
Amoxicillin	cell wall synthesis	≥32	R	≥32	R
Piperacillin	cell wall synthesis	≥128	R	≥128	R
Ceftriaxone	cell wall synthesis	≥64	R	≥64	R
Cefoperazone	cell wall synthesis	≥64	R	≥64	R
Doripenem	cell wall synthesis	≥8	R	≥8	R
Ertapenem	cell wall synthesis	≥8	R	≥8	R
Imipenem	cell wall synthesis	8	R	≥16	R
Meropenem	cell wall synthesis	≥16	R	≥16	R
Amikacin	protein synthesis	≥64	R	≤2	S
Tigecycline	protein synthesis	2	S	≥8	R
Ciprofloxacin	DNA replication	≥4	R	≥4	R
Levofloxacin	DNA replication	≥8	R	≥8	R

Note: S; Susceptible, I; intermediate, R; Resistant

Table 7 Antibiotic susceptibility profiles of *E. coli* strains

Antibiotic	**Mode of action**	***E. coli* ATCC 2452**		***E. coli* ATCC 25922**	
		MICs	**Interpretation**	**MICs**	**Interpretation**
Ceftazidime	cell wall synthesis	≥64	R	≤1	S
Amoxicillin	cell wall synthesis	≥32	R	4	S
Piperacillin	cell wall synthesis	≥128	R	≤4	S
Ceftriaxone	cell wall synthesis	≥64	R	≤1	S
Cefoperazone	cell wall synthesis	≥64	R	≤8	S
Doripenem	cell wall synthesis	≥8	R	≤0.12	S
Ertapenem	cell wall synthesis	≥8	R	≤0.5	S
Imipenem	cell wall synthesis	≥16	R	≤0.25	S
Meropenem	cell wall synthesis	≥16	R	≤0.25	S
Amikacin	protein synthesis	≥64	R	≤2	S
Tigecycline	protein synthesis	≤0.5	S	≤0.5	S
Ciprofloxacin	DNA replication	≤0.25	S	≤0.25	S
Levofloxacin	DNA replication	≤0.12	S	≤0.12	S

Note: S; Susceptible, I; intermediate, R; Resistant

Table 8 Antibiotic susceptibility profiles of *S. aureus* strains

Antibiotic	**Mode of action**	***S. aureus* ATCC 29213**		***S. aureus* ATCC 25923**	
		MICs	**Interpretation**	**MICs**	**Interpretation**
Oxacillin	cell wall synthesis	0.5	S	0.5	S
Vancomycin	cell wall synthesis	1	S	1	S
Erythromycin	protein synthesis	≤ 0.25	S	≤ 0.25	S
Linezolid	protein synthesis	4	S	2	S
Tetracycline	protein synthesis	≤ 1	S	≤ 1	S
Gentamicin	protein synthesis	≤ 0.5	S	≤ 0.5	S
Trimethoprim /Sulfamethoxazole	DNA synthesis	≤ 10	S	≤ 10	S
Rifampicin	DNA replication	≤ 0.5	S	≤ 0.5	S
Ciprofloxacin	DNA replication	≤ 0.5	S	≤ 0.5	S
Moxifloxacin	DNA replication	≤ 0.25	S	≤ 0.25	S

Note: S; Susceptible, I; intermediate, R; Resistant

1.2 Antibacterial activity of hydroquinine against several microorganisms

The antibacterial activity of hydroquinine against gram-positive and gram-negative bacteria tested in this study was reported by MIC and MBC values. The values of hydroquinine against the bacterial strains tested were investigated using broth microdilution and macrodilution methods. It was found that all bacteria tested were inhibited by hydroquinine with the same results from both methods, showing MIC values between 650 and 2,500 µg/mL and MBC values between 1,250 and 5,000 µg/mL (Table 9). Hydroquinine inhibited all gram-positive bacteria tested with MIC value was 1,250 µg/mL and MBC values between 1,250 and 2,500 µg/mL (Table 9). *E. coli* ATCC 25922 was inhibited with the lowest MIC values (650 µg/mL), whereas *P. aeruginosa* ATCC 27853 was inhibited with the highest MIC values (2,500 µg/mL). Moreover, hydroquinine showed the killing of all strains tested at specific concentrations, showing MBC values between 1,250 and 5,000 µg/mL (Table 9). It was noticeable that both *P. aeruginosa* strains were killed with the highest MBC values of 5,000 µg/mL, approximately 2–4-fold higher than other strains tested (Table 9) (221).

Table 9 The minimum inhibitory and minimum bactericidal concentrations (MIC and MBC) values of hydroquinine against the microorganisms tested.

Microorganisms	MICs of hydroquinine (µg/mL)	MBCs of hydroquinine (µg/mL)	Vehicle control [1] (%v/v)	MICs of CIP [2] (µg/mL)
Gram positive bacteria				
S. aureus ATCC 25923	1,250	1,250	>25%	ND
S. aureus ATCC 29213	1,250	2,500	>25%	0.5 (0.12-0.50)
Gram negative bacteria				
E. cloacae ATCC 2341	1,250	2,500	>25%	ND
E. coli ATCC 2452	1,250	1,250	>25%	ND
E. coli ATCC 25922	625	1,250	>25%	0.008 (0.004-0.016)
K. pneumoniae ATCC 1705	1,250	2,500	>25%	ND
P. aeruginosa ATCC BAA-2108	1,250	5,000	>25%	ND
P. aeruginosa ATCC 27853	2,500	5,000	>25%	0.5 (0.12-1.00)

[1] Vehicle control, DMSO and Tween-80 solution was used to dissolve hydroquinine. The MIC of >25% vehicle control means that the solvent did not influence the antibacterial results.

[2] ND means "not determined" because no MIC QC ranges provided in the CLSI document M100. The values in the blankets were the MIC QC ranges of the corresponding microorganisms shown in the CLSI document M100 (192).

1.3 Time-kill curve of hydroquinine against both DS and MDR *P. aeruginosa* reference strains

The time to kill both DS *P. aeruginosa* ATCC 27853 and MDR *P. aeruginosa* ATCC BAA-2108 of hydroquinine was investigated by time-kill curve analysis. It was found that without hydroquinine the number of both DS and MDR *P. aeruginosa* was almost 0% killing (Figure 16A, B). After 4 h of treatment, MIC of hydroquinine showed the killing at approximately 50%, whereas the ½ MIC of hydroquinine solution killed both strains at 20–40% after 4 h. The MBC value showed that each strain was killed by about 90% after 4 h. Hydroquinine-treated samples showed a statistically significant killing compared the untreated group by 4 h in both *P. aeruginosa* strains (p-value < 0.05), except at ¼ MIC of hydroquinine, the lowest dose tested in *P. aeruginosa* ATCC BAA-2108 (Figure 16B) (221).

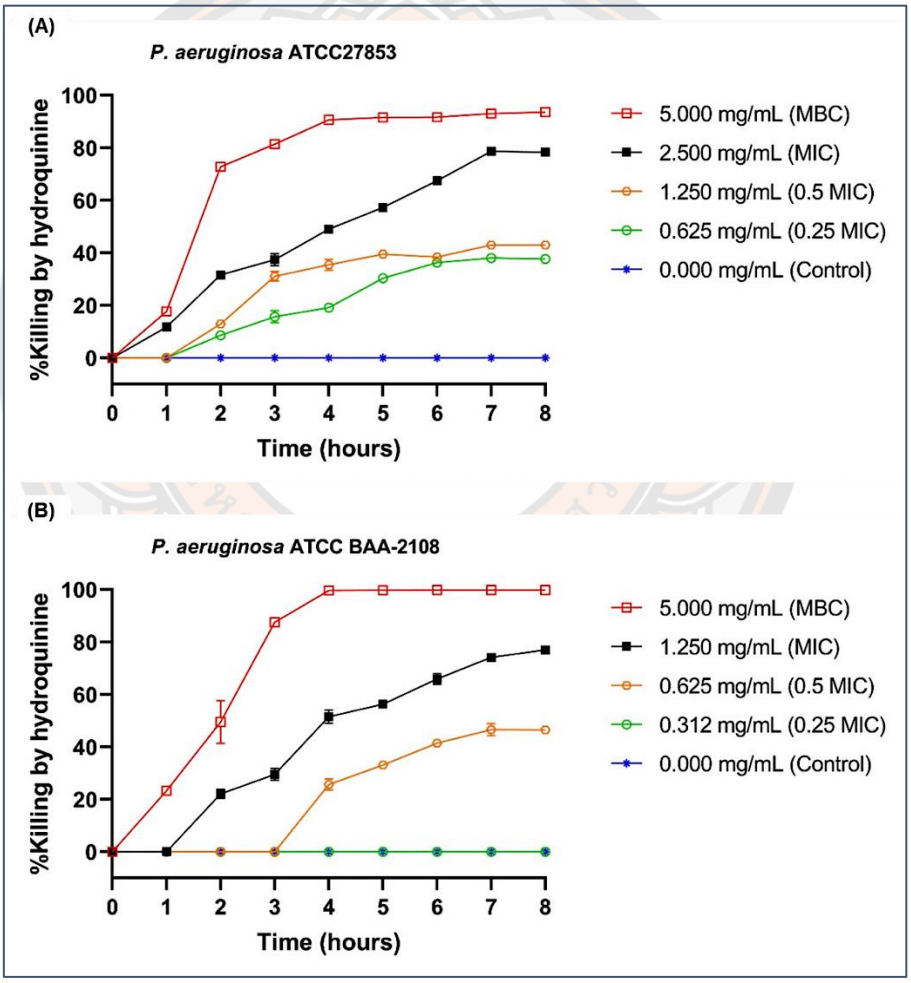

Figure 16 Time-kill curve of *P. aeruginosa* strains treated with and without hydroquinine.

(A) DS *P. aeruginosa* ATCC 27853 and (B) MDR *P. aeruginosa* ATCC BAA-2108 treated with and without indicated concentrations of hydroquinine at MBC, MIC, 0.5 × MIC, 0.25 × MIC. MBC; minimum bactericidal concentration, MIC; minimum inhibitory concentration (221).

1.4 Investigating synergistic effects of hydroquinine with antibiotics against MDR *P. aeruginosa* strains

In this experiment, we examined whether hydroquinine displayed synergistic effects with antibiotics that were ineffective against *P. aeruginosa* strain ATCC BAA-2108. The results identified that hydroquinine presented synergistic effects with imipenem, ampicillin and gentamicin with FICI values less than 1 (Table 10). The combination of hydroquinine and each antibiotic revealed the MIC values were reduced by at least 2-fold compared to the antibiotic or hydroquinine alone. Therefore, synergistic activity between each antibiotic and hydroquinine observed in *P. aeruginosa* strains suggested that hydroquinine might improve the efficacy of previously resisted antibiotics tested.

Table 10 Antibiotic resistance modulation in *P. aeruginosa* strain by hydroquinine

Antibiotics	Average of minimum inhibitory concentration (μg/mL)				FICI [a]
	Antibiotic	Antibiotic + Hydroquinine	Hydroquinine	Hydroquinine + Antibiotic	
Imipenem	32.0±0.0	12.0±5.6	1250±0.0	58.5±27.5	0.4±0.1
Gentamicin	8.0±0.0	3.6±1.1	1250±0.0	39.0±0.0	0.5±0.0
Ampicillin	128.0±0.0	0.5±0.0	1250±0.0	453.1±180.4	0.3±0.1

[a] Synergy, <1; additivity, =1; antagonism >1
FICI; Fractional inhibitory concentration index

2. Transcriptomic profiles of *P. aeruginosa* ATCC 27853 under hydroquinine treatment condition

2.1 Global transcriptomic changes in *P. aeruginosa* to hydroquinine

RNA-seq was used to investigate the molecular response of *P. aeruginosa* to hydroquinine (225). The bacteria were treated with ½ MIC of hydroquinine for a short exposure time (1 h). Total read bases were approximately 1.35×10^9 and 1.11×10^9 base pairs, respectively, with a great Phred quality score (Q20) over 97.97%. After trimming low-quality reads using FastP software, the raw sequencing reads for hydroquinine-treated and untreated conditions were 4,465,440 and 3,665,572 bps, respectively. After mapping to the genome of *P. aeruginosa* (PAO1 genome reference), the read counts of functional genes assigned features in treated and untreated with hydroquinine were 3,565,444 (80.6%) and 2,968,484 (81.7%), respectively.

Data analysis of DEGs was conducted using edgeR, and the result revealed that hydroquinine at ½ MIC significantly affects the transcriptomic profile of *P. aeruginosa* ATCC 27853 compared to the untreated control. The *P. aeruginosa* treatment with hydroquinine strongly induced the differential expression genes ($\log_2$ fold change ≥ 2 and a false discovery rate (FDR) ≤ 0.05) of 254 genes, including 157 genes ($\log_2$-fold change from 2.09 to 9.47) upregulated and 97 genes ($\log_2$-fold change from -5.07 to -2.09) downregulated (Figure 17A) (Table 11) (225). The changes in genome-wide expression of *P. aeruginosa* treated with hydroquinine were

represented as a volcano plot to identify genes with substantial fold changes and statistical significance (Figure 17B).

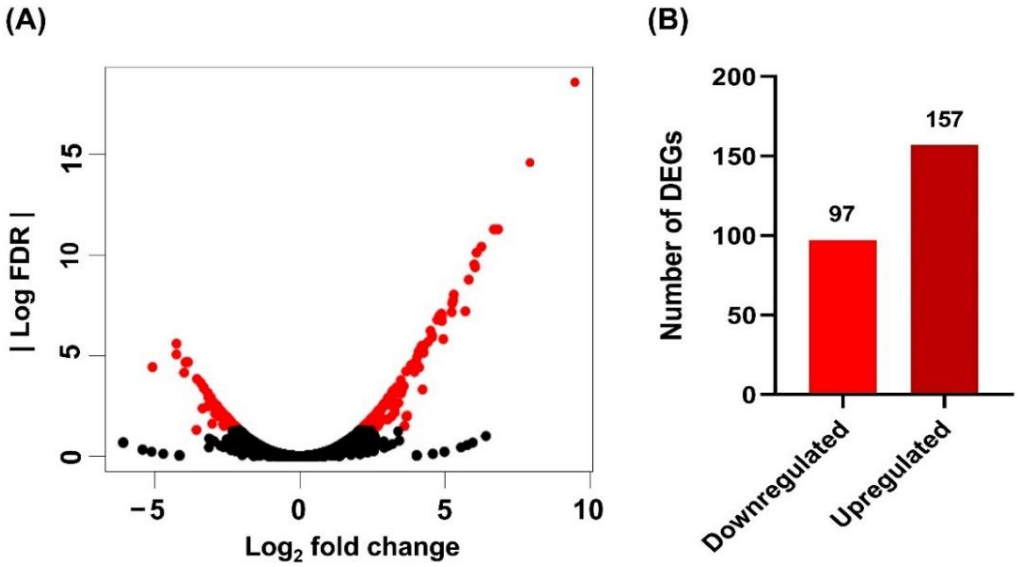

Figure 17 The differential expressed genes (DEGs) of *P. aeruginosa* ATCC 27853 in response to hydroquinine.

Showing (A) volcano plot with the statistically significant DEGs as red dots and non-significant DEGs as black dots as well as (B) the DEG number of downregulation and upregulation (225).

Table 11 List of significant differential expression genes in *P. aeruginosa* ATCC 27853 under ½ MIC of hydroquinine treatment

DEGs	logFC	FDR	Product genes	RefSeq
PA4599	9.47	2.56E-19	Resistance-Nodulation-Cell Division (RND) multidrug efflux membrane fusion protein MexC precursor	NP_253289
PA1225	7.93	2.53E-15	NAD(P)H dehydrogenase	NP_249916
PA4990	6.84	5.22E-12	SMR multidrug efflux transporter	NP_253677
PA2932	6.69	5.22E-12	morphinone reductase	NP_251622
PA4598	6.27	3.83E-11	Resistance-Nodulation-Cell Division (RND) multidrug efflux transporter MexD	NP_253288
PA4354	6.10	7.51E-11	hypothetical protein	NP_253044
PA1282	6.05	3.91E-10	major facilitator superfamily (MFS) transporter	NP_249973
PA4597	6.02	2.90E-10	Multidrug efflux outer membrane protein OprJ precursor	NP_253287
PA3720	5.83	1.66E-09	hypothetical protein	NP_252409
PA3719	5.71	6.10E-08	antirepressor for MexR, ArmR	NP_252408
PA2931	5.31	9.16E-09	CifR	NP_251621
PA0465	5.29	1.73E-08	inner membrane protein CreD	NP_249156
PA2019	5.26	2.47E-08	Resistance-Nodulation-Cell Division (RND) multidrug efflux membrane fusion protein MexX precursor	NP_250709
PA2850	5.24	6.77E-08	organic hydroperoxide resistance protein	NP_251540
PA0466	4.95	1.48E-06	hypothetical protein	NP_249157
PA4288	4.90	1.85E-07	transcriptional regulator	NP_252978
PA2018	4.90	9.60E-08	Resistance-Nodulation-Cell Division (RND) multidrug efflux transporter MexY	NP_250708
PA0534	4.89	1.04E-07	FAD-dependent oxidoreductase	NP_249225
PA4623	4.88	8.16E-08	hypothetical protein	NP_253313
PA3126	4.82	1.04E-07	heat-shock protein IbpA	NP_251816
PA3690	4.75	1.64E-07	metal-transporting P-type ATPase	NP_252380
PA1297	4.56	1.19E-06	metal transporter	NP_249988
PA1283	4.56	9.32E-07	transcriptional regulator	NP_249974
PA4881	4.51	5.75E-07	hypothetical protein	NP_253568
PA0125	4.42	2.04E-06	ParD antitoxin	NP_248815
PA1970	4.29	3.16E-06	hypothetical protein	NP_250660
PA4596	4.28	6.98E-06	EsrC	NP_253286
PA2274	4.24	0.0005	hypothetical protein	NP_250964
PA3732	4.22	3.10E-06	Uncharacterized protein	NP_252421
PA3731	4.19	3.53E-06	hypothetical protein	NP_252420
PA0124	4.19	6.12E-06	ParE toxin	NP_248814

Table 11 List of significant differential expression genes in *P. aeruginosa* ATCC 27853 under ½ MIC of hydroquinine treatment (Cont.)

DEGs	logFC	FDR	Product genes	RefSeq
PA1290	4.12	3.75E-05	transcriptional regulator	NP_249981
PA4355	4.10	6.22E-06	PyeM	NP_253045
PA0736a	4.06	1.09E-05	hypothetical protein	NP_249427
PA1744	4.03	2.06E-05	hypothetical protein	NP_250435
PA0737	3.98	2.06E-05	hypothetical protein	NP_249428
PA1298	3.96	6.30E-05	hypothetical protein	NP_249989
PA1223	3.95	3.61E-05	transcriptional regulator	NP_249914
PA1137	3.84	2.88E-05	oxidoreductase	NP_249828
PA0474	3.71	0.0096	hypothetical protein	NP_249165
PA1503	3.67	0.0104	hypothetical protein	NP_250194
PA1030	3.67	5.97E-05	hypothetical protein	NP_249721
PA2782	3.61	0.0306	biofilm-associated metzincin Inhibitor, BamI	NP_251472
PA2277	3.59	0.0003	ArsR protein	NP_250967
PA2054	3.53	0.0005	transcriptional regulator CynR	NP_250744
PA2433	3.50	0.0007	hypothetical protein	NP_251123
PA1942	3.49	0.0002	hypothetical protein	NP_250632
PA1291	3.47	0.0003	hypothetical protein	NP_249982
PA3390	3.41	0.0022	hypothetical protein	NP_252079
PA3062	3.40	0.0005	PelC	NP_251752
PA4986	3.38	0.0004	oxidoreductase	NP_253673
PA1343	3.33	0.0004	hypothetical protein	NP_250034
PA0424	3.32	0.0005	multidrug resistance operon repressor MexR	NP_249115
PA2469	3.28	0.0023	transcriptional regulator	NP_251159
PA0476	3.28	0.0065	permease	NP_249167
PA2746a	3.27	0.0007	hypothetical protein	NP_251436
PA2933	3.27	0.0044	major facilitator superfamily (MFS) transporter	NP_251623
PA3962	3.24	0.0006	hypothetical protein	NP_252651
PA4762	3.23	0.0005	heat shock protein GrpE	NP_253450
PA4600	3.21	0.0007	transcriptional regulator NfxB	NP_253290
PA4985	3.19	0.0009	Uncharacterized protein	NP_253672
PA1743	3.19	0.0016	hypothetical protein	NP_250434
PA3819	3.18	0.0007	hypothetical protein	NP_252508
PA1290	4.12	3.75E-05	transcriptional regulator	NP_249981
PA0779	2.93	0.0022	AsrA	NP_249470
PA3552	2.90	0.0028	ArnB	NP_252242
PA4495	2.89	0.0026	hypothetical protein	NP_253185
PA3718	2.89	0.0138	major facilitator superfamily (MFS) transporter	NP_252407
PA5054	2.09	0.0468	heat shock protein HslU	NP_253741

Table 11 List of significant differential expression genes in *P. aeruginosa* ATCC 27853 under ½ MIC of hydroquinine treatment (Cont.)

DEGs	logFC	FDR	Product genes	RefSeq
PA1457	-2.09	0.0480	chemotaxis protein CheZ	NP_250148
PA1561	-2.11	0.0441	aerotaxis receptor Aer	NP_250252
PA5030	-2.14	0.0432	major facilitator superfamily (MFS) transporter	NP_253717
PA5027	-2.15	0.0405	hypothetical protein	NP_253714
PA1456	-2.16	0.0413	two-component response regulator CheY	NP_250147
PA4921	-2.16	0.0448	cholinesterase, ChoE	NP_253608
PA3912	-2.17	0.0431	hypothetical protein	NP_252601
PA5207	-2.17	0.0405	phosphate transporter	NP_253894
PA3613	-2.17	0.0367	hypothetical protein	NP_252303
PA1083	-2.18	0.0413	flagellar L-ring protein precursor FlgH	NP_249774
PA0518	-2.19	0.0364	cytochrome c-551 precursor	NP_249209
PA4523	-2.20	0.0356	hypothetical protein	NP_253213
PA3350	-2.20	0.0431	hypothetical protein	NP_252040
PA0519	-2.21	0.0328	nitrite reductase precursor	NP_249210
PA1086	-2.21	0.0370	flagellar hook-associated protein 1 FlgK	NP_249777
PA0526	-2.22	0.0405	hypothetical protein	NP_249217
PA5159	-2.22	0.0442	multidrug resistance protein	NP_253846
PA1102	-2.23	0.0322	flagellar motor switch protein FliG	NP_249793
PA4348	-2.24	0.0305	hypothetical protein	NP_253038
PA4074	-2.25	0.0367	transcriptional regulator	NP_252763
PA3429	-2.26	0.0425	epoxide hydrolase	NP_252119
PA1101	-2.26	0.0292	Flagella M-ring outer membrane protein precursor	NP_249792
PA4551	-2.27	0.0355	type 4 fimbrial biogenesis protein PilV	NP_253241
PA4796	-2.28	0.0405	hypothetical protein	NP_253484
PA4535	-2.29	0.0328	hypothetical protein	NP_253225
PA4536	-2.31	0.0345	hypothetical protein	NP_253226
PA3394	-2.31	0.0283	NosF protein	NP_252084
PA3913	-2.32	0.0258	protease	NP_252602
PA1085	-2.33	0.0241	flagellar protein FlgJ	NP_249776
PA1079	-2.33	0.0276	flagellar basal-body rod modification protein FlgD	NP_249770
PA4359	-2.33	0.0306	hypothetical protein	NP_253049
PA1555	-2.34	0.0216	Cytochrome c oxidase, cbb3-type, CcoP subunit	NP_250246
PA2119	-2.35	0.0216	alcohol dehydrogenase (Zn-dependent)	NP_250809

Table 11 List of significant differential expression genes in *P. aeruginosa* ATCC 27853 under ½ MIC of hydroquinine treatment (Cont.)

DEGs	logFC	FDR	Product genes	RefSeq
PA3432	-2.35	0.0265	hypothetical protein	NP_252122
PA1736	-2.36	0.0226	acyl-CoA thiolase	NP_250427
PA1557	-2.37	0.0187	Cytochrome c oxidase, cbb3-type, CcoN subunit	NP_250248
PA1077	-2.38	0.0243	flagellar basal-body rod protein FlgB	NP_249768
PA4550	-2.39	0.0257	type 4 fimbrial biogenesis protein FimU	NP_253240
PA5497	-2.43	0.0152	class II (cobalamin-dependent) ribonucleotide-diphosphate reductase subunit, NrdJa	NP_254184
PA4100	-2.43	0.0154	dehydrogenase	NP_252789
PA0951a	-2.44	0.0219	ribonuclease	NP_249642
PA4517	-2.46	0.0226	chemotaxis protein CheZ	NP_250148
PA1103	-2.46	0.0157	flagellar assembly protein	NP_249794
PA5160	-2.46	0.0226	drug efflux transporter	NP_253847
PA2126	-2.48	0.0157	cupA gene regulator C, CgrC	NP_250816
PA1546	-2.48	0.0130	oxygen-independent coproporphyrinogen III oxidase	NP_250237
PA1555	-2.48	0.0131	Cytochrome c oxidase, cbb3-type, CcoP subunit	NP_250246
PA4465	-2.48	0.0130	hypothetical protein	NP_253155
PA4571	-2.49	0.0128	cytochrome c	NP_253261
PA4328	-2.49	0.0130	hypothetical protein	NP_253018
PA5496	-2.50	0.0130	class II (cobalamin-dependent) ribonucleotide-diphosphate reductase subunit, NrdJb	NP_254183
PA0141	-2.51	0.0117	hypothetical protein	NP_248831
PA3431	-2.52	0.0152	hypothetical protein	NP_252121
PA4587	-2.52	0.0109	cytochrome c551 peroxidase precursor	NP_253277
PA4073	-2.58	0.0093	aldehyde dehydrogenase	NP_252762
PA1556	-2.59	0.0087	Cytochrome c oxidase, cbb3-type, CcoO subunit	NP_250247
PA3416	-2.60	0.0306	pyruvate dehydrogenase E1 component, beta chain	NP_252106
PA0527	-2.61	0.0091	transcriptional regulator Dnr	NP_249218
PA3614	-2.62	0.0081	hypothetical protein	NP_252304
PA0517	-2.63	0.0087	c-type cytochrome precursor nirC	NP_249208
PA2380	-2.64	0.0252	hypothetical protein	NP_251070
PA3049	-2.64	0.0081	ribosome modulation factor	NP_251739
PA0515	-2.66	0.0077	transcriptional regulator	NP_249206
PA3919	-2.68	0.0062	hypothetical protein	NP_252608

Table 11 List of significant differential expression genes in *P. aeruginosa* ATCC 27853 under ½ MIC of hydroquinine treatment (Cont.)

DEGs	logFC	FDR	Product genes	RefSeq
PA2567	-2.72	0.0053	hypothetical protein	NP_251257
PA5026	-2.74	0.0104	hypothetical protein	NP_253713
PA2118a	-2.74	0.0104	O6-methylguanine-DNA methyltransferase	NP_250808
PA0512	-2.78	0.0051	NirH	NP_249203
PA0178	-2.79	0.0098	two-component sensor	NP_248868
PA5475	-2.83	0.0032	hypothetical protein	NP_254162
PA1920	-2.85	0.0031	class III (anaerobic) ribonucleoside-triphosphate reductase subunit, NrdD	NP_250610
PA3458	-2.88	0.0031	transcriptional regulator	NP_252148
PA0276	-2.89	0.0046	hypothetical protein	NP_248967
PA4071	-2.91	0.0032	hypothetical protein	NP_252760
PA1918	-2.91	0.0074	hypothetical protein	NP_250608
PA1078	-2.93	0.0039	flagellar basal-body rod protein FlgC	NP_249769
PA0516	-2.94	0.0023	heme d1 biosynthesis protein NirF	NP_249207
PA0514	-2.97	0.0023	heme d1 biosynthesis protein NirL	NP_249205
PA1916	-3.01	0.0235	amino acid permease	NP_250606
PA4072	-3.06	0.0012	amino acid permease	NP_252761
PA2318	-3.06	0.0012	hypothetical protein	NP_251008
PA0513	-3.15	0.0012	NirG	NP_249204
PA3337	-3.16	0.0007	ADP-L-glycero-D-mannoheptose 6-epimerase	NP_252027
PA5231	-3.17	0.0007	ATP-binding/permease fusion ABC transporter	NP_253918
PA0714	-3.17	0.0033	hypothetical protein	NP_249405
PA2317	-3.29	0.0004	oxidoreductase	NP_251007
PA5172	-3.32	0.0004	ornithine carbamoyltransferase, catabolic	NP_253859
PA4681	-3.35	0.0041	hypothetical protein	NP_253370
PA5173	-3.41	0.0002	carbamate kinase	NP_253860
PA5230	-3.54	0.0001	permease of ABC transporter	NP_253917
PA1917	-3.56	0.0480	hypothetical protein	NP_250607
PA5171	-3.85	2.06E-05	arginine deiminase	NP_253858
PA1919	-3.94	2.09E-05	class III (anaerobic) ribonucleoside-triphosphate reductase activating protein, 'activase', NrdG	NP_250609
PA4682	-3.98	6.90E-05	hypothetical protein	NP_253371
PA5170	-4.24	2.51E-06	arginine/ornithine antiporter	NP_253857
PA4683	-4.25	8.54E-06	hypothetical protein	NP_253372
PA0713	-5.07	3.66E-05	hypothetical protein	NP_249404

DEGs; Difference expression genes

LogFC; log_2 gene expression fold changes.
FDR; false discovery rate with a statistical significance of p value ≤ 0.05.
RefSeq_protein; code of genes for analysis

2.2 Analysis of the most up- and down-regulated DEGs of *P. aeruginosa* ATCC 27853 in response to hydroquinine

A heatmap of the top 25 most significantly up- and downregulated DEGs of *P. aeruginosa* ATCC 27853 following treatment with ½ MIC of hydroquinine is shown in Figure 18. The top 25 up-regulated genes showed the most function involved in the Resistance-Nodulation-Cell Division (RND) multidrug efflux pump, including *mexC*, *mexD*, *OprJ*, *mexX*, and *mexY* with log_2-fold change was 9.47, 6.27, 6.02, 5.26 and 4.90, respectively (Table 11). These genes encode membrane fusion protein (*mexC*, *mexX*), multidrug efflux transporter protein (*mexD*, *mexY*), and multidrug efflux outer membrane protein (*OprJ*). Interestingly, four of the top 25 down-regulated genes associated the arginine deiminase (ADI)-pathway, namely *arcA*, *arcB*, *arcC*, and *arcD* genes, with log_2-fold changes were -3.85, -3.32, - 3.41, and -4.24, respectively (Table 11). These genes encode enzyme arginine deiminase (*arcA*), ornithine carbamoyltransferase (*arcB*), carbamate kinase (*arcC*) and protein arginine/ornithine antiporter (*arcD*).

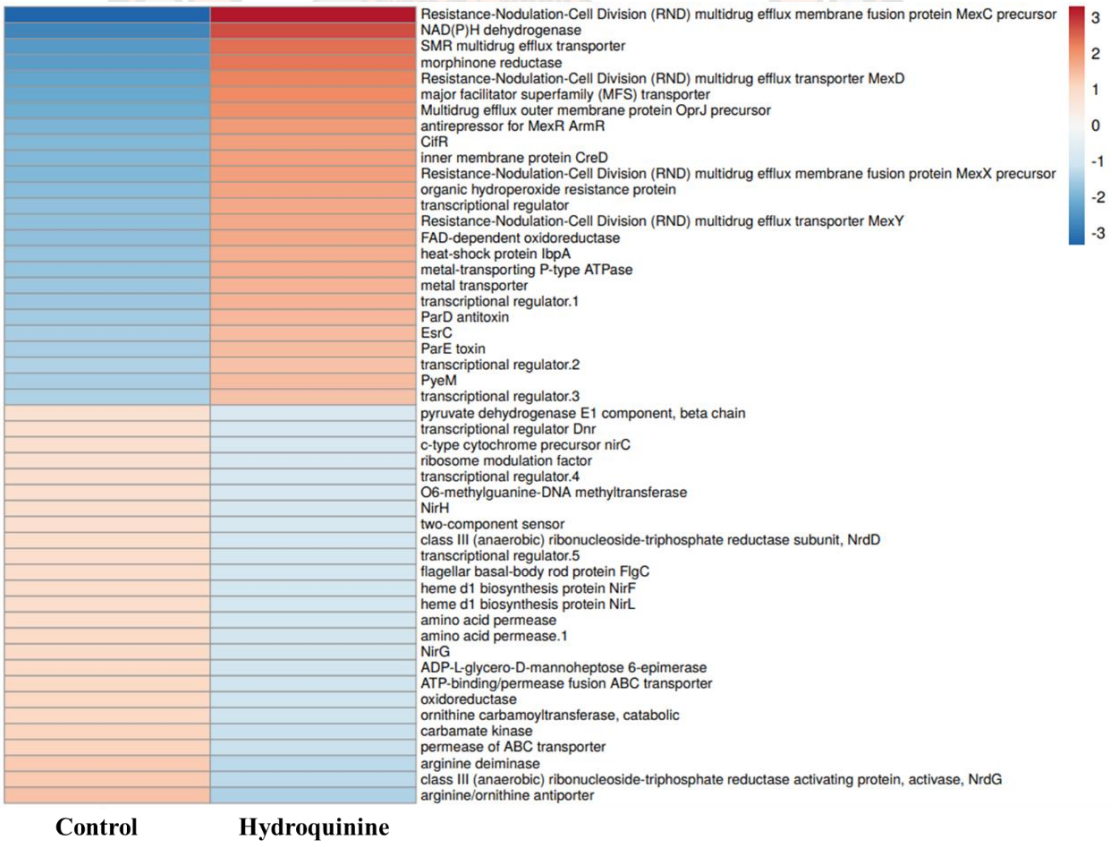

Figure 18 Clustered heatmap of transcriptional response in top 25 up and downregulated DEGs of *P. aeruginosa* ATCC 27853 after treatment with and without hydroquinine for one hour.
Each column represents one sample, and each row represents one gene.

2.3 Gene Ontology (GO) enrichment analysis of up- and down-regulated DEGs of *P. aeruginosa* ATCC 27853 in response to hydroquinine

GO analysis was performed by the DAVID online database to further investigate the biological functions of DEGs of *P. aeruginosa* ATCC 27853 exposed to ½ MIC of hydroquinine. The enrichment scores of 254 DEGs were ordered and represented various biological processes (BP), cellular components (CC), and molecular functions (MF) (Figure 19). The upregulated DEG functions in ½ MIC of hydroquinine exposure are annotated in Figure 18A. The most significantly enriched BP for up-regulated DEGs in the presence of hydroquinine was related to the regulation of transcription (Figure 19A). Protein-DNA complex showed the highest number of up-regulated DEGs for the CC category. For MF of up-regulated DEGs, it showed that the most significant enrichment is involved in the transcription factor activity of sequence-specific DNA binding. The function of down-regulated DEGs in the presence of hydroquinine of *P. aeruginosa* ATCC 27853 is shown in Figure 18B. Interestingly, the most significantly enriched BP, MF and CC for downregulated DEGs were related to function of flagella (Figure 19B).

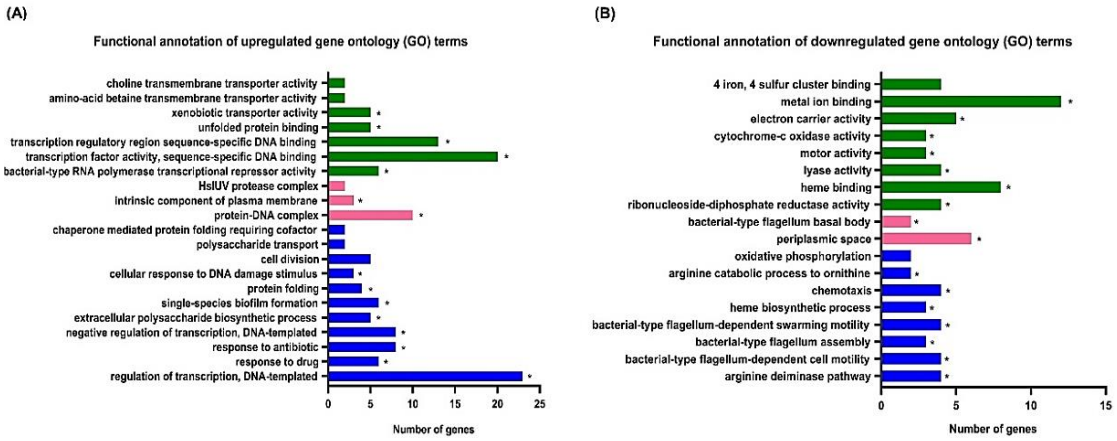

Figure 19 Enrichment scores by gene ontology (GO) analysis of 254 DEGs after *P. aeruginosa* ATCC 27853 was treated with hydroquinine for one hour.

Showing (A) functional annotation of significantly upregulated DEGs, and (B) functional annotation of significantly downregulated DEGs. The blue bars represent biological processes, the pink bars represent cellular components, and the green bars represent molecular functions. The asterisk (*) symbol is $p < 0.05$ as considered significant (225).

2.4 Kyoto Encyclopedia of Genes and Genomes (KEGG) pathway enrichment analysis of up and down-regulated DEGs of *P. aeruginosa* ATCC 27853 in response to hydroquinine

KEGG pathway analysis of significantly up- and downregulated DEGs was performed by the DAVID online database to further investigate the gene functions into pathways of *P. aeruginosa* ATCC 27853 exposed to ½ MIC of hydroquinine. In terms of upregulated DEGs of *P. aeruginosa* ATCC 27853 treated with hydroquinine for 1 h, the KEGG pathway enrichment revealed that hydroquinine significantly affected several cellular pathways and induced the gene functions involved in beta-

lactam resistance, biofilm formation, amino sugar and nucleotide sugar metabolism, and cationic antimicrobial peptide (CAMP) resistance (Figure 20-23). The number of genes involved in beta-lactam resistance and biofilm formation were the most affected KEGG pathways in *P. aeruginosa* exposed hydroquinine (Table 12). The relative fold change of the DEGs involved in beta-lactam resistance mechanism showed significant upregulation log_2-fold change from 5.71 to 2.37, as shown in Table12. Five genes, namely *armR*, *mexR*, *mexZ*, *PA2018*, and *PA2019*, involving beta-lactam resistance, were transcribed in response to hydroquinine (Figure 20). These genes encoded protein MexR anti-repressor ArmR, multidrug resistance operon repressor MexR, MexZ, multidrug efflux protein MexY, and multidrug efflux lipoprotein MexX, respectively. Regarding the biofilm formation pathway, KEEG analysis revealed that five genes (*pelA*, *pelB*, *pelC*, *pelF*, and *pelG*) in the group of upregulated DEGs of *P. aeruginosa* (log_2-fold change from 3.40 to 2.14) were affected by hydroquinine (Figure 21). These genes encoded hypothetical protein PelA, biofilm biosynthesis protein PelB, biofilm biosynthesis outer membrane protein PelC, biofilm biosynthesis glycosyltransferase PelF and biofilm biosynthesis Wzx-like polysaccharide transporter PelG, respectively. Four upregulated DEGs *arnA*, *arnB*, *arnC* and *PA3559* (log_2-fold change from 2.90 to 2.35) encoded UDP-glucuronic acid decarboxylase enzyme, UDP-4-amino-4-deoxy-L-arabinose-oxoglutarate aminotransferase, undecaprenyl-phosphate 4-deoxy-4-formamido-L-arabinose transferase and nucleotide sugar dehydrogenase, respectively, which involved in amino sugar and nucleotide sugar metabolism functions (Figure 22). Interestingly, upregulated *arn* genes, including *arnA*, *arnB*, and *arnC*, were also shown in KEGG pathway enrichment with significantly induced the cationic antimicrobial peptide (CAMP) resistance pathway after exposure to hydroquinine (Figure 23).

Table 12 Lits of up- regulated genes in KEGG pathway of in *P. aeruginosa* ATCC 27853 under ½ MIC hydroquinine treatment

No.	KEGG pathway	Number of genes	Up-regulated genes	Log_2 FC	FDR	*p*-Value
1	Beta-lactam resistance	5	*armR*	5.71	6.10×10^{-8}	1.48×10^{-10}
			PA2019	5.26	2.47×10^{-8}	5.55×10^{-11}
			PA2018	4.90	9.60×10^{-8}	2.88×10^{-10}
			mexR	3.32	5.00×10^{-4}	5.47×10^{-6}
			mexZ	2.37	2.26×10^{-2}	7.00×10^{-4}
2	biofilm formation	5	*pelC*	3.40	5.00×10^{-4}	5.02×10^{-6}
			pelA	2.79	4.20×10^{-3}	7.46×10^{-5}
			pelB	2.55	1.08×10^{-2}	3.00×10^{-4}
			pelf	2.27	2.93×10^{-2}	1.10×10^{-3}
			pelG	2.14	4.80×10^{-2}	2.20×10^{-3}
3	amino sugar and nucleotide sugar metabolism, and	4	*arnB*	2.90	2.80×10^{-3}	4.38×10^{-5}
			arnA	2.86	3.10×10^{-3}	4.96×10^{-5}
			arnC	2.35	2.26×10^{-2}	7.00×10^{-4}
			PA3559	2.35	2.34×10^{-2}	8.00×10^{-4}
4	cationic antimicrobial peptide (CAMP) resistance	3	*arnB*	2.90	2.80×10^{-3}	4.38×10^{-5}
			arnA	2.86	3.10×10^{-3}	4.96×10^{-5}
			arnC	2.35	2.26×10^{-2}	7.00×10^{-4}

Log_2FC; log_2 gene expression fold changes.
FDR; false discovery rate with a statistical significance of p-value ≤ 0.05

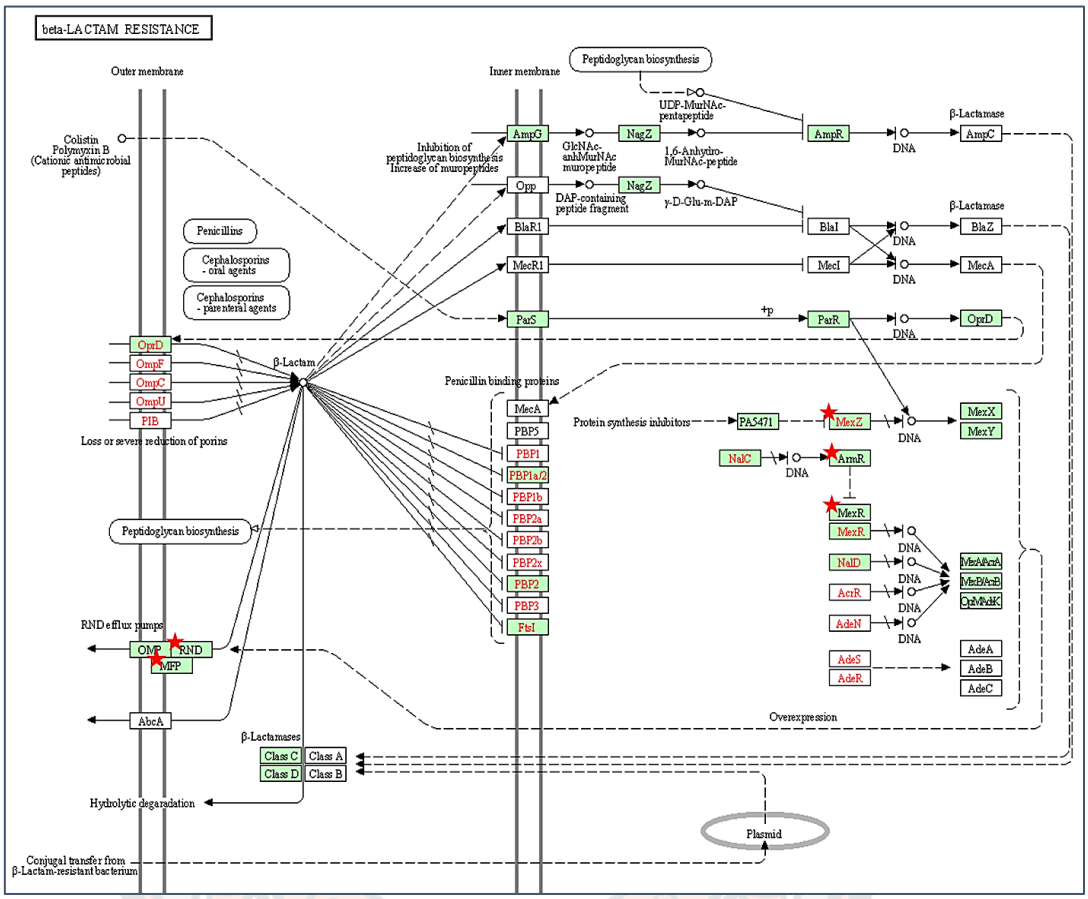

Figure 20 The KEGG pathways analyzed based on RNA sequencing analysis of beta-lactam resistance.

The red stars represent up-regulated DEGs of *P. aeruginosa* ATCC 27853 responded to half-hydroquinine concentration for 1 hour. Data from https://david.ncifcrf.gov/ 2021 updated database, accessed on 20 September 2022.

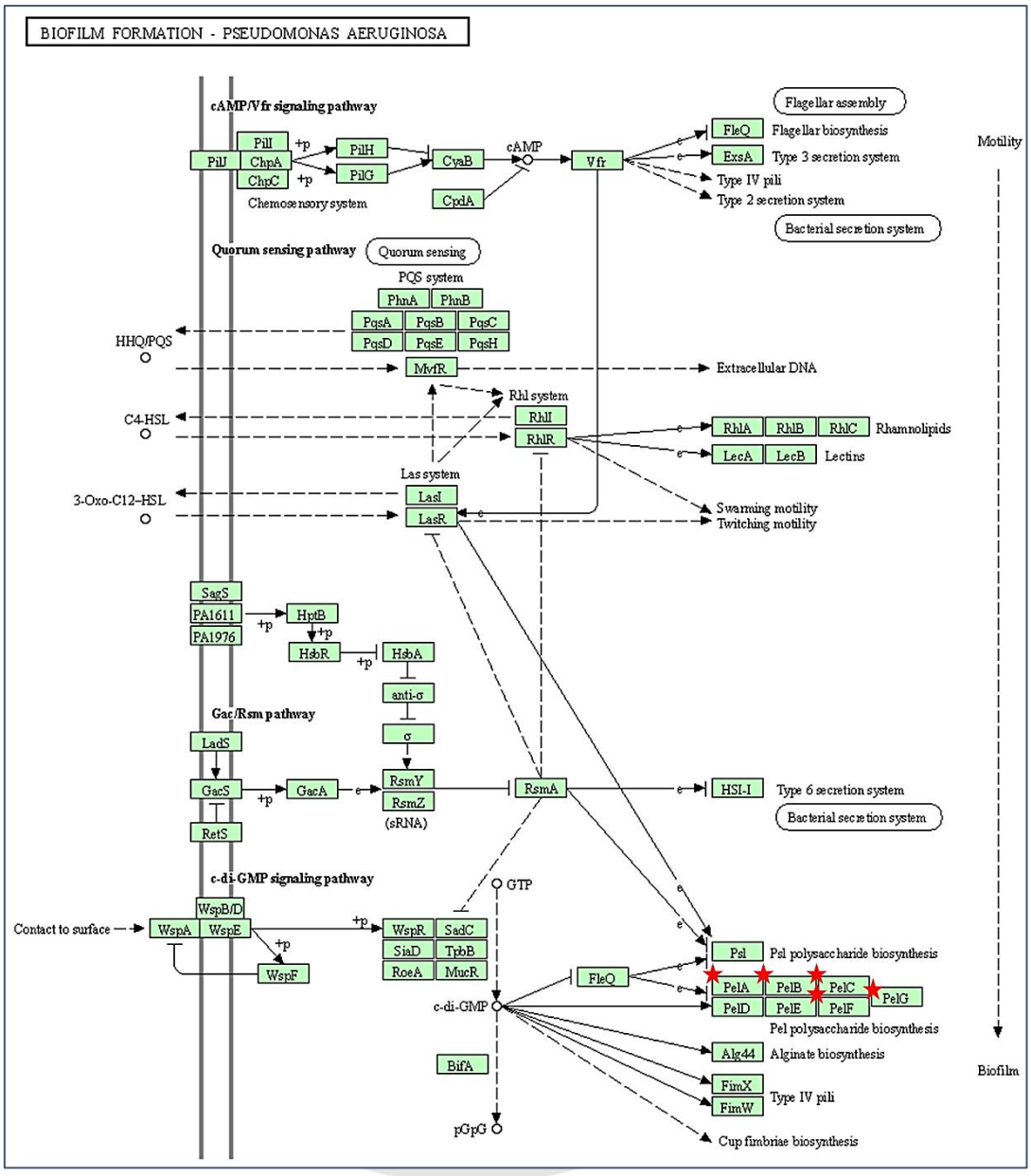

Figure 21 The KEGG pathways analyzed based on RNA sequencing analysis of biofilm formation.

The red stars represent up-regulated DEGs of *P. aeruginosa* ATCC 27853 responded to half-hydroquinine concentration for 1 hour. Data from https://david.ncifcrf.gov/ 2021 updated database, accessed on 20 September 2022.

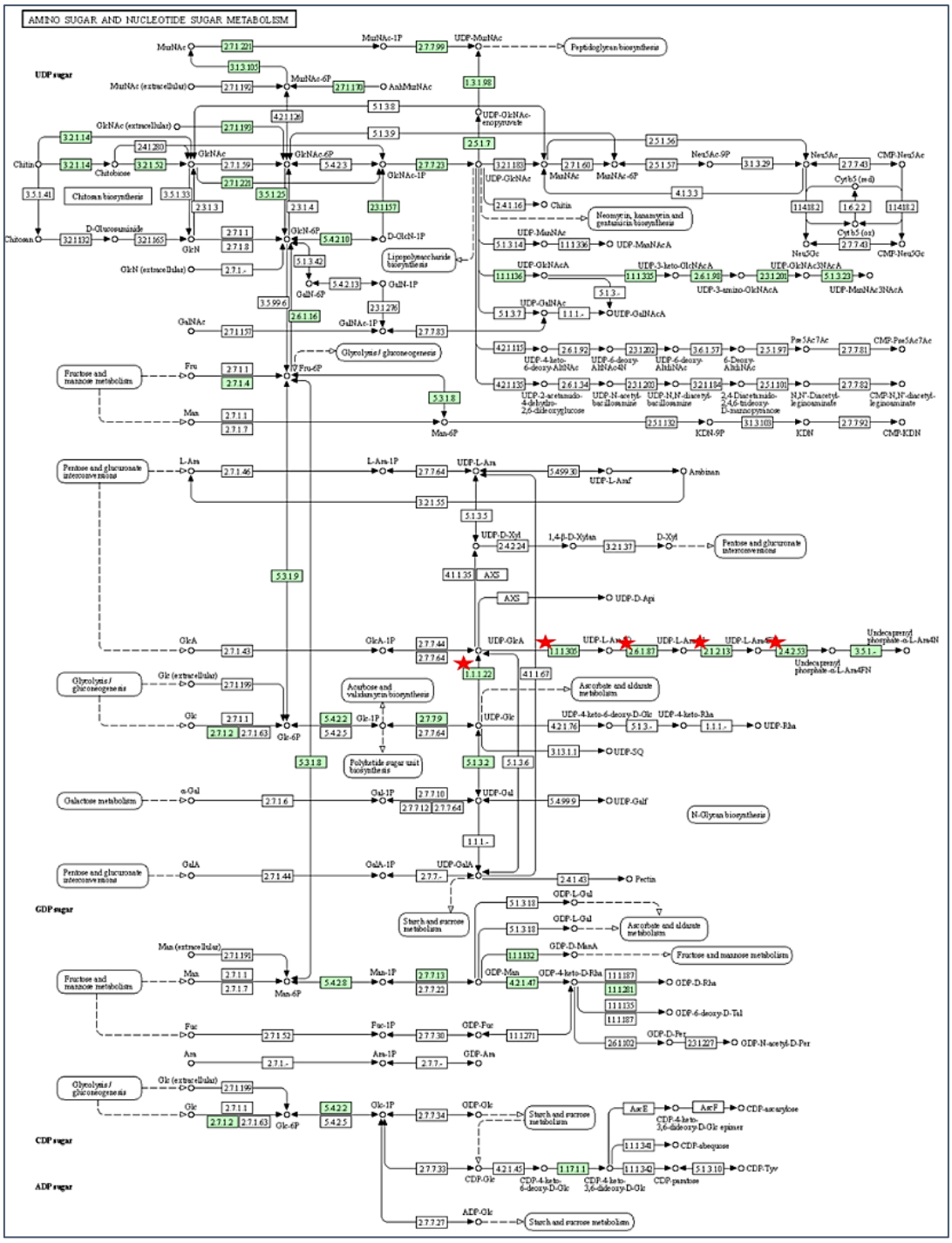

Figure 22 The KEGG pathways analyzed based on RNA sequencing analysis of amino sugar and nucleotide sugar metabolism.

The red stars represent up-regulated DEGs of *P. aeruginosa* ATCC 27853 responded to half-hydroquinine concentration for 1 hour. Data from https://david.ncifcrf.gov/ 2021 updated database, accessed on 20 September 2022.

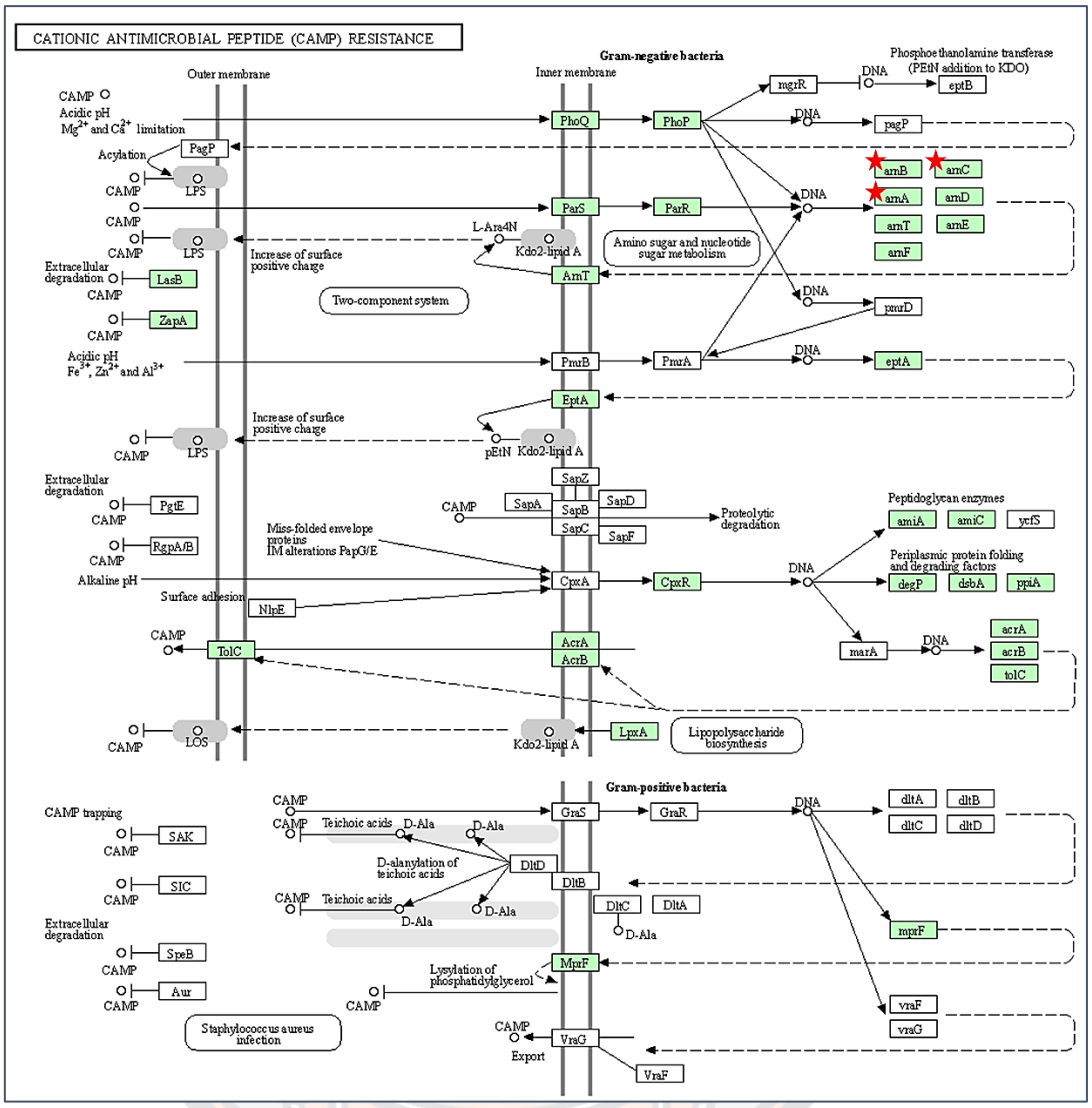

Figure 23 The KEGG pathways analyzed based on RNA sequencing analysis of cationic antimicrobial peptide (CAMP) resistance.

The red stars represent up-regulated DEGs of *P. aeruginosa* ATCC 27853 responded to half-hydroquinine concentration for 1 hour. Data from https://david.ncifcrf.gov/ 2021 updated database, accessed on 20 September 2022.

KEGG pathway analysis of down-regulated DEGs in *P. aeruginosa* ATCC 27853 revealed that genes associated with the mechanism of flagella assembly and bacterial chemotaxis were significantly affected in response to hydroquinine in *P. aeruginosa* ATCC 27853 for 1 h (Table 13). The relative fold change of the DEGs involved in flagella assembly showed significant downregulation $\log_2$-fold change from -2.93 to -2.18, as shown in Table 13. Ten genes associated flagella assembly encoded flagellar basal body rod proteins (*flgB*, *flgC*, *flgH*, *flgJ*, *fliF*), flagellar assembly protein (PA1103), flagellar basal-body rod modification protein FlgD (*flgD*), flagellar motor switch protein FliG (*fliG*), flagellar hook-associated protein FlgK (*flgK*), hypothetical protein (*PA3350*) and flagellar L-ring protein precursor FlgH (*flgH*) (Figure 24). Regarding the bacterial chemotaxis pathway, KEGG analysis

of down-regulated DEGs in *P. aeruginosa* revealed that five genes, namely PA0178, *cheZ*, *fliG*, *cheY*, and *aer* (log_2-fold change from -2.79 to -2.11) were affected by hydroquinine (Figure 25). These genes encored two-component sensor protein, protein phosphatase CheZ, flagellar motor switch protein FliG, chemotaxis protein CheY and aerotaxis receptor Aer, respectively.

Table 13 Lits of down- regulated genes in KEGG pathway of in *P. aeruginosa* ATCC 27853 under ½ MIC hydroquinine treatment

No.	KEGG pathway	Number of genes	Down-regulated genes	Log_2 FC	FDR	*p*-Value
1	Flagellar assembly	10	*flgC*	-2.93	3.866×10^{-3}	6.66×10^{-5}
			PA1103	-2.46	1.574×10^{-2}	4.51×10^{-4}
			flgB	-2.38	2.433×10^{-2}	8.29×10^{-4}
			flgD	-2.33	2.760×10^{-2}	9.77×10^{-4}
			flgJ	-2.33	2.414×10^{-2}	8.18×10^{-4}
			fliF	-2.26	2.923×10^{-2}	1.04×10^{-3}
			fliG	-2.23	3.219×10^{-2}	1.22×10^{-3}
			flgK	-2.21	3.698×10^{-2}	1.51×10^{-3}
			PA3350	-2.19	4.309×10^{-2}	1.87×10^{-3}
			flgH	-2.18	4.130×10^{-2}	1.76×10^{-3}
2	Bacterial chemotaxis	5	PA0178	-2.79	9.771×10^{-3}	2.18×10^{-4}
			cheZ	-2.46	2.260×10^{-2}	7.13×10^{-4}
			fliG	-2.23	3.219×10^{-2}	1.22×10^{-3}
			cheY	-2.15	4.130×10^{-2}	1.76×10^{-3}
			aer	-2.11	4.409×10^{-2}	1.94×10^{-3}

Log_2FC; log_2 gene expression fold changes.
FDR; false discovery rate with a statistical significance of *p*-value ≤ 0.05

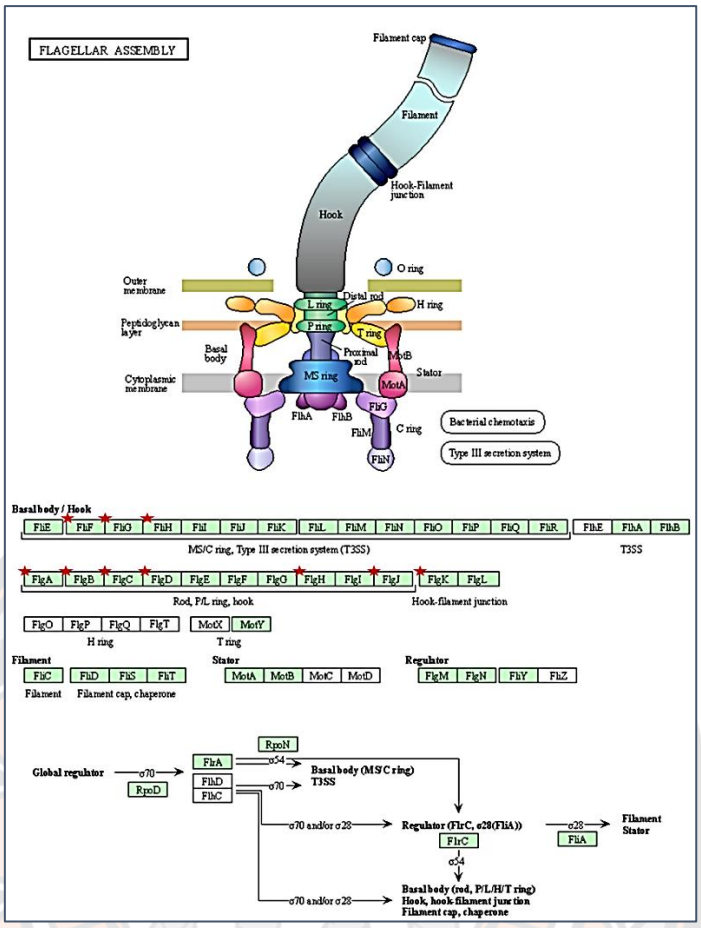

Figure 24 The KEGG pathways analyzed based on RNA sequencing analysis of flagellar assembly.

The red stars represent down-regulated DEGs of *P. aeruginosa* ATCC 27853 responded to half-hydroquinine concentration for 1 hour. Data from https://david.ncifcrf.gov/ 2021 updated database, accessed on 20 September 2022.

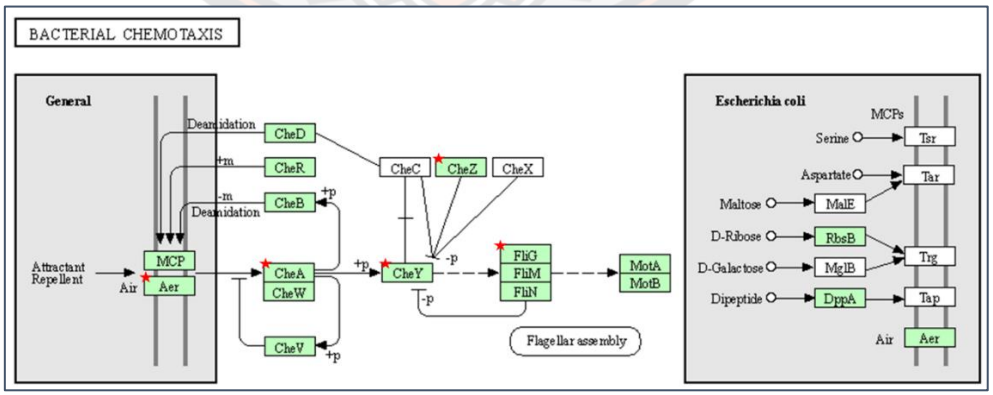

Figure 25 The KEGG pathways analyzed based on RNA sequencing analysis of bacterial chemotaxis.

The red stars represent down-regulated DEGs of *P. aeruginosa* ATCC 27853 responded to half-hydroquinine concentration for 1 hour. Data from

https://david.ncifcrf.gov/ 2021 updated database, accessed on 20 September 2022.

3. Determining the mechanism by which hydroquinine can target *P. aeruginosa*

3.1 RND-type efflux pump genes are upregulated in *P. aeruginosa* following treatment with hydroquinine

Analysis of DEGs identified that RND-type efflux pumps were up-regulated in *P. aeruginosa* ATCC 27853 in response to the ½ MIC (1,250 µg/mL) of hydroquinine for 1 hour. The DEGs results indicated that RND-type efflux pump genes, namely *mexC*, *mexD*, *oprJ*, *mexX*, and *mexY*, were highly overexpressed in response to the ½ MIC of hydroquinine (Table 11 and 14) (221). The RND multidrug efflux membrane fusion protein MexC precursor was most upregulated by a 9.47 Log_2-fold change, whereas the efflux transporter MexD and the efflux outer membrane protein OprJ precursor were upregulated by a 6.27 and 6.02 Log_2-fold change, respectively. Moreover, the multidrug efflux membrane fusion protein precursor MexX and the efflux transporter MexY were upregulated by 5.26 and 4.90 Log_2-fold changes, respectively. As a result, 1,250 µg/mL of hydroquinine induced up-regulated transcriptional response of RND-type efflux pumps in *P. aeruginosa* ATCC 27853 for 1 h.

Table 14 Differentially expressed genes (DEGs) of *P. aeruginosa* ATCC 27853 associated with the RND-type efflux pumps as determined by transcriptome analysis

RefSeq	Gene name	Gene description	Log_2 FC[1]	FDR[2]
NP_253289	*mexC*	Resistance-Nodulation-Cell Division (RND) multidrug efflux membrane fusion protein MexC precursor	9.47	2.56×10^{-9}
NP_253288	*mexD*	Resistance-Nodulation-Cell Division (RND) multidrug efflux transporter MexD	6.27	3.83×10^{-11}
NP_253287	*oprJ*	Multidrug efflux outer membrane protein OprJ precursor	6.02	2.90×10^{-10}
NP_250709	*mexX*	Resistance-Nodulation-Cell Division (RND) multidrug efflux membrane fusion protein MexX precursor	5.26	2.47×10^{-8}
NP_250708	*mexY*	Resistance-Nodulation-Cell Division (RND) multidrug efflux transporter MexY	4.90	9.60×10^{-8}

[1] Log_2 FC, Log_2 relative fold changes in expressed genes in response to hydroquinine, compared to the untreated control.
[2] FDR, false discovery rate with a statistical significance of p value ≤ 0.05.

3.1.1 Optimizing annealing/extension temperatures for amplification of the RND-type efflux pump genes of *P. aeruginosa* using multiplex qPCR (mqPCR) system

In order to amplify representative RND-type efflux pump genes (namely *mexB, mexD, mexY*) of *P. aeruginosa* strains, the optimal mqPCR annealing/extension temperature of these genes needed to be determined (224). Five annealing/extension

temperatures, including 58 °C, 59 °C, 60 °C, 61 °C, and 62 °C were tested using mqPCR system. Resulting Ct values of representative *mex* genes and reference gene (*16s rRNA*) of DS and MDR *P. aeruginosa* strains are shown in Table 15 (224). The Ct values of the genes ranged from 13.17–23.17 cycles, as shown in Table 15. The different annealing/extension temperatures tested of *the mexB* gene amplifying were detected in both DS and MDR *P. aeruginosa* strains, with the Ct values ranging from 16.47–23.17 cycles. At the temperatures tested, the Ct values of *mexD* and *mexY* genes were detected at 15.57–17.66 and 15.38–17.42 cycles, respectively. For Ct values of *16s rRNA* gene at the different annealing/extension temperatures tested were 13.17–18.92 cycles. This result indicated that *mexB, mexD, mexY,* and *16s rRNA* genes were successfully amplified in both DS *P. aeruginosa* ATCC27853 and MDR *P. aeruginosa* ATCC BAA-2108 with no significant (*p*-values > 0.9999) of all annealing/extension temperatures tested in this study (between 58 and 62 °C).

Table 15 The cycle threshold (Ct) values of each gene in two *P. aeruginosa* reference strains using multiplex qPCR at various annealing/extension temperatures

Strains	**Genes**	**Cycle threshold values in gradient annealing/extension temperature (°C)**					***p*-value**
		58	**59**	**60**	**61**	**62**	
P. aeruginosa ATCC27853	*mexB*	16.50±1.1	16.47±1.1	16.53±1.3	16.48±1.7	16.99±1.8	>0.9999
	mexD	16.24±0.9	15.57±0.9	15.99±1.5	16.69±1.0	17.66±1.1	>0.9999
	mexY	16.12±0.9	15.38±1.1	15.76±1.8	16.38±1.1	17.31±1.4	>0.9999
	16S rRNA	13.17±1.	13.50±0.3	14.03±0.9	14.56±1.4	14.67±0.4	>0.9999
P. aeruginosa ATCC BAA-2108	*mexB*	19.77±0.9	20.61±1.3	20.81±0.8	21.21±0.6	23.17±1.0	>0.9999
	mexD	16.87±0.6	16.78±1.2	16.40±0.1	16.20±0.1	16.85±1.5	>0.9999
	mexY	16.75±0.3	16.79±1.2	16.30±0.3	16.47±0.2	17.42±0.2	>0.9999
	16S rRNA	13.37±0.6	16.99±0.5	17.35±1.3	18.92±0.6	18.58±1.2	>0.9999

3.1.2 Optimizing gDNA concentration of *P. aeruginosa* ATCC strains for amplification of RND-type efflux pump genes using mqPCR

In order to amplify representative RND-type efflux pump genes of both DS and MDR *P. aeruginosa* ATCC strains, the optimal gDNA concentrations using the mqPCR system were investigated (224). The optimal annealing/extension temperature at 59 °C was used in this study. The result showed Ct values of *mexB, mexD, mexY,* and *16s rRNA* genes in all gDNA concentrations tested (5.0, 2.5, 1.0, and 0.5 ng) ranging from 15.49–27.31 cycles (Table 16) (224). At the gDNA concentrations tested of both *P. aeruginosa* gDNA samples, the Ct values of *mexB* ranged from 17.97 to 27.31 cycles. At the same time, the Ct values of *mexD* were shown in the range of 19.80–22.93 cycles. For the *mexY* gene, Ct values ranged from 18.98–22.17 cycles. For the reference gene, *16s rRNA*, at gDNA concentrations tested, the Ct value was shown in the range from 15.49–21.04 cycles

(Table 16). Overall, the result showed that the gDNA samples of both DS *P. aeruginosa* ATCC27853 and MDR *P. aeruginosa* ATCC BAA-2108 in all concentrations tested had strong positive reactions, indicating that they are suitable for detection of the representative RND-type efflux pump genes in these samples.

Table 16 The cycle threshold (Ct) values at various gDNA concentrations of *P. aeruginosa* for each *mex* gene detection using multiplex qPCR

Strains	Target genes	The Ct values in the different gDNA concentrations				*p*-value
		5.0 ng	2.5 ng	1.0 ng	0.5 ng	
P. aeruginosa ATCC27853	*mexB*	17.97±1.3	18.93±0.9	22.65±0.6	23.07±1.2	>0.9999
	mexD	20.56±0.9	19.92±0.9	21.74±0.4	22.50±0.5	>0.9999
	mexY	19.39±0.6	18.98±0.6	21.70±0.8	22.17±1.1	>0.9999
	16S rRNA	15.49±0.9	17.80±0.6	21.04±0.9	20.80±0.3	>0.9999
P. aeruginosa ATCC BAA-2108	*mexB*	20.14±0.2	22.98±0.7	23.86±0.2	27.31±1.2	>0.9999
	mexD	21.23±0.5	19.80±0.2	20.92±0.4	22.93±0.9	>0.9999
	mexY	19.16±0.9	19.18±0.9	20.61±0.5	20.65±1.5	>0.9999
	16s rRNA	17.44±1.2	16.34±0.3	19.61±1.3	20.97±0.6	>0.9999

3.1.3 The bands of representative RND-type efflux pump genes (*mexB*, *mexD*, *mexY*, and *16s rRNA*) were detected in all *P. aeruginosa* strains using agarose gel electrophoresis

The representative mex gene amplicons generated under optimal mqPCR conditions with agarose gel electrophoresis (Figure 26B) were verified according to the expected size (Table 3) (224). The mex and reference primer sets were amplified with 5 ng of gDNA at 59 °C. The results showed that the amplicons of *mexB*, *mexD*, and *mexY* genes in all *P. aeruginosa* gDNA samples had the expected size near 199 bp, 131 bp, and 168 bp, respectively (Figure 26A, B). At the same time, in all *P. aeruginosa* gDNA samples, the amplicons for the reference gene (*16s rRNA*) were shown as the anticipated size of 225 bp (Figure 26A, B). The results confirmed that the optimal conditions of the mqPCR system for amplifying representative RND-type efflux pump genes of all *P. aeruginosa* strains, including the annealing/extension temperatures, the gDNA concentration and specific primer sets, were suitable to use.

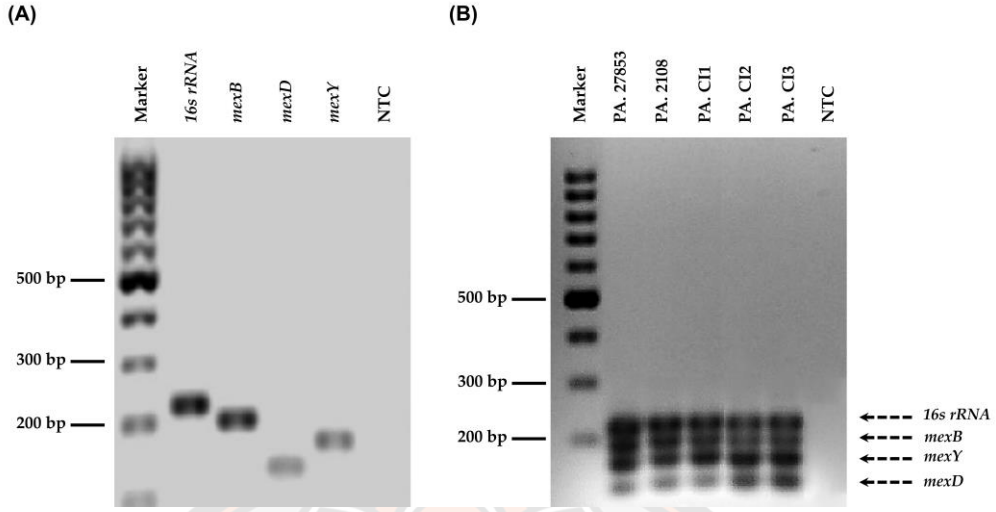

Figure 26 Agarose gel electrophoresis analysis of the reference (*16s rRNA*) and *mex* efflux pump genes (*mexB*, *mexD*, and *mexY*) of *P. aeruginosa* strains.

Amplification with (A) singleplex PCR system from representative *P. aeruginosa* ATCC 27853 strains and (B) multiplex PCR system from five representative *P. aeruginosa* strains. The PCR products amplified were run on a 2% agarose gel. The gDNA concentration was 5 ng/µL (the gDNA amount was 5 ng). The first lane contains a DNA ladder of fragments of known sizes. "PA. 27853" is the sample from *P. aeruginosa* ATCC27853. "PA. 2108" is the sample from *P. aeruginosa* ATCC BAA-2108. "PA. CI1, PA. CI2, and PA. CI3", are the samples from *P. aeruginosa* clinical isolate no. 1, no. 2, and no. 3, respectively. NTC denotes the non-template control (224).

3.1.4 The representative RND-type efflux pump genes were detected at a range of gDNA concentrations in *P. aeruginosa* using the *effluxR* detection assay with the mdPCR system

The representative RND-type efflux pump genes, including *mexB*, *mexD*, and *mexY* of *P. aeruginosa* ATCC27853 were determined at various gDNA concentrations using the *effluxR* detection assay with the mdPCR system (224). The result showed that positive and negative partitions of each *mex* gene in *P. aeruginosa* gDNA samples were showed as the relative fluorescent intensity units on a 1D scatter plot (Figure 27). At the same time, microscopic image validation was used to identify the specific *mex* target genes using specific fluorescent dyes in the filled partitions (Figure 28). All the studied genes showed concentration-dependent signals with significant fluorescence intensities in the combined findings from all three replicates, allowing for the absolute quantification of gene copies. At 5.00 ng/µL of *P. aeruginosa* gDNA concentrations, *mexB*, *mexD*, and *mexY* genes showed the positive partitions were 100%. For gDNA concentrations at 2.50 ng/µL of *P. aeruginosa* strain, the positive partitions of *mexB*, *mexD*, and *mexY* genes were 100%, 100%, and 96.33%, respectively. The positive partitions with 1.00 ng/µL of gDNA of *P. aeruginosa* strain were 99.33%, 97.00% and 82.00% for *mexB*, *mexD*, and *mexY* genes, respectively. At the same time, with 0.50 ng/µL gDNA concentrations of *P. aeruginosa*, positive partitions of *mexB*, *mexD*, and *mexY* genes

were 88.67%, 84.67%, and 72.33%, respectively. Finally, the gDNA concentrations of *P. aeruginosa* at 0.05 ng/µL, the positive partitions were 58.00%, 36.67%, and 31.67% for *mexB*, *mexD*, and *mexY*, respectively.

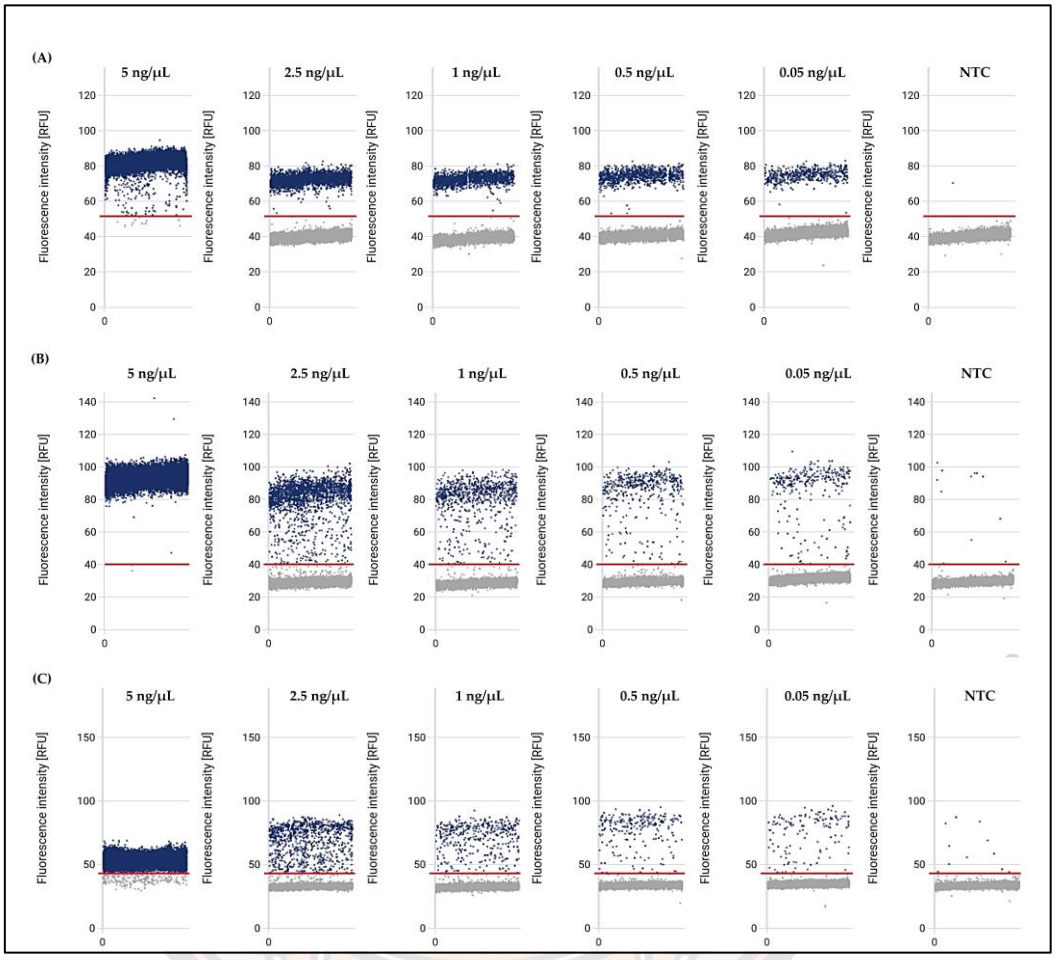

Figure 27 The fluorescence intensity of *mex* efflux pump genes at various gDNA concentrations of *P. aeruginosa* ATCC27853, detected by the *effluxR* detection assay with the mdPCR system; (A) *mexB*, (B) *mexD*, and (C) *mexY*.

Abbreviation; RFU: relative fluorescence units, NTC: Non-template control. The red lines represent the fluorescence threshold. Blue dots above the threshold line are considered as positive partitions, whereas grey dots below the threshold line are considered as negative partitions (224).

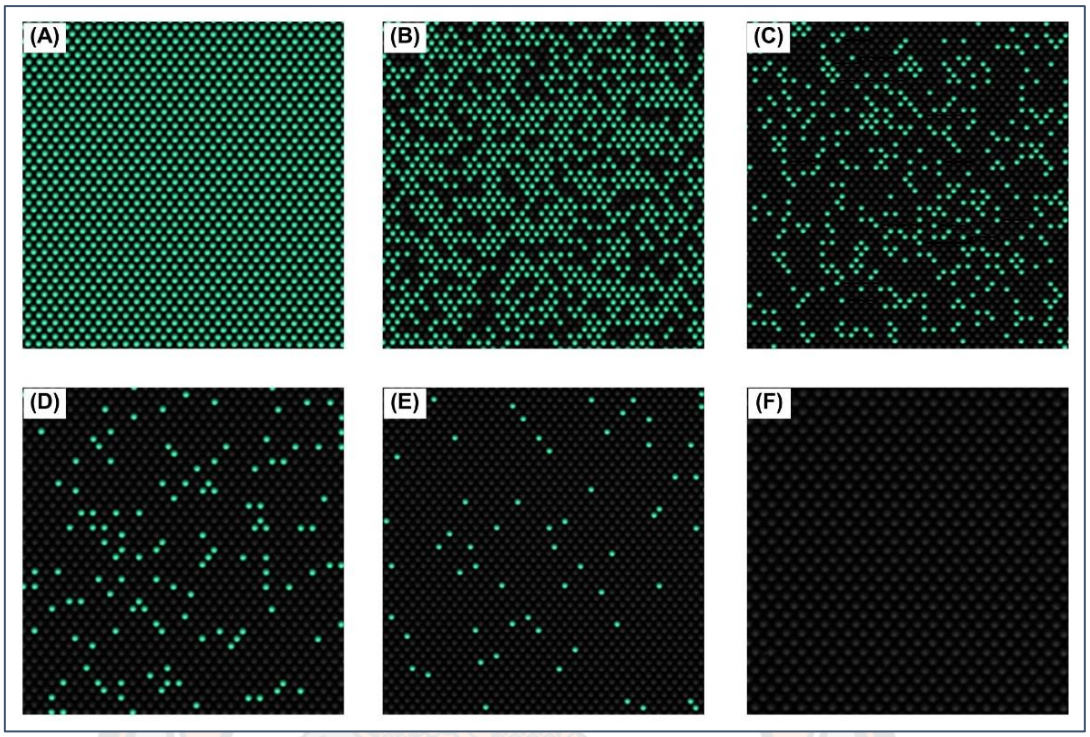

Figure 28 The validated microscopic images of *mexB* gene, detected by the *effluxR* detection assay with the mdPCR system.

The *mexB* gene as representative for positive reactions (A–E) and a negative reaction (F) in various gDNA concentrations of *P. aeruginosa* ATCC27853; (A) 5 ng/µL; (B) 2.5 ng/µL; (C) 1.0 ng/µL; (D) 0.5 ng/µL; (E) 0.05 ng/µL and (F) non template (224).

3.1.5 Limit of detection (LOD) of the *effluxR* detection assay with the mdPCR system for detecting representative RND-type efflux pump genes of *P. aeruginosa* ATCC27853

The limit of detection (LOD) of the assay was performed by detecting the presence of representative RND-type efflux pump genes at a range of gDNA concentrations of the *P. aeruginosa* ATCC 27853 (224). Various gDNA concentrations of *P. aeruginosa* ATCC 27853 at 2.50 ng/µL, 1.25 ng/µL, 0.50 ng/µL, 0.05 ng/µL, 0.005 ng/µL, 0.003 ng/µL, and 0.001 ng/µL were measured. In all three replicates of each PCR reaction, the result successfully detected and determined the absolute number of the *mex* genes (copies/µL) in the samples with gDNA concentrations ranging from 0.001–2.50 ng/µL (Table 17) (224). The non-template controls had small amounts of background signals, which resulted in absolute quantification values lower than 0.5 copies/µL. This study proved that decreased gDNA quantities would result in a reduction in the absolute quantification of *mexB*, *mexD*, and *mexY*. The ranges of the absolute quantification of *mexB*, *mexD*, and *mexY* in the samples were 34.81–10,388.27, 15.52–9121.83, and 7.04–5626.67 copies/µL, respectively. Hence, the absolute quantification was attainable from gDNA concentrations of 0.001 ng/µL or higher. As a result, it can conclude that the detection limit for the representative RND-type efflux pump target genes using *effluxR* detection assay with the mdPCR system was 0.001 ng/µL with the absolute number of

the genes being 7.04 copies/µL. Moreover, the absolute quantification of *mexB*, *mexD*, and *mexY* also showed a strong correlation with the gDNA quantities, with R^2 values of 0.78 (p = 0.0035), 0.87 (p = 0.0007), and 0.95 (p < 0.0001), respectively. Additionally, with a maximum Youden's index (J) of 1, was also reported a cut-off value of 3.72 copies/L for determining the existence of RND-type efflux pump genes in this study (Table 18) (224).

Table 17 Absolute quantification (copies/µL) and 95% confidence interval (95% CI) of representative RND-type efflux pump genes in various *P. aeruginosa* ATCC27853 gDNA concentrations

gDNA conc. samples (ng/µL)	**Mean of absolute quantification (copies/µL) and 95% confidence interval of *mex* efflux pump genes**					
	mexB*		***mexD****		***mexY****	
	copies/µL	**95% CI**	**copies/µL**	**95% CI**	**copies/µL**	**95% CI**
0.001	34.81±9.00	32–37	15.52±2.83	13–17	7.04±1.58	5–8
0.003	87.43±20.37	83–91	38.32±9.09	35–4	14.71±1.32	13–16
0.005	183.82±12.86	176–191	70.50±12.04	66–74	33.00±11.53	30–35
0.050	1923.07±445	1891–1954	1721.94±79	1689–1754	442.64±198	431–453
0.500	7106.50±44	6821–7391	4820.07±919	4698–4942	2086.37±144	2050–2121
1.250	10184.83±782	8901–11468	7729.60±640	7350–8108	4117.87±643	4031–4204
2.500	10388.27±597	9092–11683	9121.83±1298	8300–9942	5626.67±733	5465–5787
NTC	0.04±0.03	-0.02–0.09	0.40±0.08	0.085–0.72	0.30±0.04	0.06–0.53

*Note: R^2 values between the gDNA concentrations and the absolute quantification of *mexB*, *mexD* and *mexY* were 0.78 (p=0.0035), 0.87 (p=0.0007), and 0.95 (p<0.0001), respectively.

Table 18 The cut-off values of the *effluxR* detection assay with mdPCR using ROC analysis and Youden's index

Cut-off values of the copy number of genes (µg/mL)	Sensitivity	Specificity	1 – Specificity	Youden's index (J)
-0.960000	1.000	0.000	1.000	0.000
0.170000	1.000	0.333	0.667	0.333
0.350000	1.000	0.667	0.333	0.667
3.720000	1.000	1.000	0.000	1.000
10.875000	0.952	1.000	0.000	0.952
15.115000	0.905	1.000	0.000	0.905
24.260000	0.857	1.000	0.000	0.857
33.905000	0.810	1.000	0.000	0.810
36.565000	0.762	1.000	0.000	0.762
54.410000	0.714	1.000	0.000	0.714
78.965000	0.667	1.000	0.000	0.667
135.62500	0.619	1.000	0.000	0.619
313.23000	0.571	1.000	0.000	0.571
1082.29000	0.524	1.000	0.000	0.524
1822.50500	0.476	1.000	0.000	0.476
2004.72000	0.429	1.000	0.000	0.429
3102.12000	0.381	1.000	0.000	0.381
4468.97000	0.333	1.000	0.000	0.333
5223.37000	0.286	1.000	0.000	0.286
6366.58500	0.238	1.000	0.000	0.238
7418.05000	0.190	1.000	0.000	0.190
8425.71500	0.143	1.000	0.000	0.143
9653.33000	0.095	1.000	0.000	0.095
10286.55000	0.048	1.000	0.000	0.048
10389.27000	0.000	1.000	0.000	0.000

3.1.6 Sensitivity and specificity of *effluxR* detection assay using mdPCR system for detecting the representative RND-type efflux pump genes in the *P. aeruginosa* strains

The sensitivity and specificity of the *effluxR* detection assay using mdPCR system for detecting representative RND-type efflux pump genes in *P. aeruginosa* strains were also investigated in this experiment (224). A sample-blinded was prepared, which included 69 known positive samples and 15 known negative samples for the representative RND-type efflux pump genes (*mexB*, *mexD*, and *mexY*). The blinded samples were randomly numbered from samples 1 to 84 (Table 19) (224). The cut-off value for interpretation was applied among all blinded samples and non-template control. The system detected the positive partitions of *mexB*, *mexD*, and *mexY* in all positive samples (100%), showing the relative fluorescence intensity in Figure 29. Whereas all *mex* genes were not detected in all negative samples (100%) (Table 19). Interestingly, in negative blinded samples from other bacterial strains, including *S. aureus* ATCC 29213, *S. aureus* ATCC 25923, *E. coli* ATCC 25922, *E. coli* ATCC 2452, *K. pneumoniae* ATCC 1705 and *E. cloacae* ATCC 2341 (Table

18), three *mex* genes tested were not detected. As a result, the sensitivity and specificity of the blinded investigation with the assay were 100% for detecting representative RND-type efflux pump genes in *P. aeruginosa* strains.

Table 19 The *effluxR* detection assay with mdPCR system detected the 69 positive samples from 84 blinded bacterial reference and clinical isolate strains

Sample no.	Bacterial species	Present of *mex* genes			Result of *effluxR* detection assay
		mexB	*mexD*	*mexY*	
1	*P. aeruginosa*	+	+	+	Positive for three genes
2	*P. aeruginosa*	+	+	+	Positive for three genes
3	*E. coli*	-	-	-	Negative for three genes
4	*P. aeruginosa*	+	+	+	Positive for three genes
5	*P. aeruginosa*	+	+	+	Positive for three genes
6	*P. aeruginosa*	+	+	+	Positive for three genes
7	*S. aureus*	-	-	-	Negative for three genes
8	*E. cloacae*	-	-	-	Negative for three genes
9	*P. aeruginosa*	+	+	+	Positive for three genes
10	*P. aeruginosa*	+	+	+	Positive for three genes
11	*P. aeruginosa*	+	+	+	Positive for three genes
12	*P. aeruginosa*	+	+	+	Positive for three genes
13	*E. cloacae*	-	-	-	Negative for three genes
14	*P. aeruginosa*	+	+	+	Positive for three genes
15	*P. aeruginosa*	+	+	+	Positive for three genes
16	*P. aeruginosa*	+	+	+	Positive for three genes
17	*P. aeruginosa*	+	+	+	Positive for three genes
18	*P. aeruginosa*	+	+	+	Positive for three genes
19	*P. aeruginosa*	+	+	+	Positive for three genes
20	*K. pneumoniae*	-	-	-	Negative for three genes
21	*P. aeruginosa*	+	+	+	Positive for three genes
22	*P. aeruginosa*	+	+	+	Positive for three genes
23	*P. aeruginosa*	+	+	+	Positive for three genes
24	*P. aeruginosa*	+	+	+	Positive for three genes
25	*P. aeruginosa*	+	+	+	Positive for three genes
26	*P. aeruginosa*	+	+	+	Positive for three genes
27	*P. aeruginosa*	+	+	+	Positive for three genes
28	*S. aureus*	-	-	-	Negative for three genes
29	*P. aeruginosa*	+	+	+	Positive for three genes
30	*P. aeruginosa*	+	+	+	Positive for three genes
31	*S. aureus*	-	-	-	Negative for three genes
32	*P. aeruginosa*	+	+	+	Positive for three genes
33	*P. aeruginosa*	+	+	+	Positive for three genes
34	*P. aeruginosa*	+	+	+	Positive for three genes
35	*E. coli*	-	-	-	Negative for three genes

Table 19 The *efflux*R detection assay with mdPCR system detected the 69 positive samples from 84 blinded bacterial reference and clinical isolate strains (Cont.)

Sample no.	Bacterial species	Present of *mex* genes			Result of *efflux*R detection assay
		mexB	*mexD*	*mexY*	
36	*P. aeruginosa*	+	+	+	Positive for three genes
37	*P. aeruginosa*	+	+	+	Positive for three genes
38	*P. aeruginosa*	+	+	+	Positive for three genes
39	*P. aeruginosa*	+	+	+	Positive for three genes
40	*K. pneumoniae*	-	-	-	Negative for three genes
41	*P. aeruginosa*	+	+	+	Positive for three genes
42	*P. aeruginosa*	+	+	+	Positive for three genes
43	*P. aeruginosa*	+	+	+	Positive for three genes
44	*P. aeruginosa*	+	+	+	Positive for three genes
45	*E. coli*	-	-	-	Negative for three genes
46	*K. pneumoniae*	-	-	-	Negative for three genes
47	*P. aeruginosa*	+	+	+	Positive for three genes
48	*P. aeruginosa*	+	+	+	Positive for three genes
49	*P. aeruginosa*	+	+	+	Positive for three genes
50	*P. aeruginosa*	+	+	+	Positive for three genes
51	*P. aeruginosa*	+	+	+	Positive for three genes
52	*P. aeruginosa*	+	+	+	Positive for three genes
53	*P. aeruginosa*	+	+	+	Positive for three genes
54	*P. aeruginosa*	+	+	+	Positive for three genes
55	*P. aeruginosa*	+	+	+	Positive for three genes
56	*P. aeruginosa*	+	+	+	Positive for three genes
57	*P. aeruginosa*	+	+	+	Positive for three genes
58	*S. aureus*	-	-	-	Negative for three genes
59	*P. aeruginosa*	+	+	+	Positive for three genes
60	*P. aeruginosa*	+	+	+	Positive for three genes
61	*P. aeruginosa*	+	+	+	Positive for three genes
62	*P. aeruginosa*	+	+	+	Positive for three genes
63	*P. aeruginosa*	+	+	+	Positive for three genes
64	*P. aeruginosa*	+	+	+	Positive for three genes
65	*P. aeruginosa*	+	+	+	Positive for three genes
66	*P. aeruginosa*	+	+	+	Positive for three genes
67	*P. aeruginosa*	+	+	+	Positive for three genes
68	*E. coli*	-	-	-	Negative for three genes
69	*P. aeruginosa*	+	+	+	Positive for three genes
70	*P. aeruginosa*	+	+	+	Positive for three genes
71	*P. aeruginosa*	+	+	+	Positive for three genes
72	*P. aeruginosa*	+	+	+	Positive for three genes
73	*P. aeruginosa*	+	+	+	Positive for three genes

Table 19 The *effluxR* detection assay with mdPCR system detected the 69 positive samples from 84 blinded bacterial reference and clinical isolate strains (Cont.)

Sample no.	Bacterial species	Present of *mex* genes			Result of *effluxR* detection assay
		mexB	*mexD*	*mexY*	
74	*K. pneumoniae*	-	-	-	Negative for three genes
75	*P. aeruginosa*	+	+	+	Positive for three genes
76	*P. aeruginosa*	+	+	+	Positive for three genes
77	*K. pneumoniae*	-	-	-	Negative for three genes
78	*P. aeruginosa*	+	+	+	Positive for three genes
79	*P. aeruginosa*	+	+	+	Positive for three genes
80	*P. aeruginosa*	+	+	+	Positive for three genes
81	*P. aeruginosa*	+	+	+	Positive for three genes
82	*P. aeruginosa*	+	+	+	Positive for three genes
83	*P. aeruginosa*	+	+	+	Positive for three genes
84	*P. aeruginosa*	+	+	+	Positive for three genes
	Total	69	69	69	
	Percentage	100	100	100	

Note: symbol (+) is gene presence and (-) is gene absence.

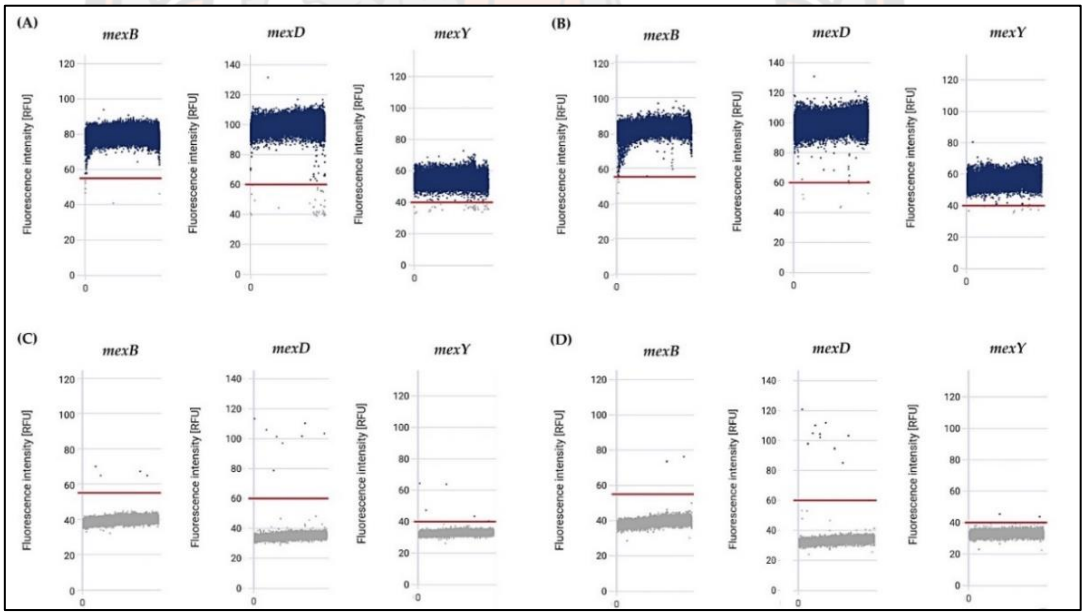

Figure 29 Representative fluorescence intensity of positive-*mex* efflux pump gene samples and negative samples, detected by the *effluxR* detection assay with the mdPCR system.

Showing (A) 5 ng/µL of *P. aeruginosa* ATCC27853; (B) 5 ng/µL of *P. aeruginosa* clinical isolate; (C) 5 ng/µL of *K. pneumoniae* ATCC1705; and (D) non-template. The red lines represent the fluorescence threshold. Blue dots above the threshold line are considered as positive partitions, whereas grey dots below the threshold line are considered as negative partitions (224).

3.1.7 RND-type efflux pump gene expression of *P. aeruginosa* strains exposed to hydroquinine

3.1.7.1 Detection of representative RND-type efflux pump gene expression in *P. aeruginosa* strains with mRT-qPCR method

To confirm transcriptomic result, the overexpression of representative RND-type efflux pump genes, including *mexB*, *mexD*, and *mexY*, in both DS and MDR *P. aeruginosa* strains was investigated with mRT-qPCR method at different times after 1, 2, and 4 h treatment with hydroquinine. Consistently, after *P. aeruginosa* ATCC 27853 exported hydroquinine for 4 h, the expression level of *mexB* was not significant in up-or down-regulation. At the same time, the expression level of *mexD* and *mexY* genes were increased between 8- and 30-fold and 3- and 30-fold, respectively (Figure 30A). In contrast, the overexpression levels of *mexD* and *mexY* genes of *P. aeruginosa* ATCC BAA-2108 were shown after hydroquinine treatment for 1 h, which increased approximately 7-fold and 6-fold, respectively (Figure 30B). As a result, hydroquinine induced transcriptional responses of *mexD* and *mexY* in both DS and MDR *P. aeruginosa* treatment with ½ MIC of hydroquinine at 1–4 h (221).

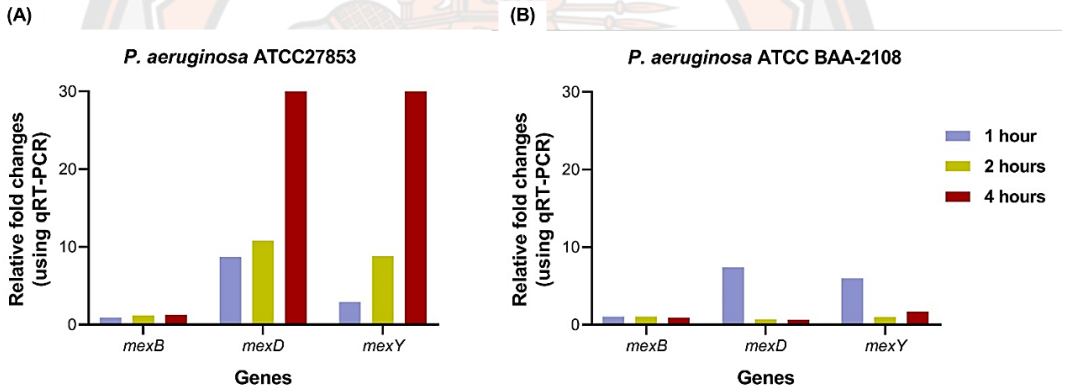

Figure 30 The expression of representative RND-type efflux pump genes in *P. aeruginosa* strains treated with ½ MIC of hydroquinine compared to the untreated conditions.

Showing (A) *P. aeruginosa* ATCC 27853 strain and (B) *P. aeruginosa* ATCC BAA-2108 strain (221).

3.1.7.2 Detection of representative RND-type efflux pump gene expression in *P. aeruginosa* strain using the *effluxR* detection assay with mRT-dPCR method

In order to validate the transcriptomic result, the *effluxR* detection assay with mRT-dPCR method was also used to evaluate whether hydroquinine induced the transcriptional levels of representative RND-type efflux pump genes (*mexB*, *mexD* and *mexY*) in DS *P. aeruginosa* ATCC 27853 (221). The result showed that after 1 h treatment of ½ MIC of hydroquinine, the relative fold changes of gene expression of *mexD* and *mexY* in DS *P. aeruginosa* ATCC 27853 were 20.8±4.31-fold and 11.8±5.01-fold, respectively. In contrast, the expression of *mexB* was not significant in up-or down-regulation (1.6±0.15-fold) (Figure 31). The result confirmed

that hydroquinine induced the *mexD* and *mexY* expression of *P. aeruginosa* in response to hydroquinine at ½ MIC at 1 h.

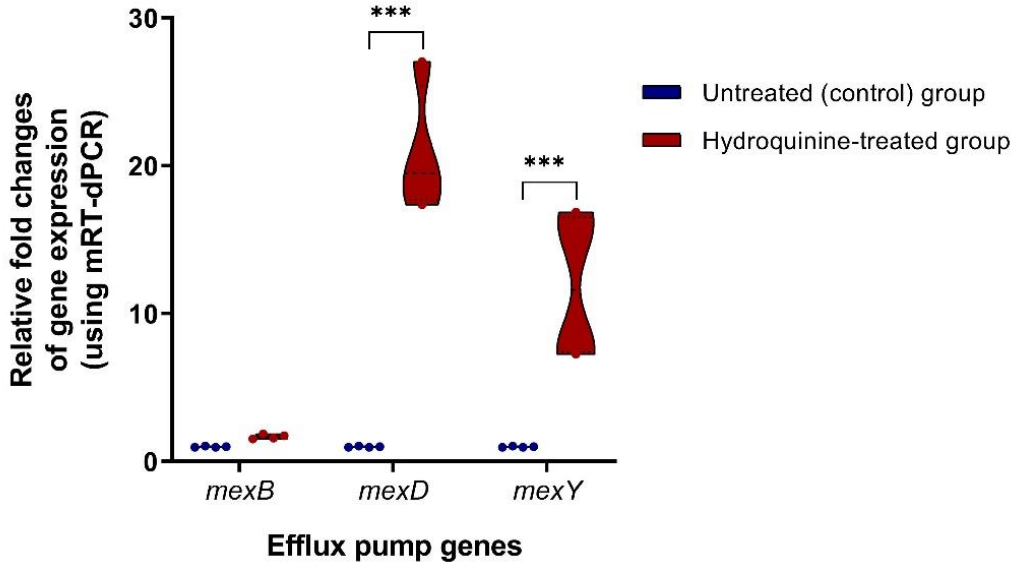

Figure 31 Expression levels of representative RND-type efflux pump genes (*mexB*, *mexD* and *mexY*) in *P. aeruginosa* ATCC27853 using the *effluxR* detection assay with mRT-dPCR between untreated and treated with hydroquinine at ½ MIC for 1 hour. The asterisk (*) symbol was considered significant ($p < 0.05$) (221).

3.2 Down-regulation of virulence factor genes in *P. aeruginosa* following treatment with hydroquinine

Transcriptomic analysis revealed virulence factor down-regulation in *P. aeruginosa* ATCC 27853 in response to treatment with ½ MIC of hydroquinine for 1 h. The DEGs results indicated that virulence factors associated with constructing the flagellar assembly, namely *flgC*, *flgB*, *flgJ*, *flgD*, *fliF*, *fliG*, *flgK* and *flgH*, were down regulated in response to the ½ MIC of hydroquinine (Figure 32). The relative fold change of the DEGs associated flagella assembly showed significant downregulation $\log_2$-fold change ranging from -2.93 to -2.18 (Table 11 and 20) (225). The flagellar L-ring protein precursor FlgH (*flgH*) was most downregulated by -2.18 $\log_2$-fold change. At the same time, proteins involved in flagellar hook-associated protein 1 FlgK (*flgK*) and flagellar motor-switch protein 1 FliG (*fliG*) showed downregulated by -2.23 $\log_2$-fold change. Moreover, the $\log_2$-fold change of downregulated *fliF*, *flgD* and *flgJ* genes, which encoded flagellar M-ring outer membrane protein precursor FliF, flagellar basal-body rod modification protein FlgD and flagellar protein FlgJ were -2.26, -2.33 and -2.33, respectively. In addition, *P. aeruginosa* ATCC 27853 exposed half-hydroquinine concentration showed downregulated DEGs of genes encoding flagellar basal-body rod proteins FlgB and FlgC were -2.38 and -2.93 $\log_2$-fold change, respectively (Table 20).

Table 20 Differentially expressed genes (DEGs) associated with the flagellar assembly in *P. aeruginosa* under ½ MIC of hydroquinine treatment.

Gene name	Gene product	Log_2 FC[1]	FDR[2]
flgC	Flagellar basal-body rod protein FlgC	-2.93	3.90×10^{-3}
flgB	Flagellar basal-body rod protein FlgB	-2.38	2.43×10^{-2}
flgJ	Flagellar protein FlgJ	-2.33	2.41×10^{-2}
flgD	Flagellar basal-body rod modification protein FlgD	-2.33	2.76×10^{-2}
fliF	Flagellar M-ring outer membrane protein precursor FliF	-2.26	2.51×10^{-2}
fliG	Flagellar motor-switch protein 1 FliG	-2.23	2.29×10^{-2}
flgK	Flagellar hook-associated protein 1 FlgK	-2.23	3.22×10^{-2}
flgH	Flagellar L-ring protein precursor FlgH	-2.18	4.13×10^{-2}

[1] Log_2 FC, Log_2 relative fold changes in expressed genes in response to hydroquinine, compared to the untreated control.
[2] FDR, false discovery rate with a statistical significance of p value ≤ 0.05.

3.2.1 The observed downregulation of flagellar related genes was further validated by RT-qPCR

Downregulated DEGs associated virulence factor genes in *P. aeruginosa* treated with ½ MIC of hydroquinine for 1 h were verified with the RT-qPCR method (225). Four representative virulence factor genes (*flgK*, *flgH*, *flgC* and *fliF*), involved in flagellar assembly, were selected for further validation (Figure 33). Both DS and MDR *P. aeruginosa* strains treated either with or without 1.250 and 0.625 mg/mL of hydroquinine for 1 h, respectively, were validated in this experiment. All flagellar genes tested in the DS and MDR strains showed downregulation of relative gene expression in response to hydroquinine, as shown in Figure 33. In particular, the relative expression levels of *flgK* were significantly decreased by 0.15 ± 0.06-fold in the DS *P. aeruginosa* strain. Three genes, *flgH*, *flgC*, and *fliF*, associated with flagellar basal body showed the relative expression levels were significantly decreased by 0.52 ± 0.11, 0.53 ± 0.12, and 0.40 ± 0.03-fold, respectively (Figure 33A). After treatment with hydroquinine at 0.625 mg/mL of MDR *P. aeruginosa* ATCC BAA-2108 for 1 h, the relative expression levels of the flagella hook-associated gene (*flgK*) significantly decreased at 0.40 ± 0.06-fold (Figure 33B). For the flagellar basal body, *flgH*, *flgC*, and *fliF* genes showed significant repression of relative expression levels at 0.42 ± 0.13, 0.59 ± 0.09 and 0.59 ± 0.10-fold, respectively (Figure 33B). As a result, it confirmed that hydroquinine negatively affects the virulence factors of both DS and MDR *P. aeruginosa* strains via the expression of genes associated with flagellar assembly.

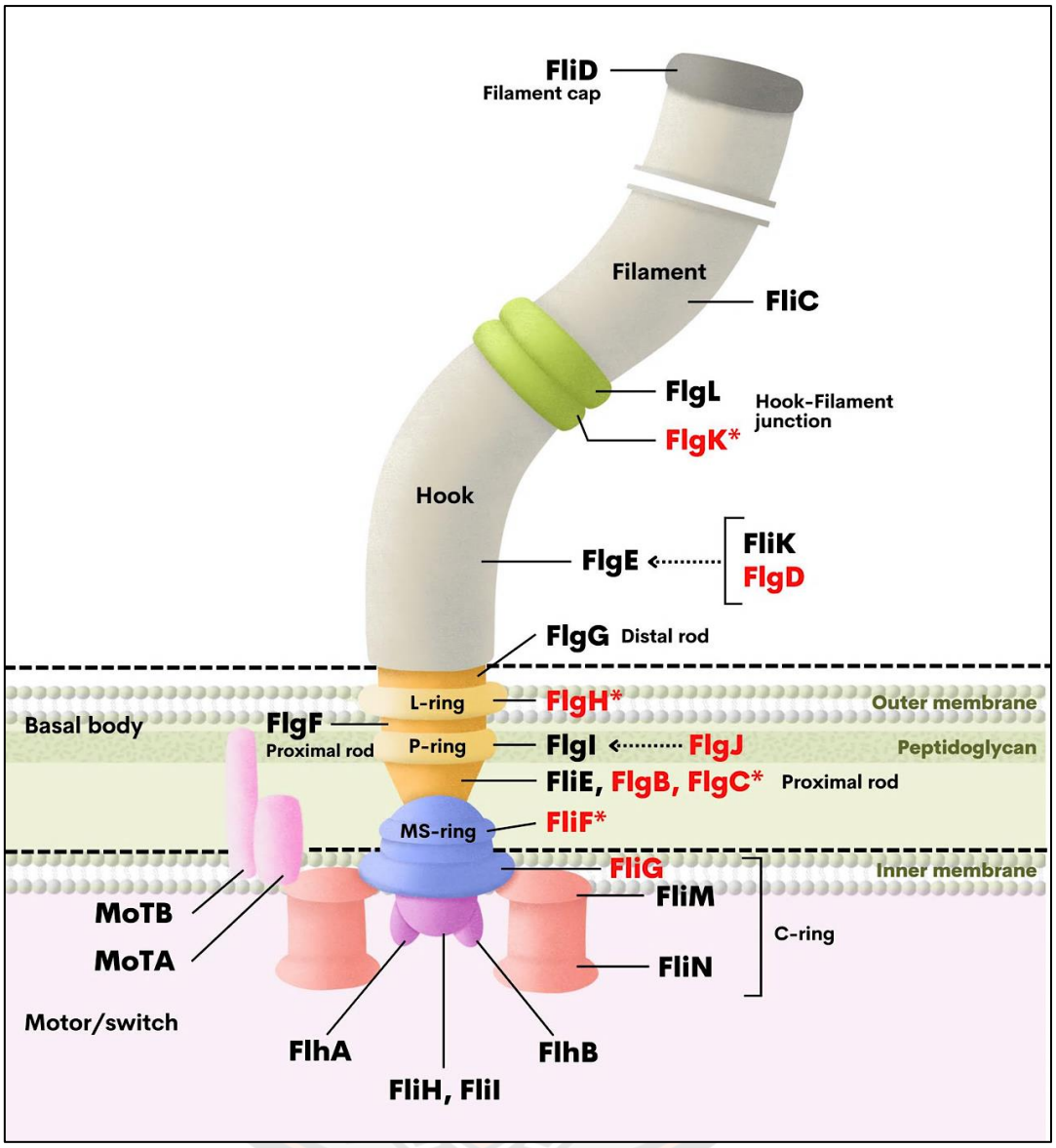

Figure 32 The flagellar structure of *P. aeruginosa* and gene products involved in flagellar assembly and/or regulation.

The red labels represent the downregulated DEGs of *P. aeruginosa* in response to hydroquinine for 1 h, according to the investigation by transcriptome analysis. The asterisk (*) symbol represents the genes selected for reverifying the expressional accuracy using RT-qPCR (225).

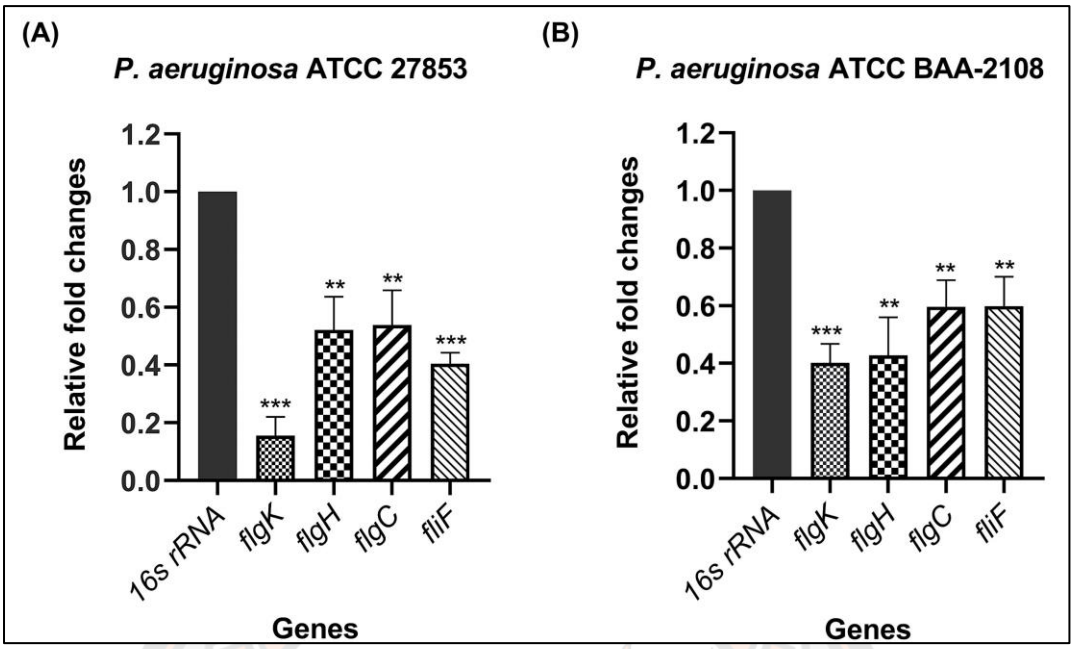

Figure 33 The relative expression of flagellar assembly genes in *P. aeruginosa* strains

(A) *P. aeruginosa* ATCC 27853 with hydroquinine at 1.250 mg/mL for 1 h and (B) *P. aeruginosa* ATCC BAA-2108 treated with hydroquinine at 0.625 mg/mL for 1 h, compared to the corresponding untreated control. The asterisk ** and *** symbols were $p < 0.01$ and $p < 0.001$, respectively (225).

3.2.2 Phenotypic result of DS and MDR *P. aeruginosa* motility following treatment with hydroquinine

This study investigated the motility of DS and MDR *P. aeruginosa* strains affected by hydroquinine at different concentrations using swimming and swarming motility assay (225). The results showed that hydroquinine had potent anti-motility effects on both the swimming and swarming capacity of both *P. aeruginosa* strains (Figure 34, Figure 35). After a 24-hour incubation, both the control and vehicle groups, without treatment, exhibited typical swimming and swarming. No statistically significant difference was observed in the motility of control groups. In contrast, swimming and swarming motility of DS and MDR *P. aeruginosa* strains were significantly inhibited with hydroquinine treatment in a dose-dependent manner compared to control groups. With hydroquinine treatment doses at 2.500, 1.250, and 0.625 mg/mL, DS *P. aeruginosa* swimming inhibition percentages were 50.0, 45.8, and 33.3%, respectively (Figure 34B). At the same time, the swarming inhibition percentages of DS *P. aeruginosa* strain exposed to those hydroquinine concentrations were 54.0, 44.0, and 36.0% ($p < 0.001$), respectively (Figure 34D). For the MDR *P. aeruginosa* strain, the percentages of swimming inhibitions by the hydroquinine concentrations of 1.250, 0.625, and 0.312 mg/mL significantly inhibited at 52.9, 35.2, and 23.5% inhibition, respectively (Figure 35B). In contrast, hydroquinine at only 1.250 mg/mL significantly inhibited swarming motility compared to the controls (30.0%) (Figure 35D).

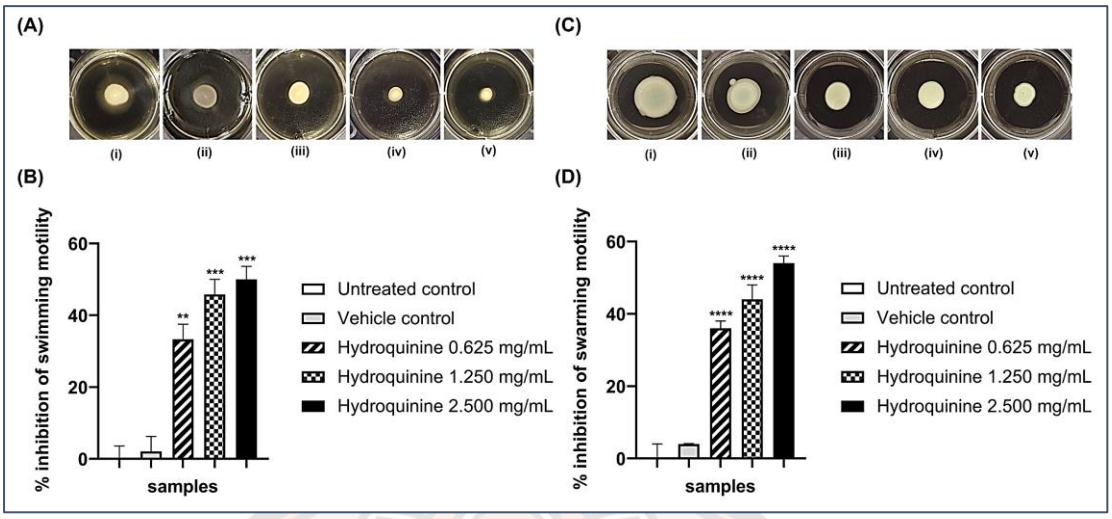

Figure 34 Anti-motility effects of hydroquinine on swimming and swarming patterns in *P. aeruginosa* ATCC 27853

Showing (A, B) swimming and (C, D) swarming patterns at 35 ± 2 °C for 24 h, labeled (i) untreated controls; (ii) vehicle controls; (iii–v) the hydroquinine concentrations at 0.625, 1.250 and 2.500 mg/mL, respectively. The percentage inhibition of (B) swimming and (D) swarming motilities by different concentrations of hydroquinine, compared with the control groups. Mean and standard deviation values from triplicate independent are shown. The asterisk **, *** and **** symbols are $p < 0.01$, $p < 0.001$, and $p < 0.0001$, respectively (225).

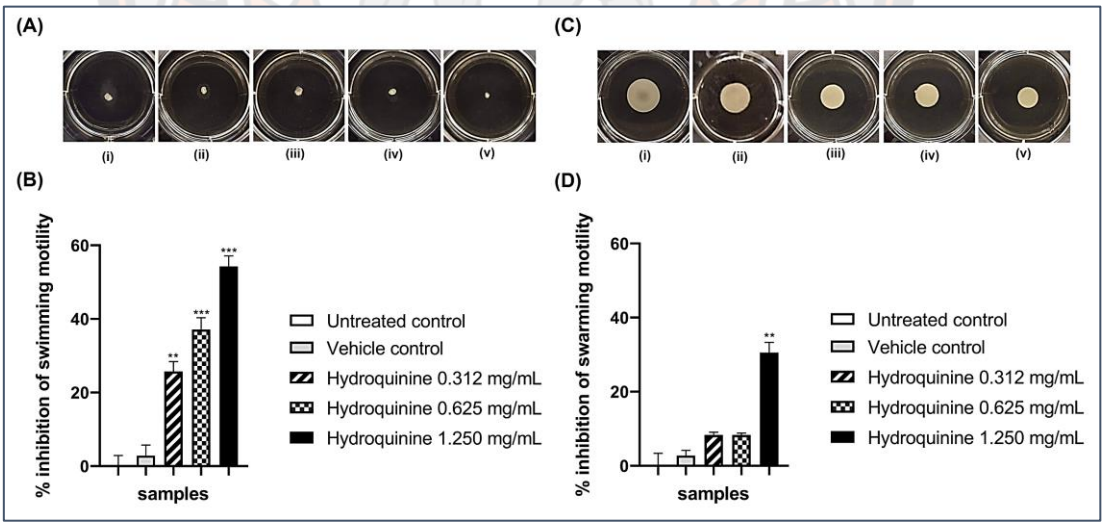

Figure 35 Anti-motility effects of hydroquinine on swimming and swarming patterns in *P. aeruginosa* ATCC BAA-2108

Showing (A, B) swimming and (C, D) swarming patterns at 35 ± 2 °C for 24 h, labeled (i) untreated controls; (ii) vehicle controls; (iii–v) hydroquinine concentrations at 0.312, 0.625 and 1.250 mg/mL, respectively. The percentage inhibition of (B) swimming and (D) swarming motilities by different concentrations of hydroquinine, compared with the control groups. Mean and standard deviation values from triplicate independent are shown. The asterisk ** and *** symbols are $p < 0.01$ and $p < 0.001$, respectively (225).

3.2.3 Hydroquinine affects gene expression of the quorum sensing (QS) system and phenotype of pyocyanin production in both DS and MDR *P. aeruginosa* strains

The relative expression of QS genes, namely *rhlI* and *rhlR* in DS and MDR *P. aeruginosa* tested strains were evaluated using the RT-qPCR method after treatment with hydroquinine at 1.250 and 0.625 mg/mL for 1 h, respectively (225). Also, virulence factors associated with pyocyanin production of DS and MDR *P. aeruginosa* strains were investigated when exposed to hydroquinine with various concentrations for 24 h (225). Hydroquinine significantly downregulated both *rhlI* and *rhlR* gene expression, as shown in Figure 35. The relative *rhlI* expression levels of DS and MDR *P. aeruginosa* strains were significantly downregulated by 0.71 ± 0.07 and 0.37 ± 0.09-fold, respectively. At the same time, the *rhlR* gene of DS and MDR *P. aeruginosa* strains were also significantly downregulated by 0.51 ± 0.17 and 0.50 ± 0.16-fold, respectively (Figure 36A, B).

The phenotype of pyocyanin production (visualized as a green pigment) of the DS and MDR *P. aeruginosa* after treatment with hydroquinine was significantly reduced with a dose-dependent response compared to control groups (Figure 37A, C). After treatment with hydroquinine at 2.500, 1.250, and 0.625 mg/mL of DS *P. aeruginosa* ATCC 27853 for 24h, the percentage of pyocyanin inhibition was shown at 27.13, 26.98, and 25.25%, respectively, when compared to the control groups (Figure 37B). In the case of MDR *P. aeruginosa* strain, the percentages of pyocyanin inhibition showed 25.12, 19.12, and 15.17% when exposed to hydroquinine at 1.250, 0.625, and 0.312 mg/mL, respectively (Figure 37D) for 24h.

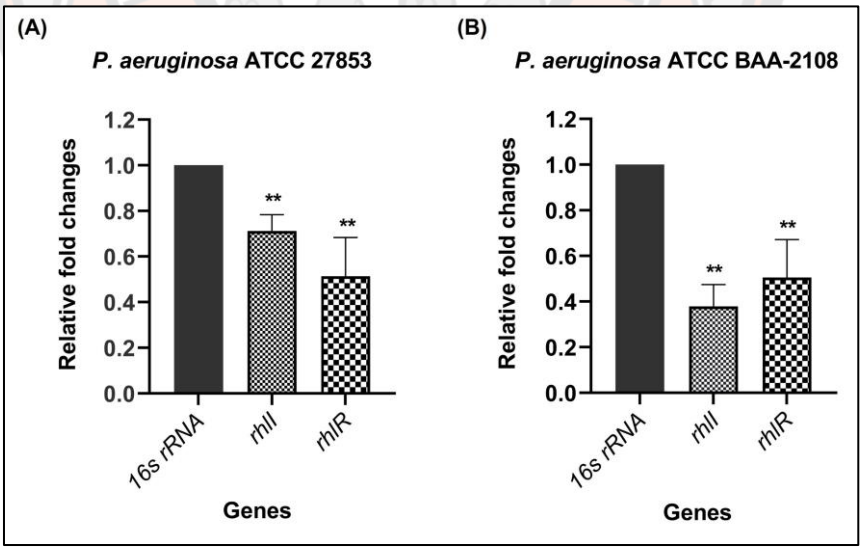

Figure 36 The relative expression of quorum sensing-related genes in *P. aeruginosa* strains.

Showing (A) *P. aeruginosa* ATCC 27853 strain with hydroquinine at 1.250 mg/mL for 1 h and (B) *P. aeruginosa* ATCC BAA-2108 strain treated with hydroquinine at 0.625 mg/mL for 1 h, compared to the corresponding untreated control. The asterisk ** symbol was $p < 0.01$ (225).

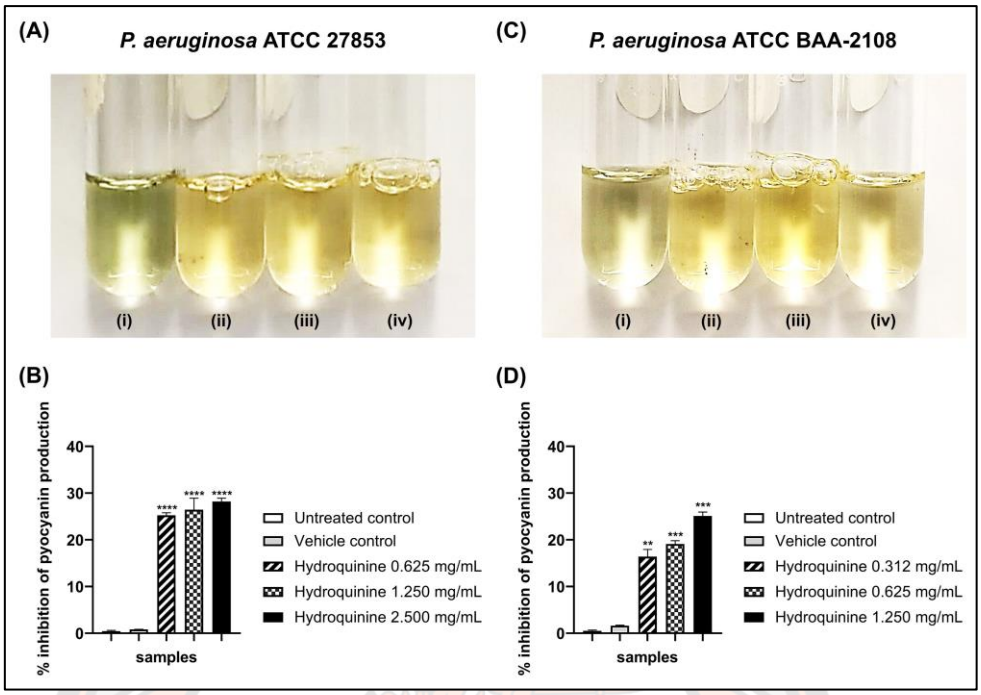

Figure 37 The effect of different concentrations of hydroquinine on pyocyanin production of *P. aeruginosa* strains

Showing (A, B) the DS *P. aeruginosa* ATCC 27853 and (C, D) the MDR *P. aeruginosa* ATCC BAA-2108 after 24 h at 35 ± 2 °C. For (A), (i) untreated control; (ii–iv) the hydroquinine concentrations at 0.625, 1.250 and 2.500 mg/mL, respectively. For (C), (i) untreated control; (ii–iv) the hydroquinine concentrations at 0.312, 0.625 and 1.250 mg/mL, respectively. The percentage inhibition of pyocyanin production in (B) the DS *P. aeruginosa* and (D) the MDR *P. aeruginosa* by the different concentrations of hydroquinine, compared with the control groups. Mean and standard deviation values from triplicate independent are shown. The asterisk **, *** and **** symbols are $p < 0.01$, $p < 0.001$ and $p < 0.0001$, respectively (225).

3.2.4 Hydroquinine affects biofilm formation in both DS and MDR *P. aeruginosa* strains

The virulence factors associated with biofilm formation of DS and MDR *P. aeruginosa* strains were validated after treatment with hydroquinine at various concentrations for 24 h (225). The result showed that the various concentrations tested of hydroquinine affected biofilm-forming ability in both *P. aeruginosa* strains compared to their controls, measured from biofilm-stained crystal violet with an optical density at 595 nm (Figure 38). Both DS and MDR *P. aeruginosa* strains in the control groups exhibited typical biofilm formation capacity (Figure 38A, C). Interestingly, the biofilm mass production of *P. aeruginosa* ATCC 27853 was significantly decreased by 57.61, 44.67, and 25.38%, when treatment with all hydroquinine concentration tasted at 2.500, 1.250, and 0.625 mg/mL, respectively compared to control groups (Figure 38B). In contrast, only hydroquinine at MIC value 1.250 mg/mL against the MDR *P. aeruginosa* strain showed significant decreased biofilm mass formation by 87.65% ($p < 0.0001$). The biofilm masses of the MDR *P. aeruginosa* strain were partially inhibited by

hydroquinine at sub-MIC dosages of 0.625 and 0.312 mg/mL, which showed biofilm mass inhibition percentages of 20.40 and 16.30%, respectively; however, this was not statistically significant (Figure 38D).

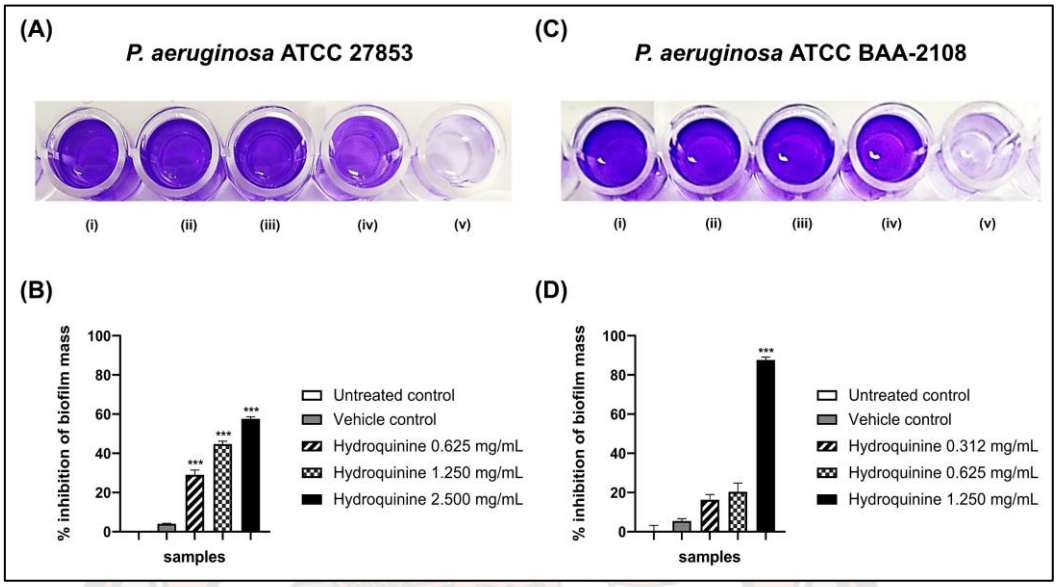

Figure 38 The effects of hydroquinine at different concentrations on biofilm formation.

The panels (A) and (B) were the DS *P. aeruginosa* ATCC 27853 results, shown as (i) untreated control; (ii) vehicle control; and (iii–v) the hydroquinine concentrations at 0.625, 1.250 and 2.500 mg/mL, respectively, while the panels (C) and (D) were the MDR *P. aeruginosa* ATCC BAA-2108 results, shown as (i) untreated control; (ii) vehicle control; and (iii–v) the hydroquinine concentrations at 0.312, 0.625 and 1.250 mg/mL, respectively. The percentage inhibition of biofilm-forming ability in (B) the DS *P. aeruginosa* and (D) the MDR *P. aeruginosa* by the different concentrations of hydroquinine, compared with the control groups. Mean and standard deviation values from triplicate independent are shown. The asterisk *** symbol indicates $p < 0.001$ (225).

CHAPTER V

DISCUSTION AND CONCLUTION

Our findings demonstrate that hydroquinine can both inhibit and kill gram-positive and gram-negative microorganisms. Specifically, hydroquinine inhibits gram-positive bacteria (*S. aureus* ATCC 25923, *S. aureus* ATCC 29213) as well as gram-negative bacteria (*E. cloacae* ATCC2341, *E. coli* ATCC 2452, *E. coli* ATCC 25922, *K. pneumoniae* ATCC 1705, *P. aeruginosa* ATCC 27853, and *P. aeruginosa* ATCC BAA-2108) at a range of MIC values ranging from 650 to 2,500 µg/mL. In addition, hydroquinine also displayed MBC values of 1,250–5,000 µg/mL against the strains tested. These findings are consistent with previous studies that found hydroquinine-containing crude extracts had antibacterial effects against *E. coli*, *S. aureus* and *P. aeruginosa* (16, 229). The MIC and MBC values of the crude extracts against *S. aureus, E. coli*, and *P. aeruginosa* were reported to range from 6,250 to >12,500 µg/mL (16, 229). In contrast, the MIC and MBC values of hydroquinine alone were 5–10 fold lower. Furthermore, this study finding suggests that hydroquinine is likely a better option for development in antibacterial activity than quinine dihydrochloride, which has a MIC of 125 g/mL, another derivative of quinine (230). Other quinine derivatives and quinine itself have antibacterial properties against a variety of harmful microorganisms, similar to hydroquinine (31). These results demonstrate that hydroquinine is one of several bioactive substances with antibacterial properties. Not many adverse effects on respiratory, ocular, or cutaneous irritation are documented in the PubChem database (231). Nonetheless, the adverse effects of hydroquinine might be similar to those of quinine-based agents (232). With the limitations of current research on the side effects of hydroquinine, there is a great need for future research on the adverse consequences of hydroquinine. Ultimately, utilizing hydroquinine as an antimicrobial agent in clinical settings, the safety and effectiveness of hydroquinine remain required for future research.

Based on the time-kill result, hydroquinine demonstrated both bacteriostatic and bactericidal effects against each of the *P. aeruginosa* strains in a dose-dependent manner within 4–8 hours of treatment. This is consistent with other derivatives of quinine or alkaloids that also showed dose-dependent bacteriostatic and bactericidal actions against microorganisms (233, 234). Particularly in the first hour after treatment, the number of viable *P. aeruginosa* cells were quite stable during the early stages of the hydroquinine treatment. This might be because cells can adapt and respond to various environmental challenges, such as chemicals, low pH, and temperatures, by reprogramming their transcriptome profiles, which in turn permits the production of protective activities in the cell (235).

The synergistic effect of hydroquinine with certain antibiotics, including imipenem, gentamicin, and ampicillin, was investigated in the *P. aeruginosa* ATCC BAA-2108 strain. These antibiotics were resisted with *P. aeruginosa* ATCC BAA-2108 strain according to antibiotic susceptibility test results and ATCC reported. As a result, it was found that hydroquinine synergized with their antibiotics as compared with hydroquinine or antibiotic alone on tested *P. aeruginosa* ATCC BAA-2108 strain (FICI values ≤ 0.5). The drug combination

effect may have resulted from different complex formations within the constituents of the respective drugs. Another study on the effects of quinine in combination with antibiotics (erythromycin) against bacteria of clinical relevance revealed interactions that were more synergistic and additive/indifferent than antagonistic (236). Since imipenem and ampicillin block cell wall synthesis to inhibit bacterial growth via binding penicillin-binding proteins associated with peptidoglycan production (196, 237). It may be possible that the mode of action of the combined antibiotic with hydroquinine may have resulted in the complexation of their loss of structural integrity of the bacterial cell wall. Moreover, gentamicin inhibits bacterial growth by attaching to the bacterial ribosome's 30S subunit, which has an adverse effect on protein synthesis (208). Consequently, the synergistic effect might have contributed to their loss of the entire 30s ribosomal subunit structure, which would have led to a loss of the mRNA translation process. These synergistic antibacterial effects of the combinations of hydroquinine with each antibiotic possibly cause a higher cure rate or a more effective treatment against bacterial infections than would be obtained if the antibiotic alone is used. This may be additional information to the present course of treatment for bacterial infections in patients. However, investigating the mechanism of hydroquinine in combination with each antibiotic in the future may help better understand their mechanism and utilize it as a basis for future development and research of hydroquinine combined with antibiotics for use in a clinical setting.

One point of note as hydroquinine exhibited antimicrobial activity, so this study also focuses on finding out the mechanisms of hydroquinine against the *P. aeruginosa* strain via molecular responses. In this study, transcriptional responses of *P. aeruginosa* strain exposed hydroquinine were examined using transcriptomic analysis. The hydroquinine killing curve data (Figure 16) were used to determine the treatment settings for transcriptomic analysis. At ½ MIC (1.250 mg/mL) of hydroquinine treatment for 1 h condition was selected because it did not result in bacterial killing but allowed for transcriptome change profiling (235). The 254 DEGs were identified hydroquinine-treated cells, compared to the untreated controls. Of the 254 DEGs, 157 genes were upregulated while 97 genes were downregulated.

The top 25 most upregulated DEGs *P. aeruginosa* ATCC 27853 following treatment with ½ MIC of hydroquinine for 1 h strongly suggested activation of Resistance-Nodulation-Cell Division (RND) multidrug efflux pump (*mexC*, *mexD*, *oprJ*, *mexX* and *mexY*). The RND-type efflux pump system is a tripartite complex, which is comprised of an inner membrane transporter (e.g., MexB, MexD, MexY), a periplasmic fusion protein (e.g., MexA, MexC, MexX) and an outer membrane channel (e.g., OprM, OprJ) (238). Typically, these three components pump substrate-specific out of the cells using the proton-motive force (238, 239). Efflux pump proteins are present in gram-negative and gram-positive bacteria membranes but have different families and compose units (240). These proteins play an essential role in preventing the accumulation of specific compounds inside the cell and decreasing their activity (241). As a result, an upregulated efflux pump is one of the strategies bacteria use to resist and avoid the effects of antibiotic compounds (242). Additionally, efflux pumps have differences in substrate-specificity; some are unique to a single drug, whereas others exhibit no specificity and expel various unrelated structural molecules, including specific colors, toxic compounds and antimicrobial agents with different chemical structures (240). Therefore, from our observed

transcriptional response, hydroquinine may as the substrate specific to RND efflux pumps of *P. aeruginosa* cells, which contributes to resistance to toxic compounds (in this case, hydroquinine). Generally, the tripartite efflux transporter of the RND efflux pump family is operon organization and similar in several bacterial species, especially gram-negative bacteria (240). Ultimately, hydroquinine may be a substrate specific to RND efflux pumps in other bacterial species; further investigation into other bacteria should continue.

Among the top 25 DEGs result, strongly downregulated gene associated with the arginine deiminase (ADI)-pathway (*arcA*, *arcB*, *arcC*, and *arcD*). Out of the four *arc* genes, the *arcD* gene is responsible for encoding the arginine/ornithine antiporter (AOA), a crucial membrane-bound transporter that swaps one L-arginine molecule for one L-ornithine molecule. On the other hand, the three essential enzymes-arginine deiminase (ADI), ornithine transcarbamylase (OTC), and carbamate kinase (CK) are encoded by the *arcA*, *arcB*, and *arcC* genes (243, 244). In *P. aeruginosa* strain, the ADI pathway acts as ATP mole production from every mole of L-arginine ingested via metabolic conversion stages to cell division and bacterial growth (245). The ADI pathway enables the bacterial cells to continue producing ATP from carbamoyl phosphate in the oxygen-dependent respiratory chain and to do so in anoxic conditions (246). Therefore, loss of ADI pathway function may contribute to reduced survival of bacterial growth (247-249). It is possible that hydroquinine may affect the synthesis of ATP by interfering with the protein associated with the ADI pathway and inhibiting the growth of *P. aeruginosa* ATCC 27853. Nevertheless, further verification of the mode of action of hydroquinine on ADI pathway function in the *P. aeruginosa* strain will require additional research using different methods, such as proteomic analysis and/or mutagenesis analysis. Also, developing hydroquinine as an antimicrobial agent to use in clinical settings, more research should investigate the impact of its mechanism on other pathogenic bacterial species in the future.

Using GO enrichment annotation and KEGG pathway analysis, the data suggested that approximately 23 upregulated genes, not including hypothetical proteins (*arsR*, *cynR*, *trpI*, *mexR*, *rtcR*, *lexA*, *catR*, *nfxB*, *ohrR*, *cifR*, PA0942, PA1223, PA1226, PA1229, PA1283, PA1290, PA2020, PA2469, PA4288, PA4596, PA4902, PA5382, and PA5428) involved in the regulation of the transcription system, were most significantly affected by hydroquinine (Table 11). This system is crucial for the expression of numerous genes and for integrating multiple signals to fine-tune gene expression, which enables bacteria to adapt to complex and dynamic environmental conditions (250). Based on this finding, possibly ½ MIC of hydroquinine concentration (1,250 µg/mL) induced the functions in *P. aeruginosa* displayed in the KEGG pathway analysis (Table 12), including the pathway of beta-lactam resistance, biofilm formation, amino sugar and nucleotide sugar metabolism, and CAMP resistance. In *P. aeruginosa* strain, beta-lactam resistance is one of the essential drug resistance mechanisms, which can reduce uptake or increase efflux of the drug in a group of beta-lactams (251). Regarding the biofilm formation in *P. aeruginosa* strain, three exopolysaccharides (Psl, Pel, and alginate) are essential for biofilm production (252). The seven *pel* genes, *pelA*, *pelB*, *pelC*, *pelD*, *pelE*, *pelF*, and *pelG*, encode the necessary proteins for Pel biosynthesis, a cellulose-like exopolysaccharide high in glucose (253). These genes are important for controlling pellicle formation in of

P. aeruginosa strain, the layer of polymer/cell at the air-liquid interface of a static culture (165). In gram-negative bacteria like *P. aeruginosa*, *E. coli* etc., enzymes ArnA, ArnB, ArnC and ArnT are encoded from the *arn* operon regulating by quorum sensing systems, including RcsA/RcsB/RcsC and PmrA/PmrB (254). These enzymes synthesize 4-Amino-4-deoxy-l-arabinose (L-Ara4N), a critical sugar component of the complex glycolipids that constitute gram-negative bacteria's outer layer of the cell wall (255). Typically, the cationic antimicrobial peptides (CAMPs), small positively charged peptides, are activated by lipid A (256). Many gram-negative bacteria resisted CAMPs by changing the negative groups of LPS to decrease the net negative charge, such as the addition of phosphoethanolamine and/or L-Ara4N that are encoded from *arn* gene operon to 1′ and 4′ phosphates of lipid, and decreasing the affinity of Lipid A by transferring the L-Ara4N from Undecaprenyl Phosphate-L-Ara4N to Lipid A by ArnT enzyme (254, 257-260). Therefore, based on the gene functions of *P. aeruginosa* ATCC 27853 shown in the KEGG pathway results (Table 12), the genes probably allow the bacteria to respond and survive in hydroquinine environments.

Interestingly, by combining GO enrichment annotation and KEGG analysis, the data reviewed that hydroquinine downregulates genes involved in flagella assembly in *P. aeruginosa*. Based on KEGG pathway result, approximately 8 significantly downregulated genes (*flgK, flgD, flgB, flgC, flgH, flgJ, fliF* and *fliG*) associated with flagella assembly pathway (Table 13), encoding to generate the flagellar structure. The flagellum is an important structure for the initial step of bacterial pathogenesis, enabling motility of the bacterium and allowing it to migrate, attach and colonize host cells as well as enabling its survival (81). Moreover, flagella promote the uptake of essential nutrients and as a result, has a critical role in the virulence of pathogenic organisms (261). As the results, it could be hypothesized that hydroquinine causes the downregulation of the flagellar assembly genes, possibly affecting the motility function in *P. aeruginosa*. In addition, genes associated with bacterial chemotaxis (*PA0178, cheZ, fliG, cheY,* and *aer*) were also reported in KEGG pathway analysis after exposure to ½ MIC of hydroquinine for 1 h. In *P. aeruginosa* strain, a chemosensory system is used with flagella or pili to sense changes in the amount of chemicals in their environment and respond behaviorally (262). The chemosensory gene systems control the swimming and twitching motility of *P. aeruginosa* (262). The findings suggest, hydroquinine treatment may disrupt the bacterial chemotaxis pathways and motility system, decreasing the capacity to detect environmental cues and adjust in *P. aeruginosa* strain. As a result, developing hydroquinine as an anti-virulence agent targeting bacterial chemotaxis and flagellar assembly may help decrease bacterial virulence without killing the bacteria and potentially increase the efficacy of the host immunity or traditional antibiotics (263). Moreover, anti-virulence strategies might originate a less intense evolutionary push for the emergence of resistance compared to traditional antibiotics (263). Nevertheless, the development of ant-virulence agents is still emerging at the fundamental research level, and clinical trials have not yet been performed, so they need to be investigated more to show their clinical usefulness.

Regarding further validating upregulated DEGs results, whether hydroquinine exactly induces RND-type efflux pump gene expression in *P. aeruginosa* strains, mRT-PCR base system was used to check for the expression of representative *mex*

genes, namely, *mexB*, *mexD* and *mexY*. Here, to confirm the presence of the *mex* genes, using both mqPCR and the *effluxR* detection assay with mdPCR, all three genes could be detected in bacterial genomes of DS *P. aeruginosa* ATCC27853 and MDR *P. aeruginosa* ATCC BAA-2108 (Table 15-16, Figure 26-28). Interestingly, using the *effluxR* detection assay with mdPCR, the *mex* genes were detected with high specificity in only *P. aeruginosa* strains, not found in any other investigated bacterial strains (Table 19, Figure 29). This result could be explained by the core genome of *P. aeruginosa* encoding many RND-type efflux pumps, e.g., MexXY, MexAB-OprM, MexCD-OprJ (264). In contrast, other microorganism genomes encode other unique types of the RND superfamily efflux pumps, e.g., *E. coli* (AcrAB, AcrAD, AcrEF) (265), *K. pneumoniae* (AcrAB, OqxAB, EefAB, KexD) (266), *E. cloacae* (AcrAB-TolC) (267), *S. aureus* (FarE) (268). The overexpression of the representative RND-type efflux pump genes (*mexB, mexD* and *mexY*) in both *P. aeruginosa* strains using mRT-qPCR and *effluxR* detection assay with mRT-dPCR were then checked. With technical limitations, only the *P. aeruginosa* ATCC 27853 strain was checked for the overexpression levels of the three *mex* genes with *effluxR* detection assay using mRT-dPCR. However, both methods confirmed that the expression levels of *mexD* and *mexY* increased after 1-hour treatment with ½ MIC of hydroquinine (Figure 30-31). In contrast, the expression level of *mexB* remains relatively unchanged (Figure 30-31). These data suggest that in both *P. aeruginosa* strains, hydroquinine stimulates overexpression of representative RND-type efflux pump genes, specifically *mexD* and *mexY*, but not of the *mexB*. These results, consistent with the transcriptomic results, confirm that hydroquinine induces the transcriptional levels of *mexD* and *mexY* in *P. aeruginosa* strains. It also implies that in order to prevent cellular stress brought on by hydroquinine, *P. aeruginosa* induces a defence mechanism by upregulating the MexCD-OprJ and MexXY efflux pumps. This result may be explained by the substrate specificity of RND efflux pumps provided by particular subunits, for example, amphiphilic molecules (e.g., MexB), hydrophobic solutes (e.g., MexD) and the hydrophilic polycationic aminoglycosides (e.g., MexY) (269). Moreover, Morita, *et al.* (270) reported that MexB binds negatively-charged substrates, whereas MexD and MexY do not. This may explain why the neutral charge and low water solubility of hydroquinine only affect the expression of *mexD* and *mexY* genes of *P. aeruginosa* after treatment. The findings suggest that hydroquinine may have some beneficial antimicrobial effects, but it also causes certain RND-type efflux pumps. This confirms the findings of previous research, which demonstrated that patients treated with antimalarial medications such as hydroquinine or medications based on quinine may also develop a concurrent bacterial infection (271, 272). Antibiotic treatments for active skin infections or other organ infections might be necessary in these individuals (271, 272). Notably, the resistance mechanism via RND-type efflux pumps in *P. aeruginosa* infections should be screened in these concurrent cases to identify the potential role of efflux pump overexpression.

To further validate the downregulated DEGs results, whether hydroquinine affects the flagellar assembly genes in *P. aeruginosa* strains was evaluated. Genotypic analysis with RT-qPCR and phenotypic analysis were used. Four representative flagellar assembly genes were examined, including genes that generated the basal

body (*flgH, flgC,* and *fliF*) and a hook-filament junction gene (*flgK*). All genes showed downregulated relative expression levels in DS and MDR *P. aeruginosa* strains exposed to ½ MIC of hydroquinine for one hour (Figure 33). Generally, the initial structure created for flagellar assembly is often the basal body, which is embedded in the cell membrane of gram-negative bacteria, such as *P. aeruginosa* (Figure 32) (273). Moreover, the hook-filament junction is essential in linking the hook/basal-body complex with the long flagellin filament (274). Interestingly, the phenotype of swimming and swarming motilities of both *P. aeruginosa* strains was measured to evaluate the effect of hydroquinine on motility property. The results showed that the swimming and swarming motilities of *P. aeruginosa* strains decreased following hydroquinine treatment concurrent with our genotypic analysis using high-throughput and RT-qPCR methods. Furthermore, the results correlated with previous research on the anti-motility properties of other alkaloid compounds. Caffeine, for instance, significantly decreases *P. aeruginosa* swarming motility (69, 97). Other alkaloids, such as piperine and reserpine, interfere with swimming and swarming motility properties in *E. coli* by lowering the expression levels of the motility genes, *motA* and *motB*, and the flagellar gene, *flaC*. (84). Therefore, the finding of these data strongly suggests that hydroquinine promotes the downregulation of the genes involved in flagellar assembly, which may impact *P. aeruginosa* motility. In addition, this study found that reducing other virulence factors in DS and MDR *P. aeruginosa*, which are pyocyanin production and biofilm formation, were exhibited after treatment with dose-dependent hydroquinine concentrations for 24 h (Figure 37-38). Pyocyanin is zwitterionic, it can pass through the cytoplasmic membrane of the host (275). The presence of pyocyanin is essential in oxidative stress, contributing to host cell cytotoxicity (275). Interestingly, in the *P. aeruginosa* strain, biofilm-forming potential is associated with flagella motility, which is the initial stage in attachment for colonization and biofilm production (273, 276). In *P. aeruginosa*, the QS systems play an essential role in regulating the production of virulence factors, including pyocyanin and biofilm (20, 277). In particular, *rhl* (*rhlI/R*) QS systems have been reported to regulate pyocyanin production and the biofilm-forming ability of the bacterium (278, 279). Moreover, according to previous observations, the biofilm mass of the *rhlI* mutant or null *rhl* QS genes showed biofilm mass reductions higher than those of the wild-type strain (279). Therefore, after hydroquinine treatment, *rhlI* and *rhlR* gene expression were examined in DS and MDR *P. aeruginosa* strains to confirm whether hydroquinine affects pyocyanin production and biofilm formation through the QS-dependent system. It was found that hydroquinine significantly decreased the mRNA expression levels of the *rhl* QS system (*rhlI* and *rhlR*) in both *P. aeruginosa* strains, indicating that hydroquinine may be able to reduce pyocyanin production and biofilm formation by interfering with the *rhl* QS system. This was consistent with findings from Park *et al.* (2008) (20), who reported an association between the *rhlI*/*R* QS system and pyocyanin production. It has been reviewed that *P. aeruginosa* produces less pyocyanin when C4-HSL, a recognized autoinducer for activating the *rhl* QS system, is absent. Furthermore, other alkaloids (such as solenopsin A) and their derivatives demonstrated anti-QS action and anti-pyocyanin production in *P. aeruginosa* by preventing the synthesis of QS molecules (20, 69, 97). Moreover, other alkaloid derivative compounds have been reported for anti-biofilm formation activity in the

P. aeruginosa strain (21, 79, 97). The findings suggest hydroquinine might be an anti-pyocyanin production and anti-biofilm formation agent. Also, as a result, hydroquinine may be used as an alternative agent in combination with other antibiotics. However, a crystal violet retention assay was used to test the biofilm formation of the bacterial living cells only. To reduce this limitation, both living and dead cells in the biofilm and biofilm matrix of *P. aeruginosa* after treatment with hydroquinine should be further investigated with other methods, e.g., staining with SYTO9 and propidium iodide (280), a wheat germ agglutinin-Alexa Fluor 488 fluorescent conjugate (228) etc.

In conclusion, hydroquinine has anti-bacterial properties with concentrations ranging from 625-2,500 µg/mL. It can inhibit and kill several strains of clinically significant bacteria, namely *S. aureus*, *E. cloacae*, *E. coli*, *K. pneumoniae* and, in particular, *P. aeruginosa*. Moreover, hydroquinine improves the efficiency of antibiotics (imipenem, gentamicin and ampicillin) with synergistic properties in the MDR *P. aeruginosa* ATCC BAA-2108 treatment. In addition, the present study is the first to uncover a global molecular response of *P. aeruginosa* to hydroquinine with high-throughput transcriptomic analysis. Overall, 254 genes were transcribed in *P. aeruginosa* ATCC 27853 exposed to ½ MIC of hydroquinine (1,250 µg/mL) for one hour, including upregulating 97 genes and downregulating 157 genes. As an upregulated DEGs result, the *P. aeruginosa* strain showed the transcriptional response of RND-type efflux pump systems with the most significant overexpression. Moreover, the upregulated relative expression levels of representative RND-type efflux pump genes in *P. aeruginosa* hydroquinine treatment were also shown by mRT-qPCR and the *effluxR* detection assay with mRT-dPCR methods. Hydroquinine exhibited the most significantly downregulated DEGs of arginine deiminase genes, which play a role in ATP synthesis and contribute to bacterial growth in the *P. aeruginosa* strain. The GO enrichment and KEGG pathway analysis of downregulated genes exhibited the hydroquinine effect with flagellar assembly and motility functions in the *P. aeruginosa* ATCC 27853. Specifically, hydroquinine treatment reduced swimming and swarming motility functions in DS and MDR *P. aeruginosa* strain. Interestingly, ½ MIC of hydroquinine showed downregulating of QS genes (*rhlI* and *rhlR*) as well as reduced the exhibition of the phenotypic properties in *P. aeruginosa* strains when treated, including green pigment and biofilm-stained crystal violet, suggesting that hydroquinine may inhibit pyocyanin production and biofilm formation. The findings of this study demonstrate that the low dose of hydroquinine treatment is sufficient to induce specific RND-type efflux pump systems, especially the MexCD-OprJ and MexXY efflux pump, as well as interfere with the ATP synthesis mechanism via the ADI pathway in *P. aeruginosa* strain. Moreover, hydroquinine has anti-infection properties via inhibition of the virulence factor of DS and MDR *P. aeruginosa* strains. These findings suggest hydroquinine might be used as an anti-bacterial and anti-infective, or anti-virulence factor agent in treating bacterial infection, especially *P. aeruginosa* strains. Although our current study provided global transcriptomic changes of *P. aeruginosa* triggered by hydroquinine treatment, further studies will be required to investigate the protein expression level of the target genes and find the molecular target of hydroquinine. Exploring the efficacy, potential, and safety of hydroquinine will also be necessary for further work to be done in clinical settings. It will be a significant step in developing

new therapeutic approaches for treating pathogenic microorganisms.

ABBREVIATIONS LIST

°C	Degree Celsius
λ	Total number of copies of the target molecule
µg	Microgram
µg/mL	Microgram per milliliter
µL	Microliter
µM	Micromolar
Ab	Antibodies
ABC	ATP binding cassette
ADI	Arginine deiminase
AHLs	Nacylated L-homoserine lactones
AIP	Autoinducer peptides
AKP	Alkaline phosphatase
AOA	Arginine/ornithine antiporter
AP	Ampicillin
AST	Antibiotic susceptibility test
ATCC	American Type Culture Collection
ATP	Adenosine triphosphate
B cell	B lymphocyte
BHI	Brain Heart Infusion broth
BP	Biological process
bp	Base pair
BSL-2	Biosafety Level 2 Laboratory
CAI-1	(S)- 3-hyroxytridecan-4-one
CAMP	Cationic antimicrobial peptide
CC	Cellular component
CDC	Centers for Disease Control and Prevention
c-di-GMP	Bis-(3′-5′)-cyclic dimeric guanosine monophosphate
CFU/mL	Colony-forming units per milliliter
95%CI	95% confidence interval
CIP	Ciprofloxacin
CK	Carbamate kinase
CLSI	Clinical and Laboratory Standards
Ct	Cycle threshold
DAVID	Annotation, Visualization, and Integrated Discovery
DEGs	Differentially expressed genes
DMSO	Dimethyl sulfoxide
DNA	Deoxyribonucleic acid
DS	Drug sensitive
eDNA	Extracellular DNA
eNEEs	Ethanolic Nest Entrances Extracts
EPS	Exopolysaccharide
EPSs	Extracellular polymeric substances

ESBLs	Extended-spectrum-ß-lactamases
EtBr	Ethidium Bromide
FDR	False discovery rate
FICI	fractional inhibitory concentration index
FIM	Florence imipenemase
FPKM	Fragments per kilobase of transcript per million
FtsZ	Filamentous temperature-sensitive protein Z
gDNA	Genomic deoxyribonucleic acid
GIM	Germany imipenemase
GO	Gene Ontology
GT	Gentamicin
h	Hour
HQ	Hydroquinine
I	Intermediate
IC50	Half maximal inhibitory concentration
IgG	Immunoglobulin G
IM	Imipenem
IMP	Imipenemase
kb	kilobase
kDa	Kilo Dalton
KEGG	Kyoto encyclopedia of genes and genomes
LB	Luria-Bertani
LOD	Limit of detection
Log_2FC	log_2 gene expression fold changes
LPS	Lipopolysaccharides
MATE	Multidrug and toxic efflux
MBC	Minimum bactericidal concentration
mdPCR	Multiplex digital PCR
MDR	Multidrug resistance
MF	Major facilitator
MF	Molecular function
mg	Milligram
mg/mL	Milligram per milliliter
MHA	Mueller Hinton agar
MHB	Mueller Hinton broth
MIC	Minimum inhibitory concentration
min	Minute
mm	Millimeter
mqPCR	Multiplex quantitative PCR
mRNA	Messenger ribonucleic acid
mRT-dPCR	Multiplex Quantitative Reverse Transcription Digital PCR
mRT-qPCR	Multiplex Quantitative Reverse Transcription PCR
NADH	Nicotinamide adenine dinucleotide (NAD) + hydrogen (H)
NCBI	National Center for Biotechnology Information

ND	Not determine
NDM	New delhi metallo- ß-lactamase
ng	Nanogram
nL	Nanoliters
nm	Nanometer
nM	Nanomolar
NNIS	The National Nosocomial Infections Surveillance
NSS	Normal saline solution
nt	Nucleotide
NTC	Non-template control
O_2	oxygen radicals
OD	Optical Density
OTC	Ornithine transcarbamylase
PBS	Phosphate-buffered saline
PCR	Polymerase chain reaction
PMF	Proton motive force
Q20	Phred quality score 20
Q30	Phred quality score 30
QC	Quality control
qPCR	Quantitative Polymerase Chain Reaction
QS	Quorum sensing
R	Resistant
RIN	RNA integrity number
RNA	Ribonucleic acid
RNA-Seq	RNA-Sequencing
RND	Resistance-nodulation-division
ROS	Reactive oxygen species
rpm	Revolutions per minute
rRNA	Ribosomal ribonucleic acid
RT-PCR	Reverse transcription polymerase chain reaction
S	Susceptible
SAM	S-adenosylmethionine
SD	Standard deviation
Sec or s.	Second
SMR	Small multidrug resistance
SNP	Single nucleotide polymorphisms
T cell	T lymphocyte
T_a	Annealing temperature
TBE	Tris-borate-EDTA
T_m	Melting temperature
tRNA	Transfer ribonucleic acid
TSA	Tryptone Soya agar
TSB	Tryptone Soya broth
UTI	Urinary tract infections
V	Estimated partition volume
V/V	Volume per volume

VIM	Verona integron-encoded metallo-ß-lactamase
SPM	Sao paulo metallo-ß-lactamase
W/V	Weight per volume
WHO	World Health Organization

REFERENCES

1. World Health Organization. antimicrobial resistance. Global Report on Surveillance. Geneva 2014. [Internet]. [cited 2021 Oct 9]. Available from: https://www.who.int/home/search?indexCatalogue=genericsearchindex1&searchQuery=Antimicrobial%20resistance&wordsMode=AllWords.
2. Ventola CL. The antibiotic resistance crisis: part 1: causes and threats. P T. 2015;40(4):277-83.
3. Golkar Z, Bagasra O, Pace DG. Bacteriophage therapy: a potential solution for the antibiotic resistance crisis. J Infect Dev Ctries. 2014;8(2):129-36.
4. Centers for Disease Control and Prevention. antibiotic resistance threats in the United States, 2013. [Internet]. [cited 2021 Oct 28]. Available from: http://www.cdc.gov/drugresistance/threat-report-2013
5. Pang Z, Raudonis R, Glick BR, Lin TJ, Cheng Z. Antibiotic resistance in *Pseudomonas aeruginosa:* mechanisms and alternative therapeutic strategies. Biotechnol Adv. 2019;37(1):177-92.
6. *Pseudomonas aeruginosa*. [Internet]. [cited 2021 Oct 28]. Available from: http://www.antimicrobe.org/b112-index.asp.
7. Livermore DM. Multiple mechanisms of antimicrobial resistance in *Pseudomonas aeruginosa*: our worst nightmare. Clin Infect Dis. 2002;34(5):634-40.
8. Cohen AL, Calfee D, Fridkin SK, Huang SS, Jernigan JA, Lautenbach E, et al. Recommendations for metrics for multidrug-resistant organisms in healthcare settings: SHEA/HICPAC position paper. Infect Control Hosp Epidemiol. 2008;29(10):901-13.
9. Falagas ME, Koletsi PK, Bliziotis IA. The diversity of definitions of multidrug-resistant (MDR) and pandrug-resistant (PDR) *Acinetobacter baumannii* and *Pseudomonas aeruginosa*. J Med Microbiol. 2006;55(12):1619-29.
10. Kallen AJ, Hidron AI, Patel J, Srinivasan A. Multidrug resistance among gram-negative pathogens that caused healthcare-associated infections reported to the National Healthcare Safety Network, 2006-2008. Infect Control Hosp Epidemiol. 2010;31(5):528-31.
11. Critchley IA, Draghi DC, Sahm DF, Thornsberry C, Jones ME, Karlowsky JA. Activity of daptomycin against susceptible and multidrug-resistant Gram-positive pathogens collected in the SECURE study (Europe) during 2000-2001. J Antimicrob Chemother. 2003;51(3):639-49.
12. Richards MJ, Edwards JR, Culver DH, Gaynes RP. Nosocomial infections in medical intensive care units in the United States. National Nosocomial Infections Surveillance System. Crit Care Med. 1999;27(5):887-92.
13. Mirzaei B, Bazgir ZN, Goli HR, Iranpour F, Mohammadi F, Babaei R. Prevalence of multi-drug resistant (MDR) and extensively drug-resistant (XDR) phenotypes of *Pseudomonas aeruginosa* and *Acinetobacter baumannii* isolated in clinical samples from Northeast of Iran. BMC Res Notes. 2020;13(1):1-6.
14. Gonelimali FD, Lin J, Miao W, Xuan J, Charles F, Chen M, et al. Antimicrobial properties and mechanism of action of some plant extracts against food pathogens and spoilage microorganisms. Front Microbiol. 2018;9:1-9.
15. Siriyong T, Srimanote P, Chusri S, Yingyongnarongkul BE, Suaisom C, Tipmanee V, et al. Conessine as a novel inhibitor of multidrug efflux pump systems in *Pseudomonas aeruginosa*. BMC Complement Altern Med. 2017;17(1):1-7.

16. Jongjitvimol T, Kraikongjit S, Paensuwan P, Jongjitwimol J. *In vitro* biological profiles and chemical contents of ethanolic nest entrance extracts of thai stingless bees *Tetrigona apicalis*. Online J Biol Sci. 2020;20(3):157-65.
17. Murauer A, Ganzera M. Quantitative determination of major alkaloids in Cinchona bark by Supercritical Fluid Chromatography. J Chromatogr A. 2018;1554:117-22.
18. Jansen PH, Veenhuizen KC, Wesseling AI, de Boo T, Verbeek AL. Randomised controlled trial of hydroquinine in muscle cramps. Lancet. 1997;349(9051):528-32.
19. Nationnal Center for Advancing Translation Science; NIH. Inxignt: Drugs, Hydroquinine 31J30Q51T6L. [Internet]. [cited 2021 Oct 2]. Available from: https://drugs.ncats.io/substance/31J3Q51T6L.
20. Park J, Kaufmann GF, Bowen JP, Arbiser JL, Janda KD. Solenopsin A, a venom alkaloid from the fire ant solenopsis invicta, inhibits quorum-sensing signaling in *Pseudomonas aeruginosa*. J Infect Dis. 2008;198(8):1198-201.
21. Lee JH, Cho MH, Lee J. 3-indolylacetonitrile decreases *Escherichia coli* O157:H7 biofilm formation and *Pseudomonas aeruginosa* virulence. Environ Microbiol. 2011;13(1):62-73.
22. Mitchell G, Lafrance M, Boulanger S, Séguin DL, Guay I, Gattuso M, et al. Tomatidine acts in synergy with aminoglycoside antibiotics against multiresistant *Staphylococcus aureus* and prevents virulence gene expression. J Antimicrob Chemother. 2012;67(3):559-68.
23. Nontprasert A, Pukrittayakamee S, Kyle DE, Vanijanonta S, White NJ. Antimalarial activity and interactions between quinine, dihydroquinine and 3-hydroxyquinine against *Plasmodium falciparum in vitro*. Trans R Soc Trop Med Hyg. 1996;90(5):553-5.
24. Polet H, Barr CF. Chloroquine and Dihydroquinine *in vitro* studies of thesis antimalarial effect upon. *Plasmodium knowlesi.* J Pharmacol Exp Ther. 1968;164(2):380-6.
25. Andersson L. A new revision of Joosia (Rubiaceae-Cinchoneae). Brittonia. 1997;49(1):24-44.
26. Kacprzak KM. Natural products: phytochemistry, botany and metabolism of alkaloids, phenolics and terpenes. Nat Prod. 2013:605-41.
27. Achan J, Talisuna AO, Erhart A, Yeka A, Tibenderana JK, Baliraine FN, et al. Quinine, an old anti-malarial drug in a modern world: role in the treatment of malaria. Malar J. 2011;144(10):1-12.
28. Edwards G. Antimalarial chemotherapy: Mechanisms of action, resistance and new directions in drug discovery. Br J Clin Pharmacol. 2001;52(4):461-4.
29. Ning X, He J, Shi Xe, Yang G. Regulation of adipogenesis by quinine through the ERK/S6 Pathway. Int J Mol Sci. 2016;17(4):1-15.
30. Krishnaveni M, K S. Induction of apoptosis by quinine in human laryngeal carcinoma cell line. Int j curr. 2015;3(3):169-78.
31. Antika LD, Triana D, Ernawati T. Antimicrobial activity of quinine derivatives against human pathogenic bacteria. IOP Conf Ser Earth Environ Sci. 2020;462:1-8.
32. Yan Y, Li X, Zhang C, Lv L, Gao B, Li M. Research progress on antibacterial activities and mechanisms of natural alkaloids: A Review. Antibiotics. 2021;10(3):3-30.
33. Elisabetsky E, Costa-Campos L. The alkaloid alstonine: a review of its pharmacological properties. Evid Based Complement Alternat Med. 2006;3(1):39-48.

34. Zhang Q, Lyu Y, Huang J, Zhang X, Yu N, Wen Z, et al. Antibacterial activity and mechanism of sanguinarine against *Providencia rettgeri in vitro*. PeerJ. 2020;8:1-19.
35. Salton MRJ. Structure and function of bacterial cell membranes. Annu Rev Microbiol. 1967;21(1):417-42.
36. RNA Functions [Internet]. Nature Education 2008 [cited 2021 Oct 28]. Available from: https://www.nature.com/scitable/topicpage/rna-functions-352/.
37. Othman L, Sleiman A, Abdel-Massih RM. Antimicrobial activity of polyphenols and alkaloids in middle eastern plants. Front Microbiol. 2019;10:1-28.
38. Maxwell A. DNA gyrase as a drug target. Trends Microbiol. 1997;5(3):102-9.
39. Heeb S, Fletcher MP, Chhabra SR, Diggle SP, Williams P, Cámara M. Quinolones: from antibiotics to autoinducers. FEMS Microbiol Rev. 2011;35(2):247-74.
40. Rukachaisirikul T, Prabpai S, Champung P, Suksamrarn A. Chabamide, a novel piperine dimer from stems of Piper chaba. Planta Med. 2002;68(9):853-5.
41. Bendaif H, Melhaoui A, Ramdani M, Elmsellem H, Douez C, El Ouadi Y. Antibacterial activity and virtual screening by molecular docking of lycorine from *Pancratium foetidum* Pom (Moroccan endemic Amaryllidaceae). Microb Pathog. 2018;115:138-45.
42. Levenfors JJ, Nord C, Bjerketorp J, Ståhlberg J, Larsson R, Guss B, et al. Antibacterial pyrrolidinyl and piperidinyl substituted 2,4-diacetylphloroglucinols from *Pseudomonas protegens* UP46. J Antibiot Res. 2020;73(11):739-47.
43. Barrows JM, Goley ED. FtsZ dynamics in bacterial division: What, how, and why?. Curr Opin Cell Biol. 2021;68:163-72.
44. Strahl H, Errington J. Bacterial membranes: structure, domains, and function. Annu Rev Microbiol. 2017;71:519-38.
45. Salton MRJ, KS K. Structure. In: S B, editor. Medical Microbiology. 4th ed. Galveston (TX): University of Texas Medical Branch at Galveston; 1996.
46. Qian LH TY, Xie J. Antibacterial mechanism of tea polyphenols against *Staphylococcus aureus* and *Pseudomonas aeruginosa*. Microbiol Rev. 2010;37:1628-33.
47. Lan WQ XJ, Hou WF, Li DW. Antibacterial activity and mechanism of compound biological preservatives against *Staphylococcus squirrel*. Res Dve Nat Prod. 2012;24:741–6.
48. Hara S, Yamakawa M. Moricin, a novel type of antibacterial peptide isolated from the silkworm, Bombyx mori. J Biol Chem. 1995;270(50):29923-27.
49. Dvorák Z, Sovadinová I, Bláha L, Giesy JP, Ulrichová J. Quaternary benzo[c]phenathridine alkaloids sanguinarine and chelerythrine do not affect transcriptional activity of aryl hydrocarbon receptor: analyses in rat hepatoma cell line H4IIE.luc. Food Chem Toxicol. 2006;44(9):1466-73.
50. Wang Y, Shou JW, Li XY, Zhao ZX, Fu J, He CY, et al. Berberine-induced bioactive metabolites of the gut microbiota improve energy metabolism. Metabolism. 2017;70:72-84.
51. Van Bambeke F, Balzi E, Tulkens PM. Antibiotic efflux pumps. Biochem Pharmacol. 2000;60(4):457-70.
52. Webber MA, Piddock LJ. The importance of efflux pumps in bacterial antibiotic resistance. J Antimicrob Chemother. 2003;51(1):9-11.
53. Wei JT QJ, Su QLY, Liu ZX, Wang XL, Wang YP. Research progress on the mechanism of bacterial biofilm induced drug resistance and the effect of antimicrobial

peptide LL-37 on biofilm. J Hexi Univ. 2020;36:38-43.
54. Lomovskaya O, Warren MS, Lee A, Galazzo J, Fronko R, Lee M, et al. Identification and characterization of inhibitors of multidrug resistance efflux pumps in *Pseudomonas aeruginosa*: novel agents for combination therapy. Antimicrob Agents Chemother. 2001;45(1):105-16.
55. Paulsen IT, Brown MH, Skurray RA. Proton-dependent multidrug efflux systems. Microbiol Rev. 1996;60(4):575-608.
56. Siriyong T, Chusri S, Srimanote P, Tipmanee V, Voravuthikunchai SP. *Holarrhena antidysenterica* extract and its steroidal alkaloid, conessine, as resistance-modifying agents against extensively drug-resistant *Acinetobacter baumannii*. Microb Drug Resist. 2016;22(4):273-82.
57. Mabhiza D, Chitemerere T, Mukanganyama S. Antibacterial properties of alkaloid extracts from *Callistemon citrinus* and *Vernonia adoensis* against *Staphylococcus aureus* and *Pseudomonas aeruginosa*. Int J Med Chem. 2016;2016:1-7.
58. Hooper DC. Efflux pumps and nosocomial antibiotic resistance: a primer for hospital epidemiologists. Clin Infect Dis. 2005;40(12):1811-17.
59. Sobti M, Ishmukhametov R, Stewart AG. ATP synthase: expression, purification, and function. Methods Mol Biol. 2020;2073:73-84.
60. Du GF, Le YJ, Sun X, Yang XY, He QY. Proteomic investigation into the action mechanism of berberine against *Streptococcus pyogenes*. J Proteomics. 2020;215:103666.
61. Wang TP GY, Zhao Q, Yuan YJ, Ma WC, Xue L. Preliminary study on the antibacterial effect and mechanism of alkaloids from *Rabdosia Rubra* on *Klebsiella pneumoniae*. J Tianshui Norm Univ. 2018;38:24–8.
62. Sharma AK, Dhasmana N, Dubey N, Kumar N, Gangwal A, Gupta M, et al. Bacterial virulence factors: Secreted for survival. Indian J Microbiol. 2017;57(1):1-10.
63. Wilson JW, Schurr MJ, LeBlanc CL, Ramamurthy R, Buchanan KL, Nickerson CA. Mechanisms of bacterial pathogenicity. Postgrad Med J. 2002;78(918):216-24.
64. Silva LN, Zimmer KR, Macedo AJ, Trentin DS. Plant natural products targeting bacterial virulence factors. Chem Rev. 2016;116(16):9162-236.
65. Miller MB, Bassler BL. Quorum sensing in bacteria. Annu Rev Microbiol. 2001;55:165-99.
66. Galloway WR, Hodgkinson JT, Bowden SD, Welch M, Spring DR. Quorum sensing in Gram-negative bacteria: small-molecule modulation of AHL and AI-2 quorum sensing pathways. Chem Rev. 2011;111(1):28-67.
67. Rutherford ST, Bassler BL. Bacterial quorum sensing: its role in virulence and possibilities for its control. Cold Spring Harb Perspect Med [Internet]. 2012 2012/11/; 2(11):[a012427 p.]. Available from: https://doi.org/10.1101/cshperspect.a012427
68. Lyon GJ, Novick RP. Peptide signaling in *Staphylococcus aureus* and other Gram-positive bacteria. Peptides. 2004;25(9):1389-403.
69. Norizan SN, Yin WF, Chan KG. Caffeine as a potential quorum sensing inhibitor. Sensors (Basel). 2013;13(4):5117-29.
70. Costerton JW, Lewandowski Z, Caldwell DE, Korber DR, Lappin-Scott HM. Microbial biofilms. Annu Rev Microbiol. 1995;49:711-45.
71. Davey ME, O'Toole G A. Microbial biofilms: from ecology to molecular genetics. Microbiol Mol Biol Rev. 2000;64(4):847-67.
72. Mikkelsen H, Duck Z, Lilley KS, Welch M. Interrelationships between colonies,

biofilms, and planktonic cells of Pseudomonas aeruginosa. J Bacteriol. 2007;189(6):2411-6.
73. del Pozo JL, Patel R. The challenge of treating biofilm-associated bacterial infections. Clin Pharmacol Ther. 2007;82(2):204-9.
74. Donlan RM. Biofilms and device-associated infections. Emerg Infect Dis. 2001;7(2):277-81.
75. Fux CA, Costerton JW, Stewart PS, Stoodley P. Survival strategies of infectious biofilms. Trends Microbiol. 2005;13(1):34-40.
76. Stewart PS, Costerton JW. Antibiotic resistance of bacteria in biofilms. Lancet. 2001;358(9276):135-8.
77. Drenkard E, Ausubel FM. Pseudomonas biofilm formation and antibiotic resistance are linked to phenotypic variation. Nature. 2002;416(6882):740-3.
78. Bjarnsholt T, Ciofu O, Molin S, Givskov M, Høiby N. Applying insights from biofilm biology to drug development - can a new approach be developed?. Nat Rev Drug Discov. 2013;12(10):791-808.
79. Lee J-H, Kim Y-G, Cho MH, Kim J-A, Lee J. 7-fluoroindole as an antivirulence compound against *Pseudomonas aeruginosa*. FEMS Microbiol Lett. 2012;329(1):36-44.
80. Artini M, Papa R, Barbato G, Scoarughi GL, Cellini A, Morazzoni P, et al. Bacterial biofilm formation inhibitory activity revealed for plant derived natural compounds. Bioorg Med Chem. 2012;20(2):920-6.
81. Haiko J, Westerlund-Wikström B. The role of the bacterial flagellum in adhesion and virulence. Biology (Basel). 2013;2(4):1242-67.
82. Kearns DB. A field guide to bacterial swarming motility. Nature Reviews Microbiology. 2010;8(9):634-44.
83. Mattick JS. Type IV pili and twitching motility. Annu Rev Microbiol. 2002;56:289-314.
84. Dusane DH, Hosseinidoust Z, Asadishad B, Tufenkji N. Alkaloids modulate motility, biofilm formation and antibiotic susceptibility of uropathogenic *Escherichia coli*. PLoS ONE. 2014;9(11):e112093.
85. Monte J, Abreu AC, Borges A, Simões LC, Simões M. Antimicrobial activity of selected phytochemicals against *Escherichia coli* and *Staphylococcus aureus* and their biofilms. Pathogens. 2014;3(2):473-98.
86. Ghazaei C. Advances in the study of bacterial toxins, their roles and mechanisms in pathogenesis. Malays J Med Sci. 2022;29(1):4-17.
87. Forbes JD. Clinically important toxins in bacterial infection: Utility of laboratory detection. Clin Microbiol Newsl. 2020;42(20):163-70.
88. Henkel JS, Baldwin MR, Barbieri JT. Toxins from bacteria. Exs. 2010;100:1-29.
89. DuMont AL, Torres VJ. Cell targeting by the *Staphylococcus aureus* pore-forming toxins: it's not just about lipids. Trends Microbiol. 2014;22(1):21-7.
90. Liu GY, Nizet V. Color me bad: microbial pigments as virulence factors. Trends Microbiol. 2009;17(9):406-13.
91. Pelz A, Wieland K-P, Putzbach K, Hentschel P, Albert K, Götz F. Structure and biosynthesis of staphyloxanthin from *Staphylococcus aureus*. J Biol Chem. 2005;280(37):32493-8.
92. Cézard C, Farvacques N, Sonnet P. Chemistry and biology of pyoverdines, *Pseudomonas* primary siderophores. Curr Med Chem. 2015;22(2):165-86.
93. Jayaseelan S, Ramaswamy D, Dharmaraj S. Pyocyanin: production, applications,

challenges and new insights. World J Microbiol Biotechnol. 2014;30(4):1159-68.
94. Dietrich LE, Price-Whelan A, Petersen A, Whiteley M, Newman DK. The phenazine pyocyanin is a terminal signalling factor in the quorum sensing network of *Pseudomonas aeruginosa*. Mol Microbiol. 2006;61(5):1308-21.
95. Balasubramanian D, Schneper L, Merighi M, Smith R, Narasimhan G, Lory S, et al. The regulatory repertoire of *Pseudomonas aeruginosa* AmpC ß-lactamase regulator AmpR includes virulence genes. PLoS ONE. 2012;7(3):e34067.
96. Lau GW, Hassett DJ, Ran H, Kong F. The role of pyocyanin in *Pseudomonas aeruginosa* infection. Trends Mol Med. 2004;10(12):599-606.
97. Husain FM, Ahmad I, Khan MS, Al-Shabib NA. *Trigonella foenum*-graceum (Seed) extract interferes with quorum sensing regulated traits and biofilm formation in the strains of *Pseudomonas aeruginosa* and *Aeromonas hydrophila*. Evid-based Complement Altern Med. 2015;2015:879540.
98. Mazhar Ali N, Rehman S, Abdullah Mazhar S, Liaqat I, Mazhar B. *Psuedomonas aeruginosa*-Associated acute and chronic pulmonary infections. In: Sahra Kırmusaoğlu, Bhardwaj SB, editors. Pathogenic Bacteria. London: IntechOpen; 2020. p. 1-21.
99. Integrated Taxonomic Information System - Report (ITIS). *Pseudomonas aeruginosa* Taxonomic Serial No.TSN 965278 [Internet]. 1900 [cited 2021 Oct 28]. Available from: https://www.itis.gov/servlet/SingleRpt/SingleRpt?search_topic=TSN&search_value=965278#null.
100. Ruiz-Roldán L, Rojo-Bezares B, Lozano C, López M, Chichón G, Torres C, et al. Occurrence of *Pseudomonas* spp. in raw vegetables: molecular and phenotypical analysis of their antimicrobial resistance and virulence-related traits. Int J Mol Sci. 2021;22(23).
101. Silby MW, Winstanley C, Godfrey SA, Levy SB, Jackson RW. *Pseudomonas genomes*: diverse and adaptable. FEMS Microbiol Rev. 2011;35(4):652-80.
102. LaBauve AE, Wargo MJ. Growth and laboratory maintenance of *Pseudomonas aeruginosa*. Curr Protoc Microbiol. 2012:2-11.
103. Schobert M, Jahn D. Anaerobic physiology of *Pseudomonas aeruginosa* in the cystic fibrosis lung. Int J Med Microbiol. 2010;300(8):549-56.
104. Iglewski. BH. Pseudomonas. 1996 [cited 2021 Oct 28]. In: Medical Microbiology [Internet]. Galveston: University of Texas Medical Branch at Galveston. 4th ed. [cited 2021 Oct 28]. Available from: https://www.ncbi.nlm.nih.gov/books/NBK8326/.
105. Sampedro I, Parales RE, Krell T, Hill JE. Pseudomonas chemotaxis. FEMS Microbiol Rev. 2014;39(1):17-46.
106. Whitchurch CB, Leech AJ, Young MD, Kennedy D, Sargent JL, Bertrand JJ, et al. Characterization of a complex chemosensory signal transduction system which controls twitching motility in *Pseudomonas aeruginosa*. Mol Microbiol. 2004;52(3):873-93.
107. Overhage J, Bains M, Brazas MD, Hancock REW. Swarming of *Pseudomonas aeruginosa* is a complex adaptation leading to increased production of virulence factors and antibiotic resistance. J Bacteriol. 2008;190(8):2671-9.
108. Ellis TN, Kuehn MJ. Virulence and immunomodulatory roles of bacterial outer membrane vesicles. MMBR. 2010;74(1):81-94.

109. Song Z, Wu H, Ciofu O, Kong K-F, Hoiby N, Rygaard J, et al. *Pseudomonas aeruginosa* alginate is refractory to Th1 immune response and impedes host immune clearance in a mouse model of acute lung infection. J Med Microbiol. 2003;52(9):731-40.
110. Kessler E, Safrin M, Gustin JK, Ohman DE. Elastase and the LasA protease of *Pseudomonas aeruginosa* are secreted with their propeptides. J Biol Chem. 1998;273(46):30225-31.
111. Tielen P, Kuhn H, Rosenau F, Jaeger K-E, Flemming H-C, Wingender J. Interaction between extracellular lipase LipA and the polysaccharide alginate of *Pseudomonas aeruginosa*. BMC Microbiology. 2013;13(1):159.
112. Sun Z, Kang Y, Norris MH, Troyer RM, Son MS, Schweizer HP, et al. Blocking phosphatidylcholine utilization in *Pseudomonas aeruginosa*, via mutagenesis of fatty acid, glycerol and choline degradation pathways, confirms the importance of this nutrient source *in vivo*. PLoS ONE. 2014;9(7):e103778.
113. Vasil ML, Graham LRM, Ostroff RM, Shortridge VD, Vasil AI. Phospholipase C: Molecular biology and contribution to the pathogenesis of *Pseudomonas aeruginosa*. In: Homma JY, Tanimoto H, Holder IA, Hoiby N, Döring G, editors. *Pseudomonas aeruginosa* in human diseases: 3rd international symposium of basic research and clinical aspects of *Pseudomonas aeruginosa* infection, Tokyo, September 1990. 44: S.Karger AG; 1991. p. 0.
114. Bradshaw JL, Caballero AR, Bierdeman MA, Adams KV, Pipkins HR, Tang A, et al. *Pseudomonas aeruginosa* protease IV exacerbates pneumococcal pneumonia and systemic disease. mSphere. 2018;3(3):10.1128/msphere.00212-18.
115. Kessler E, Safrin M. Elastinolytic and proteolytic enzymes. Methods Mol Biol. 2014;1149:135-69.
116. Sass G, Miller Conrad LC, Nguyen T-TH, Stevens DA. The *Pseudomonas aeruginosa* product pyochelin interferes with *Trypanosoma cruzi* infection and multiplication *in vitro*. Trans R Soc Trop Med Hyg. 2020;114(7):492-8.
117. Bonneau A, Roche B, Schalk IJ. Iron acquisition in *Pseudomonas aeruginosa* by the siderophore pyoverdine: an intricate interacting network including periplasmic and membrane proteins. Sci Rep. 2020;10(1):120.
118. Hall S, McDermott C, Anoopkumar-Dukie S, McFarland AJ, Forbes A, Perkins AV, et al. Cellular effects of pyocyanin, a secreted virulence factor of *Pseudomonas aeruginosa*. Toxins. 2016;8(8):236.
119. Michalska M, Wolf P. Pseudomonas exotoxin A: optimized by evolution for effective killing. Front Microbiol. 2015;6.
120. Basso P, Ragno M, Elsen S, Reboud E, Golovkine G, Bouillot S, et al. *Pseudomonas aeruginosa* pore-forming exolysin and type IV pili cooperate to induce host cell lysis. mBio. 2017;8(1):10.1128/mbio.02250-16.
121. Thi MTT, Wibowo D, Rehm BHA. *Pseudomonas aeruginosa* Biofilms. Int J Mol Sci. 2020;21(22):8671.
122. Lewis K. Riddle of biofilm resistance. Antimicrob Agents Chemother. 2001;45(4):999-1007.
123. Antibiotic resistance [Internet]. 2024 [cited 2024 January 21]. Available from: https://www.britannica.com/science/antibiotic-resistance.
124. Blair JMA, Webber MA, Baylay AJ, Ogbolu DO, Piddock LJV. Molecular mechanisms of antibiotic resistance. Nat Rev Microbiol. 2015;13(1):42-51.

125. Breidenstein EB, de la Fuente-Núñez C, Hancock RE. *Pseudomonas aeruginosa*: all roads lead to resistance. Trends Microbiol. 2011;19(8):419-26.
126. Delcour AH. Outer membrane permeability and antibiotic resistance. Biochim Biophys Acta. 2009;1794(5):808-16.
127. Hancock RE, Brinkman FS. Function of pseudomonas porins in uptake and efflux. Annu Rev Microbiol. 2002;56:17-38.
128. Welte W, Nestel U, Wacker T, Diederichs K. Structure and function of the porin channel. Kidney Int. 1995;48(4):930-40.
129. Bouffartigues E, Moscoso JA, Duchesne R, Rosay T, Fito-Boncompte L, Gicquel G, et al. The absence of the *Pseudomonas aeruginosa* OprF protein leads to increased biofilm formation through variation in c-di-GMP level. Front microbiol. 2015;6(630):1-13.
130. Li H, Luo YF, Williams BJ, Blackwell TS, Xie CM. Structure and function of OprD protein in *Pseudomonas aeruginosa:* from antibiotic resistance to novel therapies. Int J Med Microbiol. 2012;302(2):63-8.
131. Huang H, Hancock RE. Genetic definition of the substrate selectivity of outer membrane porin protein OprD of *Pseudomonas aeruginosa*. J Bacteriol. 1993;175(24):7793-800.
132. Sun J, Deng Z, Yan A. Bacterial multidrug efflux pumps: mechanisms, physiology and pharmacological exploitations. Biochem Biophys Res Commun. 2014;453(2):254-67.
133. Dreier J, Ruggerone P. Interaction of antibacterial compounds with RND efflux pumps in *Pseudomonas aeruginosa*. Front Microbiol. 2015;6:1-21.
134. Köhler T, Kok M, Michea-Hamzehpour M, Plesiat P, Gotoh N, Nishino T, et al. Multidrug efflux in intrinsic resistance to trimethoprim and sulfamethoxazole in *Pseudomonas aeruginosa*. Antimicrob Agents Chemother. 1996;40(10):2288-90.
135. Gotoh N, Tsujimoto H, Poole K, Yamagishi J, Nishino T. The outer membrane protein OprM of *Pseudomonas aeruginosa* is encoded by oprK of the mexA-mexB-oprK multidrug resistance operon. Antimicrob Agents Chemother. 1995;39(11):2567-9.
136. Li XZ, Nikaido H, Poole K. Role of mexA-mexB-oprM in antibiotic efflux in *Pseudomonas aeruginosa*. Antimicrob Agents Chemother. 1995;39(9):1948-53.
137. Li XZ, Zhang L, Srikumar R, Poole K. Beta-lactamase inhibitors are substrates for the multidrug efflux pumps of *Pseudomonas aeruginosa*. Antimicrob Agents Chemother. 1998;42(2):399-403.
138. Wright GD. Bacterial resistance to antibiotics: enzymatic degradation and modification. Adv Drug Deliv Rev. 2005;57(10):1451-70.
139. Poole K. Aminoglycoside resistance in *Pseudomonas aeruginosa*. Antimicrob Agents Chemother. 2005;49(2):479-87.
140. Bonfiglio G, Laksai Y, Franchino L, Amicosante G, Nicoletti G. Mechanisms of beta-lactam resistance amongst *Pseudomonas aeruginosa* isolated in an Italian survey. J Antimicrob Chemother. 1998;42(6):697-702.
141. Bush K, Jacoby GA. Updated functional classification of beta-lactamases. Antimicrob Agents Chemother. 2010;54(3):969-76.
142. Berrazeg M, Jeannot K, Ntsogo Enguéné VY, Broutin I, Loeffert S, Fournier D, et al. Mutations in β-Lactamase AmpC increase resistance of *Pseudomonas aeruginosa* isolates to antipseudomonal cephalosporins. Antimicrob Agents Chemother. 2015;59(10):6248-55.

143. Paterson DL, Bonomo RA. Extended-spectrum beta-lactamases: a clinical update. Clin Microbiol Rev. 2005;18(4):657-86.
144. Ratjen F, Brockhaus F, Angyalosi G. Aminoglycoside therapy against *Pseudomonas aeruginosa* in cystic fibrosis: a review. J Cyst Fibros. 2009;8(6):361-9.
145. Munita JM, Arias CA. Mechanisms of antibiotic resistance. Microbiol Spectr. 2016;4(2):1-37.
146. Mandsberg LF, Ciofu O, Kirkby N, Christiansen LE, Poulsen HE, Høiby N. Antibiotic resistance in *Pseudomonas aeruginosa* strains with increased mutation frequency due to inactivation of the DNA oxidative repair system. Antimicrob Agents Chemother. 2009;53(6):2483-91.
147. Braz VS, Furlan JPR, Fernandes AFT, Stehling EG. Mutations in NalC induce MexAB-OprM overexpression resulting in high level of aztreonam resistance in environmental isolates of *Pseudomonas aeruginosa*. FEMS Microbiol Lett. 2016;363(16):1-6.
148. Tian ZX, Yi XX, Cho A, O'Gara F, Wang YP. CpxR activates MexAB-OprM efflux pump expression and enhances antibiotic resistance in both laboratory and clinical *nalB*-type isolates of *Pseudomonas aeruginosa*. PLoS Pathog. 2016;12(10):1-22.
149. Hirai K, Suzue S, Irikura T, Iyobe S, Mitsuhashi S. Mutations producing resistance to norfloxacin in *Pseudomonas aeruginosa*. Antimicrob Agents Chemother. 1987;31(4):582-6.
150. Masuda N, Sakagawa E, Ohya S. Outer membrane proteins responsible for multiple drug resistance in *Pseudomonas aeruginosa*. Antimicrob Agents Chemother. 1995;39(3):645-9.
151. Fukuda H, Hosaka M, Hirai K, Iyobe S. New norfloxacin resistance gene in *Pseudomonas aeruginosa* PAO. Antimicrob Agents Chemother. 1990;34(9):1757-61.
152. Köhler T, Michéa-Hamzehpour M, Henze U, Gotoh N, Curty LK, Pechère JC. Characterization of MexE-MexF-OprN, a positively regulated multidrug efflux system of *Pseudomonas aeruginosa*. Mol Microbiol. 1997;23(2):345-54.
153. De Kievit TR, Parkins MD, Gillis RJ, Srikumar R, Ceri H, Poole K, et al. Multidrug efflux pumps: expression patterns and contribution to antibiotic resistance in *Pseudomonas aeruginosa* biofilms. Antimicrob Agents Chemother. 2001;45(6):1761-70.
154. Bruchmann S, Dötsch A, Nouri B, Chaberny IF, Häussler S. Quantitative contributions of target alteration and decreased drug accumulation to *Pseudomonas aeruginosa* fluoroquinolone resistance. Antimicrob Agents Chemother. 2013;57(3):1361-8.
155. Juan C, Maciá MD, Gutiérrez O, Vidal C, Pérez JL, Oliver A. Molecular mechanisms of beta-lactam resistance mediated by AmpC hyperproduction in *Pseudomonas aeruginosa* clinical strains. Antimicrob Agents Chemother. 2005;49(11):4733-8.
156. Arber W. Horizontal gene transfer among bacteria and its role in biological evolution. Life. 2014;4(2):217-24.
157. Subedi D, Vijay AK, Willcox M. Overview of mechanisms of antibiotic resistance in *Pseudomonas aeruginosa*: an ocular perspective. Clin Exp Optom. 2018;101(2):162-71.
158. Jacoby GA. Mechanisms of resistance to quinolones. Clin Infect Dis.

2005;41(2):120-6.
159. Blondeau JM. Fluoroquinolones: mechanism of action, classification, and development of resistance. Surv Ophthalmol. 2004;49(2):73-8.
160. Pandya AG, Hynan LS, Bhore R, Riley FC, Guevara IL, Grimes P, et al. Reliability assessment and validation of the Melasma Area and Severity Index (MASI) and a new modified MASI scoring method. J Am Acad Dermatol. 2011;64(1):78-83.
161. Das T, Sehar S, Manefield M. The roles of extracellular DNA in the structural integrity of extracellular polymeric substance and bacterial biofilm development. Environ Microbiol Rep. 2013;5(6):778-86.
162. Stewart PS. Mechanisms of antibiotic resistance in bacterial biofilms. Int J Med Microbiol. 2002;292(2):107-13.
163. Hoiby N, Jacobsen L, Jorgensen BA, Lykkegaard E, Weeke B. *Pseudomonas aeruginosa* infection in cystic fibrosis. Occurrence of precipitating antibodies against *Pseudomonas aeruginosa* in relation to the concentration of sixteen serum proteins and the clinical and radiographical status of the lungs. Acta Paediatr Scand. 1974;63(6):843-8.
164. Govan JR, Deretic V. Microbial pathogenesis in cystic fibrosis: mucoid *Pseudomonas aeruginosa* and *Burkholderia cepacia*. Microbiol Rev. 1996;60(3):539-74.
165. Friedman L, Kolter R. Genes involved in matrix formation in *Pseudomonas aeruginosa* PA14 biofilms. Mol Microbiol. 2004;51(3):675-90.
166. Whitchurch CB, Tolker-Nielsen T, Ragas PC, Mattick JS. Extracellular DNA required for bacterial biofilm formation. Science. 2002;295(5559):1487.
167. Allesen-Holm M, Barken KB, Yang L, Klausen M, Webb JS, Kjelleberg S, et al. A characterization of DNA release in *Pseudomonas aeruginosa* cultures and biofilms. Mol Microbiol. 2006;59(4):1114-28.
168. Pamp SJ, Tolker-Nielsen T. Multiple roles of biosurfactants in structural biofilm development by *Pseudomonas aeruginosa*. J Bacteriol. 2007;189(6):2531-9.
169. Goltermann L, Tolker-Nielsen T. Importance of the exopolysaccharide matrix in antimicrobial tolerance of *Pseudomonas aeruginosa* aggregates. Antimicrob Agents Chemother. 2017;61(4):1-7.
170. Ciofu O, Tolker-Nielsen T. Tolerance and resistance of *Pseudomonas aeruginosa* biofilms to antimicrobial agents-How *P. aeruginosa* can escape antibiotics. Front microbiol. 2019;10:1-15.
171. Balaban NQ, Gerdes K, Lewis K, McKinney JD. A problem of persistence: still more questions than answers?. Nat Rev Microbiol. 2013;11(8):587-91.
172. Mulcahy LR, Burns JL, Lory S, Lewis K. Emergence of *Pseudomonas aeruginosa* strains producing high levels of persister cells in patients with cystic fibrosis. J Bacteriol. 2010;192(23):6191-9.
173. Debnath M, Prasad GBKS, Bisen PS. Omics Technology. In: Debnath M, Prasad GBKS, Bisen PS, editors. Molecular Diagnostics: promises and possibilities. Dordrecht: Springer Netherlands; 2010. p. 11-31.
174. Lowe R, Shirley N, Bleackley M, Dolan S, Shafee T. Transcriptomics technologies. PLoS Comput Biol. 2017;13(5):e1005457.
175. Ozsolak F, Milos PM. RNA sequencing: advances, challenges and opportunities. Nat Rev Genet. 2011;12(2):87-98.
176. Wang Z, Gerstein M, Snyder M. RNA-Seq: a revolutionary tool for

transcriptomics. Nat Rev Genet. 2009;10(1):57-63.
177. Romanov V, Davidoff SN, Miles AR, Grainger DW, Gale BK, Brooks BD. A critical comparison of protein microarray fabrication technologies. Analyst. 2014;139(6):1303-26.
178. Barbulovic-Nad I, Lucente M, Sun Y, Zhang M, Wheeler AR, Bussmann M. Bio-microarray fabrication techniques-a review. Crit Rev Biotechnol. 2006;26(4):237-59.
179. Costa V, Aprile M, Esposito R, Ciccodicola A. RNA-Seq and human complex diseases: recent accomplishments and future perspectives. Eur J Hum Genet. 2013;21(2):134-42.
180. Khurana E, Fu Y, Chakravarty D, Demichelis F, Rubin MA, Gerstein M. Role of non-coding sequence variants in cancer. Nat Rev Genet. 2016;17(2):93-108.
181. Slotkin RK, Martienssen R. Transposable elements and the epigenetic regulation of the genome. Nat Rev Genet. 2007;8(4):272-85.
182. Proserpio V, Mahata B. Single-cell technologies to study the immune system. Immunology. 2016;147(2):133-40.
183. García-Sánchez S, Aubert S, Iraqui I, Janbon G, Ghigo J-M, d'Enfert C. *Candida albicans* biofilms: a developmental state associated with specific and stable gene expression patterns. Eukaryotic Cell. 2004;3(2):536-45.
184. Mok S, Ashley EA, Ferreira PE, Zhu L, Lin Z, Yeo T, et al. Population transcriptomics of human malaria parasites reveals the mechanism of artemisinin resistance. Science. 2015;347(6220):431-5.
185. Christov CP, Gardiner TJ, Szüts D, Krude T. Functional requirement of noncoding Y RNAs for human chromosomal DNA replication. Mol Cell Biol. 2006;26(18):6993-7004.
186. Kishore S, Stamm S. The snoRNA HBII-52 regulates alternative splicing of the serotonin receptor 2C. Science. 2006;311(5758):230-2.
187. Esteller M. Non-coding RNAs in human disease. Nat Rev Genet. 2011;12(12):861-74.
188. Aleksander SA, Balhoff J, Carbon S, Cherry JM, Drabkin HJ, Ebert D, et al. The gene ontology knowledgebase in 2023. Genetics. 2023;224(1).
189. CLSI. Methods for dilution antimicrobial susceptibility tests for bacteria that grow aerobically; approved Standard—Ninth Edition.: CLSI Documents M07-A9. Clinical and Laboratory Standards Institute 950 West Valley Roadn Suite 2500,Wayne, Pennsylvania 19087,USA; 2012.
190. Rakholiya KD, Kaneria MJ, Chanda SV. Chapeter 11-Medicinal plants as alternative sources of therapeutics against multidrug-resistant pathogenic microorganisms based on their antimicrobial potential and synergistic properties. In: Rai M, Kon K, editors. Fighting multidrug resistance with herbal extracts, essential oils and their components. San Diego: Academic Press; 2013. p. 165-79.
191. CLSI. M100 Performance Standards for Antimicrobial Susceptibility Testing. : CLSI Documents M100, 28th ed. Clinical and Laboratory Standards Institute 950 West Valley Roadn Suite 2500,Wayne, Pennsylvania 19087,USA; 2014.
192. CLSI. Performance Standards for antimicrobial susceptibility testing. 30th ed. CLSI supplement M100. Wayne, PA: Clinical and Laboratory Standards Institute; 2020.
193. PubChem Compound Summary for CID 5481173, Ceftazidime [Internet]. [cited 2021 Nov. 8]. Available from:

https://pubchem.ncbi.nlm.nih.gov/compound/Ceftazidime.
194. Craig WA, Gerber AU. Pharmacokinetics of cefoperazone: a review. Drugs. 1981;22(1):35-45.
195. Drug index [Internet]. [cited 2021 Nov. 8]. Available from: https://www.pediatriconcall.com/drugs.
196. Papp-Wallace KM, Endimiani A, Taracila MA, Bonomo RA. Carbapenems: past, present, and future. Antimicrob Agents Chemother. 2011;55(11):4943-60.
197. Ramirez MS, Tolmasky ME. Amikacin: uses, resistance, and prospects for inhibition. Molecules. 2017;22(12):1-23.
198. French GL. A review of tigecycline. J Chemother. 2008;20(1):3-11.
199. LeBel M. Ciprofloxacin: chemistry, mechanism of action, resistance, antimicrobial spectrum, pharmacokinetics, clinical trials, and adverse reactions. Pharmacotherapy. 1988;8(1):3-33.
200. Podder V, Sadiq NM. Levofloxacin. Treasure Island: StatPearls Publishing; 2021. Available from: https://pubmed.ncbi.nlm.nih.gov/31424764/.
201. Akhavan BJ, Khanna NR, Vijhani P. Amoxicillin. Treasure Island: StatPearls Publishing; 2021. Available from: https://pubmed.ncbi.nlm.nih.gov/29489203/.
202. Mitsuyama J, Takahata M, Yasuda T, Saikawa I. The mechanism of action of piperacillin-analogues *in vitro*; effect of the carbon number at the N-4 position of 2,3-dioxopiperazine on the outer membrane permeability, stability to beta-lactamase and binding affinity to penicillin-binding proteins. J Antibiot. 1987;40(6):868-72.
203. Richards DM, Heel RC, Brogden RN, Speight TM, Avery GS. Ceftriaxone. A review of its antibacterial activity, pharmacological properties and therapeutic use. Drugs. 1984;27(6):469-527.
204. Sugimoto A, Maeda A, Itto K, Arimoto H. Deciphering the mode of action of cell wall-inhibiting antibiotics using metabolic labeling of growing peptidoglycan in *Streptococcus pyogenes*. Sci Rep. 2017;7(1):1-12.
205. Wang F, Zhou H, Olademehin OP, Kim SJ, Tao P. Insights into key interactions between vancomycin and bacterial cell wall structures. ACS Omega. 2018;3(1):37-45.
206. Jelic D, Antolovic R. From erythromycin to azithromycin and new potential ribosome-binding antimicrobials. Antibiotics. 2016;5(3):1-13.
207. Chopra I, Roberts M. Tetracycline antibiotics: mode of action, applications, molecular biology, and epidemiology of bacterial resistance. Microbiol Mol Biol Rev. 2001;65(2):232-60.
208. Chaves BJ, Tadi P. Gentamicin. Treasure Island: StatPearls Publishing; 2021. Available from: https://pubmed.ncbi.nlm.nih.gov/32491482/.
209. Gleckman R, Blagg N, Joubert DW. Trimethoprim: mechanisms of action, antimicrobial activity, bacterial resistance, pharmacokinetics, adverse reactions, and therapeutic indications. Pharmacotherapy. 1981;1(1):14-20.
210. Wehrli W. Rifampin: mechanisms of action and resistance. Rev Infect Dis. 1983;5(3):407-11.
211. Tulkens PM, Arvis P, Kruesmann F. Moxifloxacin safety: an analysis of 14 years of clinical data. Drugs R D. 2012;12(2):71-100.
212. Balouiri M, Sadiki M, Ibnsouda SK. Methods for *in vitro* evaluating antimicrobial activity: A review. J Pharm Anal. 2016;6(2):71-9.
213. Wongkaewkhiaw S, Kanthawong S, Bolscher JGM, Nazmi K, Taweechaisupapong S, Krom BP. DNase-mediated eDNA removal enhances D-LL-31

activity against biofilms of bacteria isolated from chronic rhinosinusitis patients. Biofouling. 2020;36(9):1117-28.
214. Kanthawong S, Nazmi K, Wongratanacheewin S, Bolscher JG, Wuthiekanun V, Taweechaisupapong S. *In vitro* susceptibility of *Burkholderia pseudomallei* to antimicrobial peptides. Int J Antimicrob Agents. 2009;34(4):309-14.
215. Konaté K, Mavoungou JF, Lepengué AN, Aworet-Samseny RR, Hilou A, Souza A, et al. Antibacterial activity against ß-lactamase producing methicillin and ampicillin-resistants *Staphylococcus aureus*: Fractional Inhibitory Concentration Index (FICI) determination. Ann clin microbiol antimicrob. 2012;11(18):1-12.
216. Fratini F, Mancini S, Turchi B, Friscia E, Pistelli L, Giusti G, et al. A novel interpretation of the Fractional Inhibitory Concentration Index: The case *Origanum vulgare* L. and *Leptospermum scoparium* J. R. et G. Forst essential oils against *Staphylococcus aureus* strains. Microbiol Res. 2017;195:11-7.
217. Cheypratub P, Leeanansaksiri W, Eumkeb G. The synergy and mode of action of *Cyperus rotundus* L. extract plus ampicillin against ampicillin-resistant *Staphylococcus aureus*. Evid Based Complementary Altern Med. 2018;2018:1-11.
218. American Type Culture Collection (ATCC). *Pseudomonas aeruginosa* (Schroeter) Migula BAA-2108™ [Internet]. [cited 2021 Nov 8]. Available from: https://www.atcc.org/products/baa-2108.
219. Bassolé IH, Lamien-Meda A, Bayala B, Obame LC, Ilboudo AJ, Franz C, et al. Chemical composition and antimicrobial activity of Cymbopogon citratus and Cymbopogon giganteus essential oils alone and in combination. Phytomedicine. 2011;18(12):1070-4.
220. File:96-Well plate.svg [Internet]. [cited 2021 Oct 8]. Available from: https://commons.wikimedia.org/wiki/File:96-Well_plate.svg.
221. Rattanachak N, Weawsiangsang S, Jongjitvimol T, Baldock RA, Jongjitwimol J. Hydroquinine possesses antibacterial activity, and at half the MIC, induces the overexpression of RND-type efflux pumps using Multiplex Digital PCR in *Pseudomonas aeruginosa*. Trop Med Int Health. 2022;7(8):156.
222. Premier biosoft: accelelrating research in Life scienc. PCR Primer design guidelines [Internet]. [cited 2021 Nov 8]. Available from: http://www.premierbiosoft.com/tech_notes/PCR_Primer_Design.html.
223. Rychlik W, Spencer WJ, Rhoads RE. Optimization of the annealing temperature for DNA amplification *in vitro*. Nucleic Acids Res. 1990;18(21):6409-12.
224. Rattanachak N, Weawsiangsang S, Baldock RA, Jaifoo T, Jongjitvimol T, Jongjitwimol J. A novel and quantitative detection assay (*effluxR*) for identifying efflux-associated resistance genes using multiplex digital PCR in clinical isolates of *Pseudomonas aeruginosa*. Methods protoc. 2023;6(5):96.
225. Rattanachak N, Weawsiangsang S, Daowtak K, Thongsri Y, Ross S, Ross G, et al. High-throughput transcriptomic profiling reveals the inhibitory effect of hydroquinine on virulence factors in *Pseudomonas aeruginosa*. Antibiotics (Basel). 2022;11(10).
226. She P, Wang Y, Luo Z, Chen L, Tan R, Wang Y, et al. Meloxicam inhibits biofilm formation and enhances antimicrobial agents efficacy by *Pseudomonas aeruginosa*. Microbiologyopen. 2018;7(1).
227. Merritt JH, Kadouri DE, O'Toole GA. Growing and analyzing static biofilms. Curr Protoc Microbiol. 2006;00(1).

228. Wongkaewkhiaw S, Taweechaisupapong S, Thanaviratananich S, Bolscher JGM, Nazmi K, Anutrakunchai C, et al. D-LL-31 enhances biofilm-eradicating effect of currently used antibiotics for chronic rhinosinusitis and its immunomodulatory activity on human lung epithelial cells. PLoS ONE. 2020;15(12):e0243315.
229. Kraikongjit S, Jongjitvimol T, Mianjinda N, Sirithep N, Kaewbor T, Jumroon N, et al. Antibacterial effect of plant resin collected from *Tetrigona apicalis* (Smith, 1857) in Thung Salaeng Luang National Park, Phitsanulok. Walailak J Sci & Tech. 2017;15(8):599-607.
230. Kharal SA, Hussain Q, Ali S, Fakhuruddin. Quinine is bactericidal. J Pak Med Assoc. 2009;59(4):208-12.
231. National Center for Biotechnology Information. PubChem Compound Summary for CID 10651. Hydroquinine. (accessed on 23 July 2022). [Internet]. [cited 23 July 2022]. Available from: https://pubchem.ncbi.nlm.nih.gov/compound/Hydroquinine#section=Hazards-Summary.
232. Abed F, Baniya R, Bachuwa G. Quinine-induced disseminated intravascular coagulation. Case Rep Med. 2016;2016:9136825.
233. Leanse LG, Dong PT, Goh XS, Lu M, Cheng JX, Hooper DC, et al. Quinine enhances photo-inactivation of gram-negative bacteria. J Infect Dis. 2020;221(4):618-26.
234. Peng L, Kang S, Yin Z, Jia R, Song X, Li L, et al. Antibacterial activity and mechanism of berberine against *Streptococcus agalactiae*. Int J Clin Exp Pathol. 2015;8(5):5217-23.
235. NicAogáin K, O'Byrne CP. The role of stress and stress adaptations in determining the fate of the bacterial pathogen *Listeria monocytogenes* in the food chain. Front Microbiol. 2016;7:1865.
236. Oluremi Adejoke A, Uyi Oluwatobi E, Opeyemi Mariam A, Morenike Olutumbi A-I, Olufunmiso Olusola O. *In vitro* effects of quinine on the antibacterial activity of erythromycin against bacteria of clinical relevance. GSC biol pharm sci. 2021;14(2):077-86.
237. Peechakara BV, Basit H, Gupta M. Ampicillin. StatPearls. Treasure Island (FL): StatPearls Publishing Copyright © 2023, StatPearls Publishing LLC.; 2023.
238. Lister PD, Wolter DJ, Hanson ND. Antibacterial-resistant *Pseudomonas aeruginosa*: clinical impact and complex regulation of chromosomally encoded resistance mechanisms. Clin Microbiol Rev. 2009;22(4):582-610.
239. Piddock LJ. Multidrug-resistance efflux pumps - not just for resistance. Nat Rev Microbiol. 2006;4(8):629-36.
240. Auda IG, Ali Salman IM, Odah JG. Efflux pumps of Gram-negative bacteria in brief. Gene Reports. 2020;20:100666.
241. Soto SM. Role of efflux pumps in the antibiotic resistance of bacteria embedded in a biofilm. Virulence. 2013;4(3):223-9.
242. Hancock REW. Resistance mechanisms in *Pseudomonas aeruginosa* and other nonfermentative gram-negative bacteria. Clinical Infectious Diseases. 1998;27(Supplement_1):S93-S9.
243. Xiong L, Teng JL, Botelho MG, Lo RC, Lau SK, Woo PC. Arginine metabolism in bacterial pathogenesis and cancer therapy. Int J Mol Sci. 2016;17(3):363.
244. Mercenier A, Simon JP, Vander Wauven C, Haas D, Stalon V. Regulation of enzyme synthesis in the arginine deiminase pathway of *Pseudomonas aeruginosa*. J

Bacteriol. 1980;144(1):159-63.
245. Weawsiangsang S, Rattanachak N, Jongjitvimol T, Jaifoo T, Charoensit P, Viyoch J, et al. Hydroquinine inhibits the growth of multidrug-resistant *Pseudomonas aeruginosa* via the suppression of the arginine deiminase pathway genes. Int J Mol Sci. 2023;24(18).
246. Vander Wauven C, Piérard A, Kley-Raymann M, Haas D. *Pseudomonas aeruginosa* mutants affected in anaerobic growth on arginine: evidence for a four-gene cluster encoding the arginine deiminase pathway. J Bacteriol. 1984;160(3):928-34.
247. Kolbeck S, Abele M, Hilgarth M, Vogel RF. Comparative proteomics reveals the anaerobic lifestyle of meat-spoiling Pseudomonas species. Front Microbiol. 2021;12:664061.
248. Armitage JP, Evans MC. The motile and tactic behaviour of *Pseudomonas aeruginosa* in anaerobic environments. FEBS Lett. 1983;156(1):113-8.
249. Casiano-Colón A, Marquis RE. Role of the arginine deiminase system in protecting oral bacteria and an enzymatic basis for acid tolerance. Appl Environ Microbiol. 1988;54(6):1318-24.
250. Wang D, Kompaniiets D, Hu Y, Liu B. Editorial: Transcription and its regulation in bacteria. Front Microbiol. 2023;14.
251. Glen KA, Lamont IL. β-lactam resistance in *Pseudomonas aeruginosa*: current status, future prospects. Pathogens. 2021;10(12).
252. Ghafoor A, Hay ID, Rehm BH. Role of exopolysaccharides in *Pseudomonas aeruginosa* biofilm formation and architecture. Appl Environ Microbiol. 2011;77(15):5238-46.
253. Ghafoor A, Jordens Z, Rehm BH. Role of PelF in pel polysaccharide biosynthesis in *Pseudomonas aeruginosa*. Appl Environ Microbiol. 2013;79(9):2968-78.
254. Laverty G, Gorman S, Gilmore B. The potential of antimicrobial peptides as biocides. Int J Mol Sci. 2011;12:6566-96.
255. Müller B, Blaukopf M, Hofinger A, Zamyatina A, Brade H, Kosma P. Efficient synthesis of 4-amino-4-deoxy-L-arabinose and spacer-equipped 4-amino-4-deoxy-L-arabinopyranosides by transglycosylation reactions. Synthesis (Stuttg). 2010;2010(18):3143-51.
256. Williams GJ, Breazeale SD, Raetz CR, Naismith JH. Structure and function of both domains of ArnA, a dual function decarboxylase and a formyltransferase, involved in 4-amino-4-deoxy-L-arabinose biosynthesis. J Biol Chem. 2005;280(24):23000-8.
257. Zhou Z, Lin S, Cotter RJ, Raetz CR. Lipid A modifications characteristic of *Salmonella typhimurium* are induced by NH4VO3 in *Escherichia coli* K12. Detection of 4-amino-4-deoxy-L-arabinose, phosphoethanolamine and palmitate. J Biol Chem. 1999;274(26):18503-14.
258. Zhou Z, Ribeiro AA, Lin S, Cotter RJ, Miller SI, Raetz CR. Lipid A modifications in polymyxin-resistant *Salmonella typhimurium*: PMRA-dependent 4-amino-4-deoxy-L-arabinose, and phosphoethanolamine incorporation. J Biol Chem. 2001;276(46):43111-21.
259. Gunn JS. Bacterial modification of LPS and resistance to antimicrobial peptides. J Endotoxin Res. 2001;7(1):57-62.
260. Gunn JS, Ryan SS, Van Velkinburgh JC, Ernst RK, Miller SI. Genetic and functional analysis of a PmrA-PmrB-regulated locus necessary for lipopolysaccharide

modification, antimicrobial peptide resistance, and oral virulence of *Salmonella enterica* serovar typhimurium. Infect Immun. 2000;68(11):6139-46.
261. Schavemaker PE, Lynch M. Flagellar energy costs across the tree of life. eLife. 2022;11:e77266.
262. Sampedro I, Parales RE, Krell T, Hill JE. Pseudomonas chemotaxis. FEMS Microbiol Rev. 2015;39(1):17-46.
263. Rasko DA, Sperandio V. Anti-virulence strategies to combat bacteria-mediated disease. Nature Reviews Drug Discovery. 2010;9(2):117-28.
264. Valot B, Guyeux C, Rolland JY, Mazouzi K, Bertrand X, Hocquet D. What It takes to be a *Pseudomonas aeruginosa*? the core genome of the opportunistic pathogen updated. PLoS ONE. 2015;10(5):e0126468.
265. Anes J, McCusker MP, Fanning S, Martins M. The ins and outs of RND efflux pumps in *Escherichia coli*. Front Microbiol. 2015;6:587.
266. Ni RT, Onishi M, Mizusawa M, Kitagawa R, Kishino T, Matsubara F, et al. The role of RND-type efflux pumps in multidrug-resistant mutants of *Klebsiella pneumoniae*. Sci Rep. 2020;10(1):10876.
267. Guérin F, Lallement C, Isnard C, Dhalluin A, Cattoir V, Giard JC. Landscape of Resistance-Nodulation-Cell Division (RND)-type efflux pumps in *Enterobacter cloacae* complex. Antimicrob Agents Chemother. 2016;60(4):2373-82.
268. Dashtbani-Roozbehani A, Brown MH. Efflux pump mediated antimicrobial resistance by *Staphylococci* in health-related environments: challenges and the quest for inhibition. Antibiotics. 2021;10(12).
269. Hancock REW. The bacterial outer membrane as a drug barrier. Trends Microbiol. 1997;5(1):37-42.
270. Morita Y, Tomida J, Kawamura Y. MexXY multidrug efflux system of *Pseudomonas aeruginosa*. Front Microbiol. 2012;3.
271. Wolf R, Baroni A, Greco R, Donnarumma G, Ruocco E, Tufano MA, et al. Quinine sulfate and bacterial invasion. Ann Clin Microbiol Antimicrob. 2002;1:5.
272. Wolf R, Tufano MA, Ruocco V, Grimaldi E, Ruocco E, Donnarumma G, et al. Quinine sulfate inhibits invasion of some bacterial skin pathogens. Int J Dermatol. 2006;45(6):661-3.
273. Mariano G, Faba-Rodriguez R, Bui S, Zhao W, Ross J, Tzokov SB, et al. Oligomerization of the FliF domains suggests a coordinated assembly of the bacterial flagellum MS Ring. Front Microbiol. 2022;12.
274. Bouteiller M, Dupont C, Bourigault Y, Latour X, Barbey C, Konto-Ghiorghi Y, et al. Pseudomonas flagella: generalities and specificities. Int J Mol Sci. 2021;22(7):3337.
275. Hall S, McDermott C, Anoopkumar-Dukie S, McFarland AJ, Forbes A, Perkins AV, et al. Cellular effects of pyocyanin, a secreted virulence factor of *Pseudomonas aeruginosa*. Toxins (Basel). 2016;8(8).
276. Wu Z, Zheng R, Zhang J, Wu S. Transcriptional profiling of *Pseudomonas aeruginosa* PAO1 in response to anti-biofilm and anti-infection agent exopolysaccharide EPS273. J Appl Microbiol. 2021;130(1):265-77.
277. O'Donnell JN, Bidell MR, Lodise TP. Approach to the treatment of patients with serious multidrug-resistant *Pseudomonas aeruginosa* infections. Pharmacotherapy. 2020;40(9):952-69.
278. Geske GD, O'Neill JC, Miller DM, Mattmann ME, Blackwell HE. Modulation of

bacterial quorum sensing with synthetic ligands: Systematic evaluation of N-Acylated homoserine lactones in multiple species and new insights into their mechanisms of action. J Am Chem Soc. 2007;129(44):13613-25.
279. Favre-Bonté S, Köhler T, Van Delden C. Biofilm formation by *Pseudomonas aeruginosa*: Role of the C4-HSL cell-to-cell signal and inhibition by azithromycin. J Antimicrob Chemother. 2003;52(4):598-604.
280. Wang Y, Feng L, Lu H, Zhu J, Kumar V, Liu X. Transcriptomic analysis of the food spoilers *Pseudomonas fluorescens* reveals the antibiofilm of carvacrol by interference with intracellular signaling processes. Food Control. 2021;127:108115.